Platinum alloyed DLC and gold nanoparticle covered DLC electrodes for detection of glutamate

Iina-Maria Yrjänä

School of Electrical Engineering

Thesis submitted for examination for the degree of Master of Science in Technology.

Espoo 30.9.2015

Thesis supervisor:

Prof. Tomi Laurila

Thesis advisor:

D.Sc. (Tech.) Emilia Peltola

Aalto University
School of Electrical
Engineering

AALTO UNIVERSITY
SCHOOL OF ELECTRICAL ENGINEERING

ABSTRACT OF THE
MASTER'S THESIS

Author: Iina-Maria Yrjänä

Title: Platinum alloyed DLC and gold nanoparticle covered DLC electrodes for detection of glutamate

Date: 30.9.2015 Language: English Number of pages: 7+91

Department of Electrical Engineering and Automation

Professorship: Microsystem Technology

Supervisor: Prof. Tomi Laurila

Advisor: D.Sc. (Tech.) Emilia Peltola

Glutamate is one of the most common neurotransmitters in the vertebrate central nervous system. It is a factor in several neurological processes and dysfunction on its regulation has been suggested to play a role in different neurological conditions. The ability to detect glutamate with high spatial and temporal resolutions would give an important insight to the underlying mechanisms of these processes and conditions.

Amperometric biosensors have provided a promising method for glutamate detection. The sensors are based on the electrochemical detection of hydrogen peroxide (H_2O_2), which is produced by an enzymatic reaction of glutamate. Due to several electrochemically active endogenous interferents present in the brain, a permselective polymer layer may be deposited onto the electrode.

In this thesis the suitability of two electrode materials are evaluated, first for H_2O_2 detection and then for glutamate detection. The materials are: platinum alloyed DLC (CPt) and DLC with gold nanoparticles deposited onto it (AuNP). Two different polymer layers (polyaniline and polypyrrole) are deposited onto the electrode and their functionality as a permselective protective layer is assessed. Glutamate oxidase is immobilized onto the sample types, which performed satisfactorily in the preliminary studies of H_2O_2 detection. The stability of the enzyme layer is also evaluated.

The CPt samples seemed to be a promising electrode material for glutamate sensors. The greatest problem with the AuNP samples was the detachment of the nanoparticles. Promising results were obtained from the preliminary measurements with H_2O_2 but sensors able to detect glutamate were not produced. The deposition of the polymer layers were not successful. The major problem with them was the improper adhesion between the substrate and the polymer layer.

Keywords: Platinum alloyed DLC, Gold nanoparticles, Glutamate, Biosensors

AALTO-YLIOPISTO
SÄHKÖTEKNIIKAN KORKEAKOULU

DIPLOMITYÖN
TIIVISTELMÄ

Tekijä: Iina-Maria Yrjänä

Työn nimi: Glutamaatin havaitseminen platinaseostetulla DLC:llä ja kultananopartikkelipinnoitteisella DLC:llä

Päivämäärä: 30.9.2015 Kieli: Englanti Sivumäärä: 7+91

Sähkötekniikan ja automaation laitos

Professuuri: Mikrosysteemitekniikka

Työn valvoja: Prof. Tomi Laurila

Työn ohjaaja: TkT Emilia Peltola

Glutamaatti on yksi selkärankaisten keskushermoston yleisimmistä välittäjäaineista. Se vaikuttaa monien normaalien aivotoimintojen lisäksi myös monien neurologisten sairauksien syntyyn. Jotta näitä toimintoja ja niiden syntymekanismeja voitaisiin ymmärtää, olisi tärkeää kyetä mittaamaan glutamaatin pitoisuuksia tarkasti aivoista.
Lupaava metodi glutamaatin havaitsemiseen on amperometriset bioanturit. Ne perustuvat entsymaattisen reaktion avulla glutamaatista tuotetun vetyperoksidin (H_2O_2) sähkökemialliseen havaitsemiseen. Antureiden elektrodit päällystetään yleensä puoliläpäisevällä suojaavalla kalvolla, jotta aivoissa olevat sähkökemiallisesti aktiiviset häiriötekijät eivät häiritsisi anturin toimintaa.
Kahden eri elektrodimateriaalin soveltuvuutta arvioidaan ensin H_2O_2- ja sen jälkeen glutamaattimittauksilla. Materiaalit ovat platinalla seostettu timantinkaltainen hiili (CPt) ja kultananopartikkelein päällystetty timantinkaltainen hiili (AuNP). Elektrodit pinnoitetaan kahdella eri polymeerillä (polyaniliini ja polypyrroli) ja niiden toiminnallisuutta puoliläpäisevänä suojakalvona arvioidaan. Glutamaattioksidaasi immobilisoidaan niiden näytetyyppien päälle, jotka toimivat tyydyttävästi alustavissa H_2O_2-mittauksissa. Entsyymikerroksen stabiiliutta arvioidaan myös.
CPt näytteet vaikuttivat lupaavalta electrodimateriaalilta glutamaattiantureihin. Suurin haaste AuNP-näytteiden kanssa oli nanopartikkeleiden irtoaminen mittauksissa. H_2O_2-mittaukset tuottivat lupaavia tuloksia, mutta glutamaattia havaitsevia antureita ei kyetty valmistamaan. Polymeerikalvojen pinnoittaminen ei onnistunut, ongelmana oli puutteellinen adheesio substraatin ja kalvon välillä.

Avainsanat: Platinalla seostettu timantinkaltainen hiili, Kultananopartikkelit, Glutamaatti, Bioanturit

Preface

I would like to thank my supervisor professor Tomi Laurila for giving me the opportunity to work with this interesting topic and his helpful advice. I would also like to thank my instructor Emilia Peltola for her useful feedback and advice I received with this process.

Several others have also helped me with this thesis and they deserve to be mentioned here. Noora Tujunen for her help and support with the electrochemical measurements. Vera Propototova for preparing the CPt samples and substrates for the other samples. Vesa Vuorinen and Antti Rautiainen for their help in the sample manufacturing process. Tommi Palomäki, Niklas Wester and Sami Sainio for their help and answers for all my random questions about the electrochemical measurements. I would also like to thank Elsi and Elli for peer support.

I would also want to take this opportunity and thank all the amazing people who have made these past six years in Otaniemi so unbelievable awesome! Without you I might have graduated earlier but the journey would not have been as memorable.

Finally I would also want to thank my family for their support and believing in me that one day I will indeed finish my studies. And especially I want to thank my beloved future hubby for his support and just being there when I needed him.

Otaniemi, 30.9.2015

Iina-Maria Yrjänä

Contents

Symbols and abbreviations

Abbreviations

Ag/AgCl	Silver/silver chloride
APTES	3-aminopropyltriethoxysilane
AuNP	DLC covered with gold nanoparticles; a sample type used in this thesis.
CPt	Platinum alloyed DLC; a sample type used in this thesis
DLC	Diamond-Like Carbon
EDC	1-Ethyl-3-(3-dimethylaminopropyl)carbodiimide
GlOx	Glutamate Oxidase
H_2O_2	Hydrogen peroxide
NHE	Normal hydrogen electrode
NHS	N-Hydroxysuccinimide
PANI	Polyaniline
PPD	Phenylenediamine
PPy	Polypyrrole
PBS	Phosphate Buffered Saline
SAM	Self-Assebled Monolayer
SCE	Saturated calomel electrode
TESPSA	3-triethoxysilylpropyl succinic anhydride

1 Introduction

Glutamate is one of the most common neurotransmitters in vertebrate central nervous system (CNS). Approximately 90% of all excitatory synapses are glutamatergic i.e. they are glutamate mediated. Glutamate is a factor in several neurological processes including learning, memory, and development of the CNS [1, 2]. On the other hand abnormalities in the concentration have also been suggested to play a role in several different neurological and psychological conditions, for example depression, epilepsy and Parkinson's disease [2, 3, 4]. Ability to detect glutamate with a high spatial (< 1 mm) and temporal resolution (< 100 ms) would give more information of the normal brain activities and might help to understand the underlying mechanisms of the conditions caused by the abnormal concentrations of glutamate [5, 6].

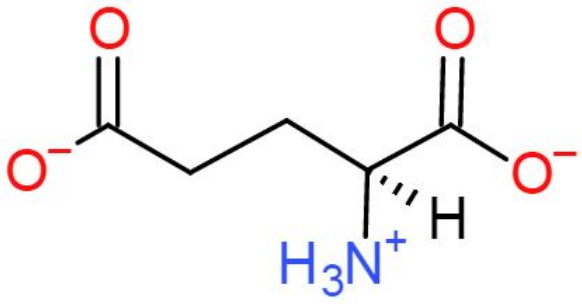

Figure 1 – Structural formula of glutamate.

Meeting the requirements for glutamate detection is challenging. Microdialysis is a traditional method but it does not provide adequate temporal or spatial resolution to detect the fast fluctuations of glutamate. Amperometric sensors on the other hand provide a better strategy for rapid glutamate detection. Glutamate is the anionic form of glutamic acid, the structural formula is shown in Figure 1. It is not electrochemically active enough, neither does it oxidase nor reduce in low enough potentials to be detected directly from the brain. Present amperometric sensors detect glutamate with the help of an enzyme. Glutamate oxidase (GlOx) is the most commonly used enzyme, but glutamate dehydrogenase is also used. As a product of the enzyme-catalyzed reaction of GlOx hydrogen peroxide (H_2O_2) is formed and it can be detected by the amperometric sensors either by oxidation or by reduction. The oxidation being the most common detection method.[5] An enzyme-free glutamate sensor has also been developed. It is based on a vertically oriented nickel nanowire array.[7] The downside of this novel enzyme-free sensor is that it only works in highly alkaline conditions and it is not therefore directly adaptable to measurements *in vivo*.

According to a study conducted by O'Neill et al. the oxidation of hydrogen peroxide is most efficient at platinum electrodes, which are also widely used in amperometric glutamate sensors. Also gold and palladium have been successfully used.[8] Even though H_2O_2 can be oxidized, requires it a relatively high potential to efficiently do

so at most electrode materials. For instance, at platinum the oxidation potential is reported to be 0.7– 0.8 V (vs. Ag/AgCl). Due to the high potential several endogenous interferents will also be oxidized and hence lower the selectivity of the electrode. This can be prevented by the use of different semipermeable protective layers deposited on the electrode.[5, 6]

This thesis is done as a part of a project which aims to manufacture an amperometric sensor for glutamate detection invasively. The aim of this thesis is to build a working glutamate sensor with a permselective polymer layer between the electrode and the enzymes. Two electrode materials are used: platinum alloyed diamond-like carbon (DLC) and gold nanoparticles deposited onto DLC surface. The electrodes' suitability for H_2O_2 detection is also compared to pure platinum and pure gold electrodes accordingly. DLC is used in the electrodes due to its antifouling properties [9, 10]. Biofouling causes major problems with pure metallic electrodes. They are still needed in the electrode due to DLCs insensitiveness towards most analytes, including H_2O_2 [11].

Prior studies of the group have led to functional platinum electrodes that can detect glutamate[12]. Gold as an electrode material has not been used before in the group. Next step in the process of glutamate sensor development would be to find a suitable protective layer for the electrode. In the theoretical part of this thesis a literature review is presented over the possible alternatives. Two of them, polyaniline and polypyrrole are deposited onto the electrodes in the experimental part of this thesis. Their suitability as permselective membranes for glutamate sensors is also evaluated. Glutamate oxidase will be immobilized on the electrodes with EDC-NHS conjugation. EDC (1-Ethyl-3-(3-dimethylaminopropyl)carbodiimide) and NHS (N-Hydroxysuccinimide) are immobilization enhancers used to activate functional groups on the surface of the electrode and the enzyme. Also immobilization with glutaraldehyde is used. Other possible enzyme immobilization techniques are also evaluated in the theoretical part of thesis.

2 Electrode materials for glutamate biosensors

The core of the biosensor is the electrode and the purpose of it is to detect the electrochemical oxidation or reduction of H_2O_2 created via the enzymatic reaction of GlOx. The principal idea behind the glutamate detection is that the rate of H_2O_2 oxidation is directly proportional to the analyte concentration. Ideally the ratio between H_2O_2 oxidation and glutamate consumed enzymatically would be 1:1 but in practice the conversation remains below 50 % depending on the immobilization method and the structure of the sensor.[6]

The material of the electrode needs to be biocompatible and stable to withstand the hostile environment of the body. The material should also be physically rigid to be suitable for implantation without being damaged in the process. To function as an amperometric biosensor the electrochemical properties have to be adequate as well. Methods for characterizing the electrochemical properties of the electrode are presented in this chapter. Afterwards the properties of platinum, gold and DLC are presented and discussed.

2.1 The basics of electrochemical measurements

Electrochemistry studies the interrelations of chemical and electrical effects. The reactions involve electron transfers from one particle to another and they are generally called redox reactions.[13, 14]

The basic set-up of an electrochemical cell consists of three electrodes: reference electrode, counter electrode, and working electrode (the sample). The reference electrode determines the zero potential of the measurement set-up. A potential is applied to the working electrode (vs. the reference electrode) and a current is measured between the working electrode and the counter electrode. Reference electrodes are stable and the potential compared to other reference electrodes is well-known. Silver/silver chloride (Ag/AgCl) is the reference electrode generally used in this thesis. The shift compared to normal hydrogen electrode (NHE) is +0.198 V and to the saturated calomel electrode (SCE) +0.043 V. NHE and SCE are also commonly used reference electrodes in the literature. The potential shifts of the electrodes are presented in Table 1.

Table 1 – Potential shifts of different reference elctrodes compared to each other.

Reference electrode	**E vs. NHE (V)**	**E vs. Ag/AgCl (V)**	**Source**
NHE	0	-0.198	[15]
Ag/AgCl (sat. KCl)	+0.198	0	[15]
SCE (sat. KCl)	+0.241	+0.043	[15]
Ag/AgCl (in 3 M KCl)	+0.194	-0.004	[15]

In this thesis two types of electrochemical measurements are utilized: cyclic voltammetry and amperometry. In cyclic voltammetry the potential of the working electrode is swept from an initial potential to the first scan limit where the direction of the sweep is switched. The sweep continues until the second scan limit where the direction of the potential sweep changes again. The applied potential as the function of time is presented in Figure 2A. The current is plotted versus the applied potential like seen in Figure 2B.

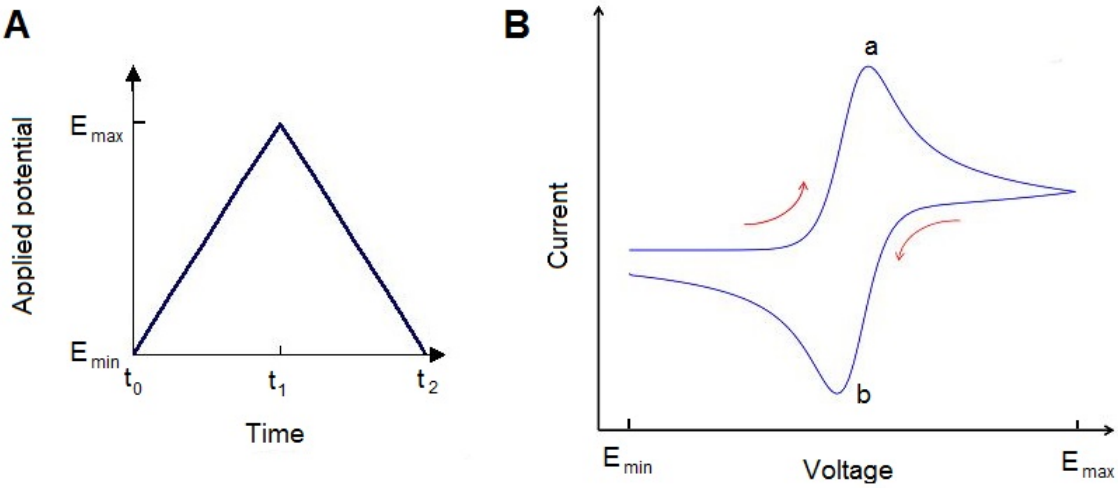

Figure 2 – (A) Applied potential vs. time in a cyclic voltammetry measurement. (B) The measured current vs. the potential in the measurement. Modified from [16].

In this example the initial potential is the lower scan limit (referred as E_{min}) and the maximum potential (E_{max}) is the first scan limit. The potential sweep can start and end in any chosen potential, it does not necessarily have to be either one of the scan limits, and the measurement may be continued as many cycles as desired. The scan limits are chosen so that the desired redox reaction will happen within the potential window. Peak (a) in Figure 2B is an anodic peak representing oxidation of an analyte at the electrode. Peak (b) is a cathodic peak and represents the corresponding reduction reaction for peak (a).

Cyclic voltammetry is a specially popular technique for the initial measurements while studying a new system. The voltammogram will give information about the redox reactions occuring at the interface between the electrode and the ambient solution. The place, shape and size of the peak is usually quite specific for a certain reaction between an analyte and an electrode, therefore voltammograms may be used in sample characterization.[14] Cyclic voltammetry may also be used as a deposition method for different layers or particles onto the electrode.

In amperometry a potential is applied at the working electrode and the current induced will be monitored. Depending of the sort of amperometry used the potential may be constant during the whole measurement (constant potential amperometry) or change once or more during the measurement (chronoamperometry). The potential

changes during the measurements are called potential steps. Figure 3A represents a single step chronoamperometry and B the data retrieved from the measurement.

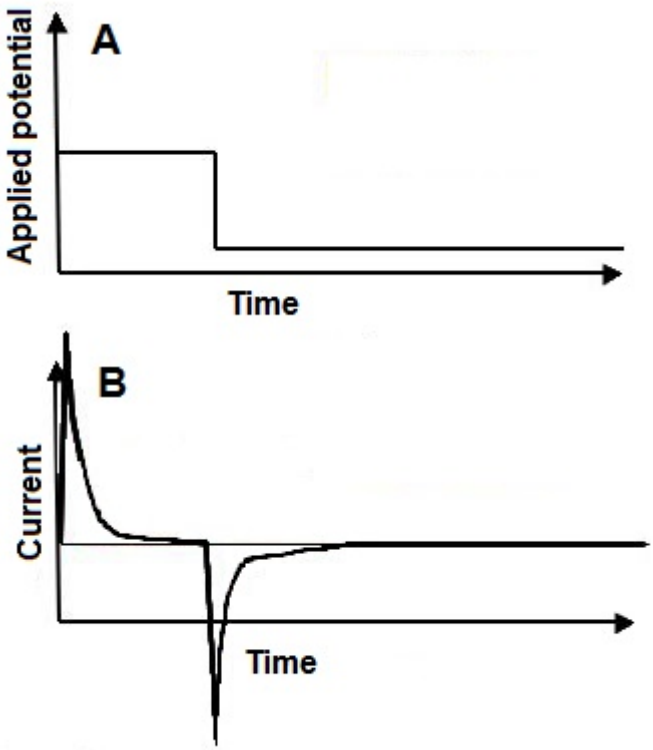

Figure 3 – (A) is the excitation waveform and (B) the response waveform of a chronoamperometric measurement. Modified from [17].

The concentration of certain analyte or the pH of ambient solution can be changed during the measurement by injecting a secondary solution at certain time points or by titration. This will give information about the current response correspondent to the changing concentration or pH. Amperometry does not provide information about the current compared to the potential changes, therefore it should only be used in situations where the identity of the oxidized or reduced analyte is known.[14] Like cyclic voltammetry amperometry may also be used in electrodeposition of layers or particles onto the electrode.

2.2 Platinum as an electrode material

Platinum has successfully been used in various medical applications due to its high biocompatibility, low corrosivity and good mechanical properties [18]. The electrical properties of the material are also excellent as will be presented later on in this chapter and hence it is widely used in amperometric sensors[8].

The characteristic voltammograms of platinum in sulfuric acid (H_2SO_4) and phosphate buffered saline (PBS) (vs. Ag/AgCl) are presented in Figure 4. Area I is the hydrogen

region. Peaks for hydrogen adsorption and desorption are clearly shown in the figure. Area II is the double layer region. Additional peaks at this region indicate the presence of impurities. Area III is the oxide growth region. Oxides form on the surface of the platinum on the anodic potential of the voltammogram until the oxygen evolution peak. The oxides are reduced when the potential decreases.[19, 20]

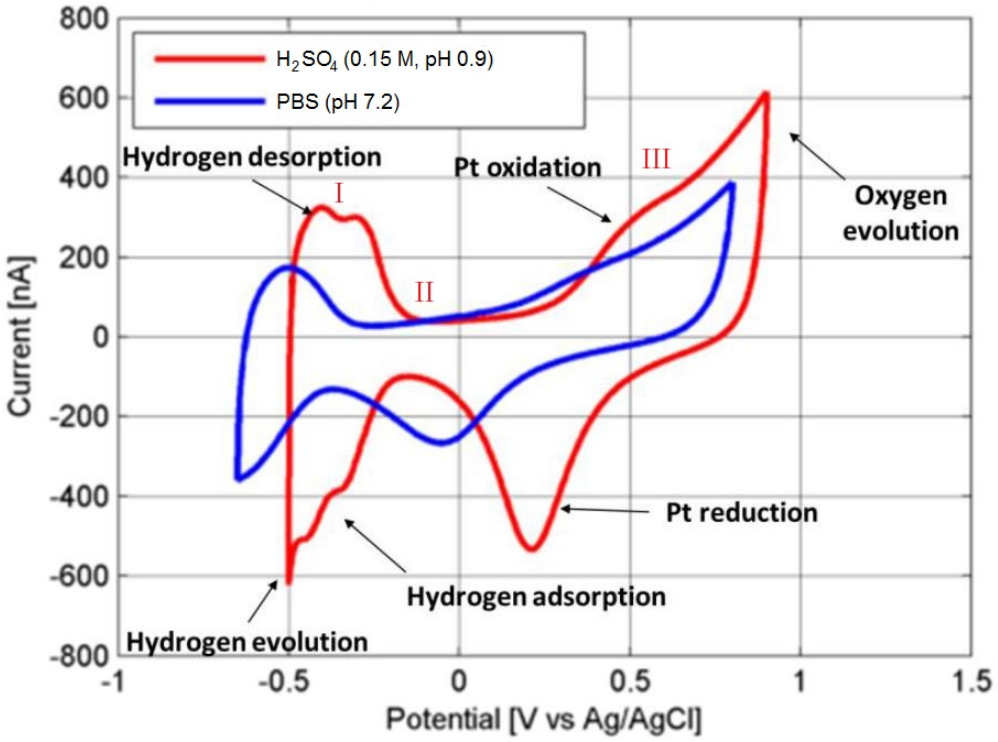

Figure 4 – Characteristic voltammogram of the platinum electrode in 0.15 M H_2SO_4 (red) and in PBS (blue) with scan rate of 400 mV/s vs. Ag/AgCl (Modified from [21]).

The peaks of hydrogen adsorption, desorption and evolution as well the oxide formation and reduction are seen in both curves. The major difference between the voltammograms is the shift of PBS curve towards the cathodic potential. This is caused by the difference in pH (7.2 for PBS and 0.9 for 0.15 M H_2SO_4). Even though H_2SO_4 reveals the characteristic hydrogen and oxygen peaks more clearly, it is also important to characterize the electrode material in solutions more relevant to the final application. PBS is commonly used due to its resemblance to the physiological saline solution.[19]

Besides the pH, the solutions differ also in their chemical composition. These differences are not yet visible while cycling in the smaller potential window like in Figure 4, but will emerge when widening the potential window to -1.0 – 1.7 V like seen in Figure 5.

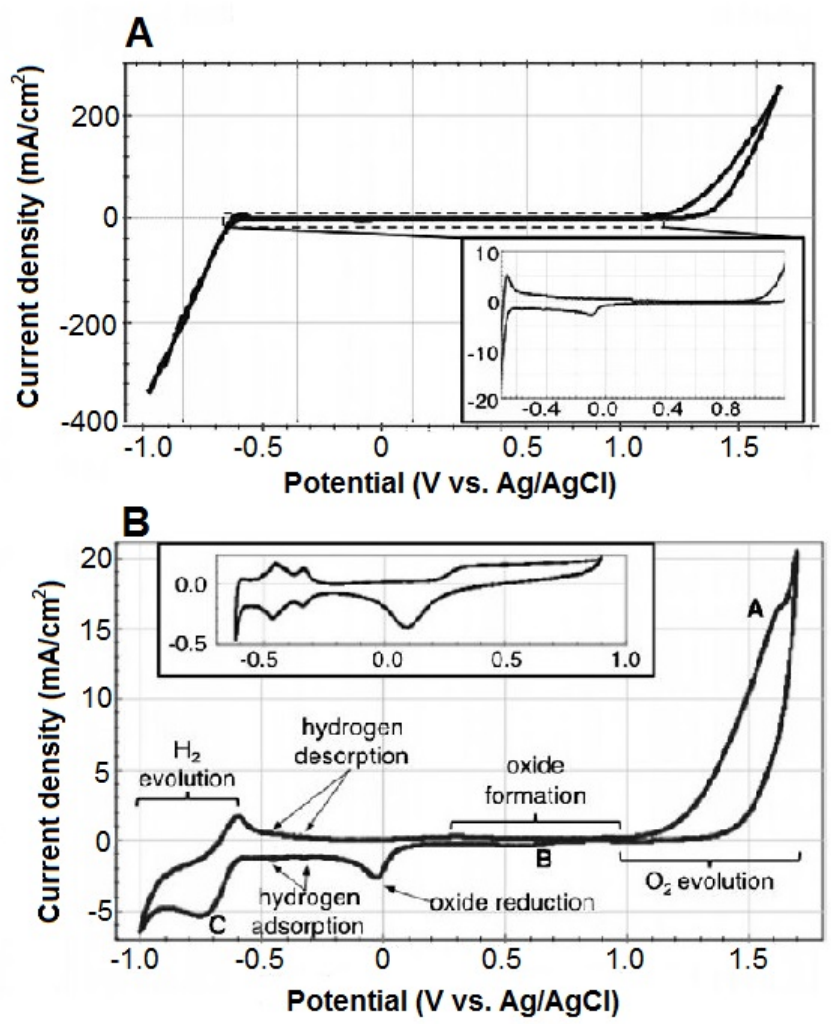

Figure 5 – Voltammograms of platinum cycled in the wide potential window in (A) 0.5 M H_2SO_4 and (B) PBS with 100 mV/s vs. Ag/AgCl. (Modified from [19]).

Three additional peaks will emerge in the PBS voltammogram, one oxidation peaks at + 1.6 V (A) and two reduction peaks at + 0.6 V (B) and -0.75 V (C). A is most likely the combination of the oxidation peaks of chloride and phosphate group, B is the reduction peak of chloride and C the reduction peak of the phosphate group.[19] Like mentioned before these peaks are not present while cycling in the smaller window which is more relevant for H_2O_2 detection.

Oxygen and oxide formation on the other hand have crucial effects in the measurements even in the smaller potential window. The formed oxide film will affect the performance of the electrode in several anodic processes. It will for example change the electronic properties of the surface, which will affect the adsorption behavior of reaction intermediates. The oxide film will also influence the reaction thermodynamics at the double layer.[22]

Measuring in O_2 -saturated solution will affect the curve like seen in Figure 6. The curve is shifted below the zero-current axis at potentials less than +0.25 V. This is most likely the reduction of the excess oxygen present in the solution.[19] The presence of oxygen and its influence on the voltammogram needs to considered while interpreting the data collected from electrochemical measurements. The concentration of oxygen is often minimized in the liquids by nitrogen bubbling prior to the measurements and performing the measurements under nitrogen atmosphere. On the other hand oxygen is needed in the enzymatic reaction with GlOx [23] and oxides are needed in H_2O_2 detection based by oxidation [24].

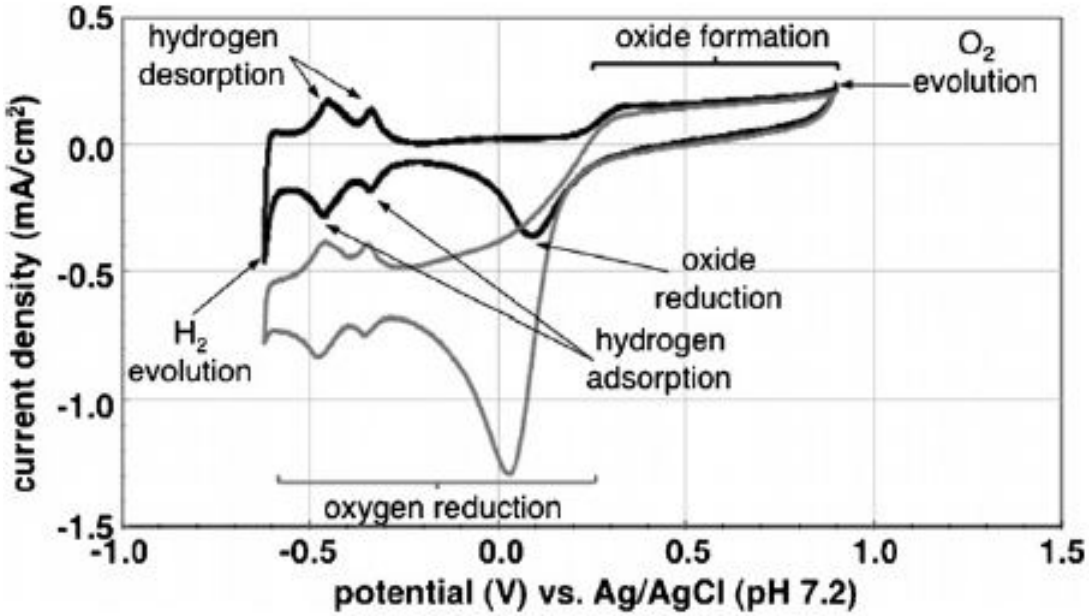

Figure 6 – The effect of oxygen saturated solution (gray line) vs. nitrogen saturated solution (black line). The measurements were done in PBS with scan rate of 100 mV/s vs. Ag/AgCl [19].

According to studies the oxidation of H_2O_2 is favorable on oxidized platinum surface[19, 24, 25, 26]. H_2O_2 will reduce the platinum oxides and the current observed is the platinum oxides reforming after H_2O_2 oxidation. This happens only at high anodic potentials (E > + 600 mV vs. Ag/AgCl) [24, 25, 26]. The reaction between platinum oxide and H_2O_2 can be seen in the equation (1) and the regeneration of the binding site is presented in equation (2) [26].

$$Pt_{BS} + H_2O_2 \rightleftharpoons Pt_{BS} \cdot H_2O_2 \rightarrow Pt + 2H^+ + O_2 \tag{1}$$

$$Pt \rightarrow Pt_{BS} + 2e^- \tag{2}$$

H_2O_2 is adsorbed to the surface onto the platinum binding site (referred as Pt_{BS} in the equations). In the oxidation reaction protons and oxygen are released as products.

The Pt_{BS} is an oxide on the surface. Free O_2 in the solution might also get adsorbed to the binding site and act as a competitive inhibitor to the H_2O_2 oxidation.[24]

2.3 Gold as an electrode material

Gold and especially gold nanoparticles are an attractive choice for electrode material due to their suitable electrical properties and biocompatibility. Enzyme modified gold electrodes are generally used for the enzymatic detection of glucose. The electrochemical detection of glucose is also based on the oxidation of H_2O_2.[27, 28, 29]

A typical voltammogram of a gold electrode in H_2SO_4 is presented in Figure 7. The oxide formation onto the electrode surface starts at peak A and the reduction of these oxides happen at peak C. Peak B is the start of oxygen evolution and peak D the start of hydrogen evolution [30, 31].

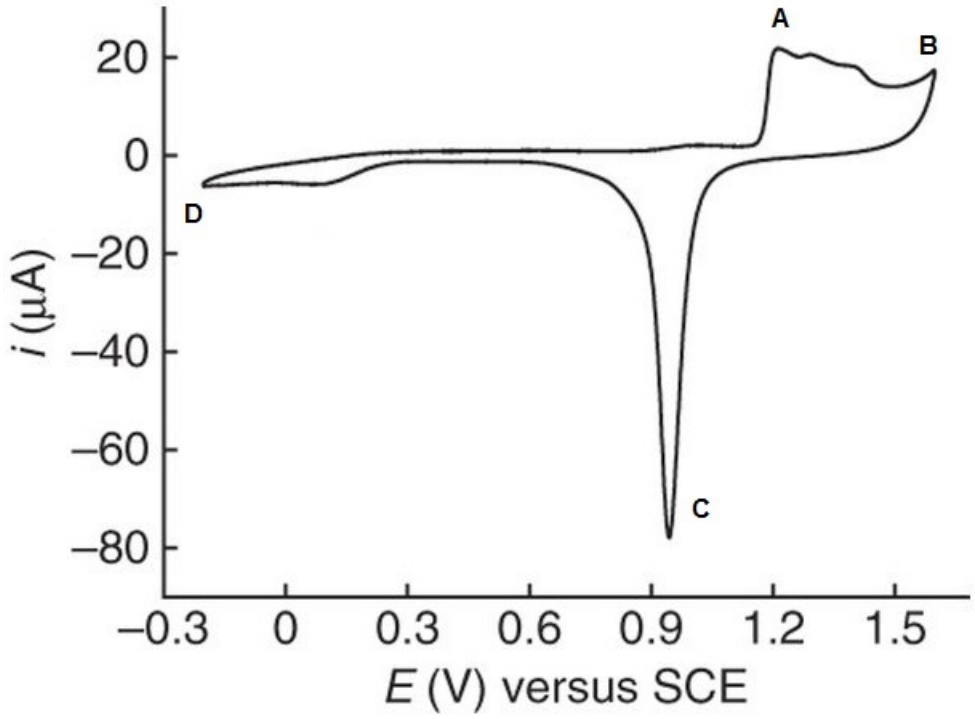

Figure 7 – Characteristic voltammogram of gold electrode in 0.5 M H_2SO_4 with scan rate of 200 mV/s vs. SCE (potential shift of +0.043 V vs. Ag/AgCl). Modified from [32]

Gold nanoparticles have shown better electrochemical properties compared to bulk gold, which is poorly active or totally inactive towards many electrochemical reactions [33, 34]. Catalytic active sites in gold are generally in crystal surface defect sites like step edges. This is the main reason why bulk planar gold is not active catalytically.[35] Gold nanoparticles on the other hand work as a catalyst for oxidation of different analytes at the surface of the electrode [35].

Another advantage for gold nanoparticles is that they are suitable for direct biomolecule immobilization [36, 37]. Direct immobilization on bare metal surfaces on the other hand will generally result in denaturation of the biomolecules. The electrochemical properties of the nanoparticles allow a direct electron transfer between the surrounding and the bulk electrode.[36]

Manufacturing of gold nanoparticles is generally done by chemical reduction of gold salt in aqueus solutions. The biggest problem in the fabrication is to control the size and morphology of the nanoparticles. Due to the high surface energy of the particles they tend to aggregate easily.[27]

Detection of H_2O_2 on gold electrodes including the bulk and electrodes modified with AuNPs will happen by the oxidation of H_2O_2. What is exceptional for the gold electrodes is that the oxidation might occur in two distinctive potentials. On a clean gold surface the oxidation of H_2O_2 gives a noticeable peak at +0.49 V (vs. Ag/AgCl) but if some impurities are adsorbed onto the surface of the electrode, the oxidation potential will be between +0.8 - +0.9 V.[31] Both potential peaks may be used for the quantitative detection of H_2O_2 though using the lower potential peak would mean that the electrodes need to be cleaned thoroughly prior to use. According to a study conducted by Fisher et al. the best cleaning method for gold electrodes would be a potential sweep between -0.2 - 1.2 V (vs. Ag/AgCl) in 50 mM potassium hydroxide (KOH) solution with the scan rate of 50 mV/s. Cycling in 50 mM H_2SO_4 solution would also give acceptable results.[38]

The high level of cleanliness required may be possible to maintain for electrodes meant for H_2O_2 detection in *in vitro* conditions but with electrodes for glutamate detection *in vivo* it would be improbable to sustain it. Therefore using gold as an electrode material in glutamate biosensors would most likely mean that the oxidation potential would be even higher than the one for platinum electrodes. Also unlike with platinum electrodes the reduction peak for H_2O_2 is not distinguishable from oxygen reduction and can not be used for H_2O_2 detection [31].

According to O'Neill et al. the oxidation of H_2O_2 is most efficient on platinum electrodes [8]. Most of the biosensors with gold or gold nanoparticles as electrode materials appeared to be for the enzymatic detection of glucose, which is also based on the oxidation of H_2O_2. Glutamate and other analytes had platinum or platinum alloys as electrode material more often than gold. No evident reason for this was found in the literature review.

2.4 Diamond-like carbon as an electrode material

Diamond-like carbon (DLC) is a metastable allotrope of carbon composed of a mixture of sp^2- and sp^3-hybridized carbons. It is disordered and isotropic with no grain boundaries. DLC possesses some excellent properties for an implantable amperometric sensor. It is mechanically robust and chemically stable. It has also been reported to be biologically inert and it is for instance widely used in cardiovascular

implants due to its excellent hemocompatibility [39]. It shares a lot of its excellent properties with diamond but it is considerably cheaper to produce. Unlike the crystalline carbon materials (e.g. diamond and graphite) DLC films can be deposited at room temperature without the need for surface pretreatment or catalysts in the process. The electrochemical properties making DLC intriguing for biosensors are the large water window and low backround current.[40, 41]

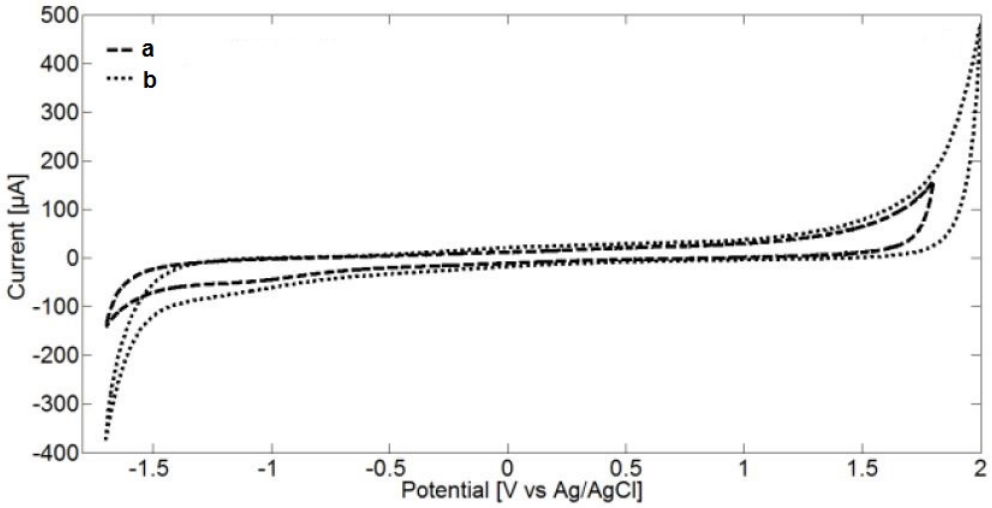

Figure 8 – Characteristic voltammograms of two different types of DLC electrodes in H_2SO_4 with the scan rate of 400 mV/s. Modified from [42]

Unfortunately DLC is electrochemically quite inactive as can be seen in the voltammogram presented in Figure 8. Detecting analytes by oxidation or reduction with a pure DLC electrode is hard if not impossible. The properties of DLC may be altered by adding other elements. For instance doping with boron or nitrogen will increase its conductivity [41]. High hydrogen concentration in DLC will for example weaken the mechanical properties and hence low hydrogen concentration is often desired.[40, 42] Metals can also be incorporated to the DLC film, though they can not be atomically distributed. Doping with metal atoms will lead to the formation of metallic carbides and metallic clusters. This will increase the electrochemical activity of DLC.[11, 41] Metal alloys enable the use of DLC electrodes in the electrochemical detection of various analytes. Doping DLC with platinum leads to nano-sized clusters forming in the film. According to Pleskov et al. platinum alloyed DLC might add active sites on the electrode surface and thus catalyst the redox reaction, though platinum does not increase the free carrier concentration in DLC.[11] Nanoparticle deposition onto the surface of the electrode has the same kind of effects to the electrochemical properties of DLC than the metallic alloys of DLC [30, 41].

2.5 Summary of electrode materials for glutamate biosensors

The purpose of an electrode in a glutamate sensor is the electrochemical detection of H_2O_2 either by oxidation or by reduction. The H_2O_2 originates from the enzyme catalyzed reaction of glutamate. The material for an electrode needs to be biocompatible and stable, it should also possess suitable electrochemical properties like a wide water window, good conductivity, and of cource the capability to detect H_2O_2.

Both platinum and gold are widely used as electrode materials in amperometric biosensors, though platinum would seem to be slightly preferable. Gold electrodes are mainly used in applications for the enzyme assisted detection of glucose while platinum is used as an electrode material for detecting various kinds of analytes including glutamate. DLC possess several desirable electrochemical properties to function as an electrode in an amperometric biosensor. Unfortunately it is insensitive towards several analytes including H_2O_2. By doping DLC with metal particles it is possible to improve the electrochemical activity of the material and enable the use of DLC electrodes in amperometric sensors.

3 Permselective polymers as protective layers

The high potential required for H_2O_2 oxidation at most electrode materials causes the nonspecific oxidation of several endogenous interferents [8]. For example dopamine (DA), ascorbic acid (AA), uric acid (UA), and some monoamine neurotransmitters like serotonin and norepinephrine are known to cause unwanted signals in the glutamate sensors *in vivo*. The interferents as well as many other biomolecules present in the brain may also cause electrode fouling. To prevent unwanted signals the electrode can be coated with a polymer layer to work as a permselective protective membrane. The basic idea of the membrane is that it would let H_2O_2 through as much as possible and block other electroactive species present in the brain.[5, 6, 43] Most common interferents are presented in Table 2.

Table 2 – Different interferents present in the brain.

Interferent	**Charge (pH 7.4)**	**Formula**	**Source**
Ascorbic acid (AA)	-	$C_6H_8O_6$	[5]
Uric acid (UA)	-	$C_5H_4N_4O_3$	[5]
Dopamine (DA)	+	$C_8H_{11}NO_2$	[5]
DOPAC (metabolite of dopamine)	-	$C_8H_8O_4$	[5]
Norepinephrine	+	$C_8H_{11}NO_3$	[44]
Serotonin	+	$C_{10}H_{12}N_2O$	[44]

The polymeric films depend on different strategies in the blocking of interferents. Most of the films control the movement through the layer by the size of their pores and let only smaller molecules (e.g. H_2O_2) through. Some polymers work as a diffusion barriers letting also the bigger molecules through but slowing them down significantly. Most of the electroactive species present in the brain are bigger than H_2O_2 as can be seen in the chemical formulas presented in Table 2. The polymers may also be charged which enables them to charge exclusion. For instance negatively charged polymer layers will repel anions (e.g. ascorbic acid and uric acid). On the other hand a negative charge might also attract positively charged molecules (e.g. dopamine) and lower the selectivity towards them.[6, 43] The electrical nature of the interferents is presented in Table 2. In physiological pH the two carboxyle groups of glutamate are deprotonated and amino group is protonated which gives glutamate a negative total charge (as can be seen in Figure 1).

Polymer synthetization by chemical or electrochemical oxidative polymerization is frequently used [45]. The main advantages of the electrochemical methods are that the thickness of the layer and the deposition density can be closely regulated by the concentration of the solution and by controlling the applied potential and electropolymerization time. A homogenous film may also be formed onto an electrode with a complex geometry.[6, 46]

The polymers can be divided into conducting and non-conducting polymers, some can be either depending on the oxidation state of the polymer. Polymer layers composed of non-conductive monomers display a self-limiting growth which leads to thin layers and shorter response times. Reproducibility is also usually higher with the non-conducting polymer layers compared to conducting polymers.[6] Even though conducting polymers tend to form thicker layers the electrical properties of the layer may compensate the thickness and lead to shorter response times. Conducting polymers can act as mediators between the enzymes active site and electrode surface during the H_2O_2 oxidation [47]. Due to the electrical nature of impulses between neurons, conducting polymers might be more suitable in the neurological environment.

Besides blocking the interferents the polymer layers block H_2O_2 or at least form a diffusion barrier hence reducing the sensitivity and lengthening the response time of the sensor[43]. This needs to be considered while choosing a suitable layer for the application.

3.1 Polyaniline as a protective layer

Aniline molecule consists of an amino group attached to a phenyl group as can be seen in the molecular formula presented in Figure 9A. Polyaniline (PANI) can be formed relatively easy either chemically or electrochemically by oxidizing aniline [6, 48]. In the polymerized form the repeating unit can either be oxidized (presented in Figure 9B) or reduced (presented in Figure 9C)[49].

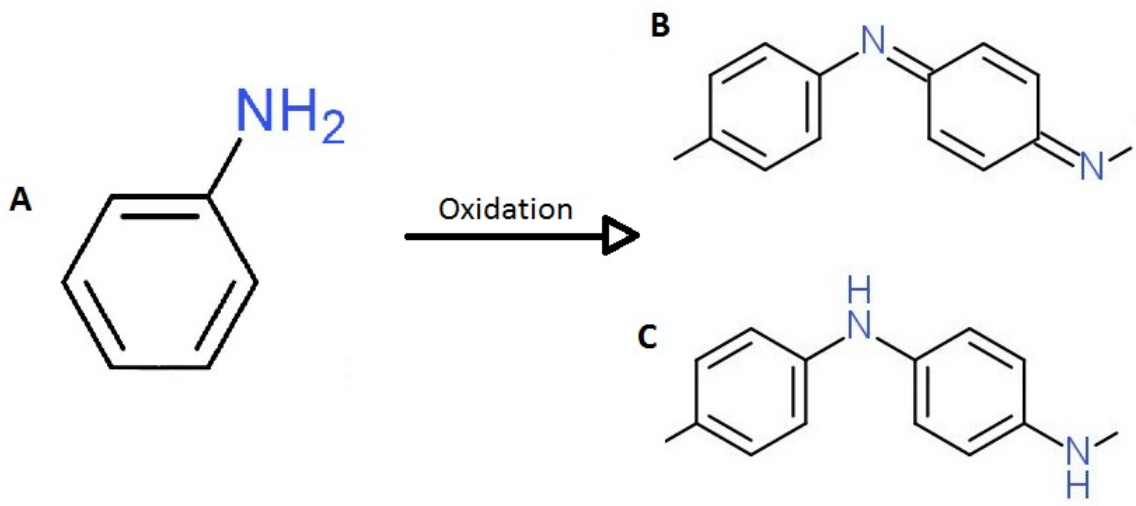

Figure 9 – Structural formulas of aniline (A) and the repeating units of polyaniline. (B) is the oxidized and (C) the reduced form.

Depending of the units the polymer is formed, it can be fully oxidized (pernigraniline), half oxidized (emeraldine), fully reduced (leucoemeraldine) or something in between

[49]. Depending on the oxidation state PANI can be either conductive (in non-oxidated form) or non-conductive (in over-oxidized form). In conductive form PANI acts also as an effective mediator for electron transfer.[6, 48, 50, 51]

PANI is an attractive alternative for the protective layer due to its environmental stability. The formed polymer should also remain stable both under air and water exposure. PANI contains fibril chains that form pores. These fibrils are also suitable for enzyme trapping.[47]

Electrochemical deposition of polyaniline can be done by amperometry or by cyclic voltammetry [47]. Voltammogram of polyaniline deposition on a platinum electrode is presented in Figure 10.

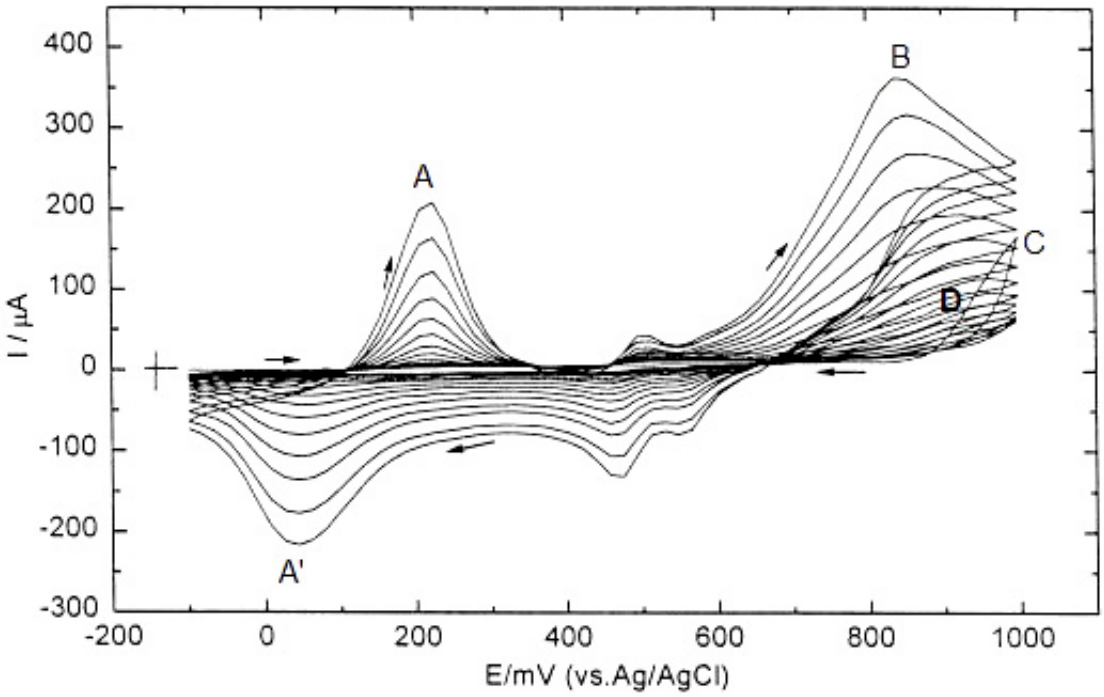

Figure 10 – Voltammogram of 15 consecutive potential cycles of PANI deposition on a platinum electrode. The electrode is cycled between -0.2 – + 1.0 V with the scan rate of 20 mV/s in a 0.5 M H_2SO_4 solution containing 0.03 M of aniline. Modified from [52]

In this representative example the polymerization is done in a 0.5 M sulfuric acid solution containing 0.03 M aniline. Peak C presents aniline oxidation on the first cycle of the polymerization. The monomer and dimer molecules saturate on the surface and after supersaturation they start to precipitate. After the first cycle the peak disappears and a smaller peak D becomes visible. Peak D shifts slowly to the left and disappears to peak B. Peak D indicates that the small oligomers formed on the surface are being oxidized. Shifting of the peak implies of the increasing chain length of the oligomers. Peak B presents the production of polymer species (i.e. membrane growth). Peak A presents anion insertion due to the p-doping of the polymer.[52]

When the film gets thick enough the degradation reaction starts to hinder the membrane growth. This becomes a problem especially at higher deposition voltages so the upper scan limit should stay under +1.0 V (vs. Ag/AgCl). Slower scan rates should be preferred, it gives aniline more time to polymerize.[52]

The sensitivity of PANI towards H_2O_2 has proven to be lower compared to the other permselective layers presented in this thesis. It has also been reported to give a substantial response to dopamine. On the other had PANI films have been reported to be fairly insensitive towards ascorbic acid.[6, 43]

3.2 Polypyrrole as a protective layer

Pyrrole is an organic heterocyclic aromatic compound with one nitrogen in the five-membered ring. It can be polymerized with oxidation to form polypyrrole (PPy). The structural formula of pyrrole and PPy is presented in Figure 11. The formed film is yellow which gets darker in air contact due to oxidation [53].

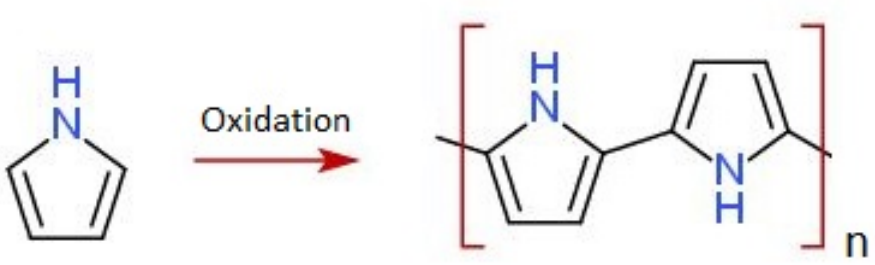

Figure 11 – Structural formulas of pyrrole and polypyrrole.

In electrochemical polymerization the PPy film is generated by the oxidation of aqueous pyrrole onto the electrode. An electrodeposition voltammogram of pyrrole can be seen in Figure 12. In this example the deposition is done in an aqueous solution containing 0.1 M $LiClO_4$ and 0.01 M pyrrole with the scan rate of 10 mV/s versus SCE reference. $LiClO_4$ works as a supporting electrolyte in the deposition process. A clear oxidation peak starts at 0.9 V (vs. SCE). It is the formation of radical cations by oxidation followed by the coupling of radicals and formation of a conductive polymer layer. The oxidation of the layer starts after the second cycle. This can be seen as an anodic peak at 0.13 V.[54] Polymerization potentials are kept low enough to avoid oxygen evolution [46].

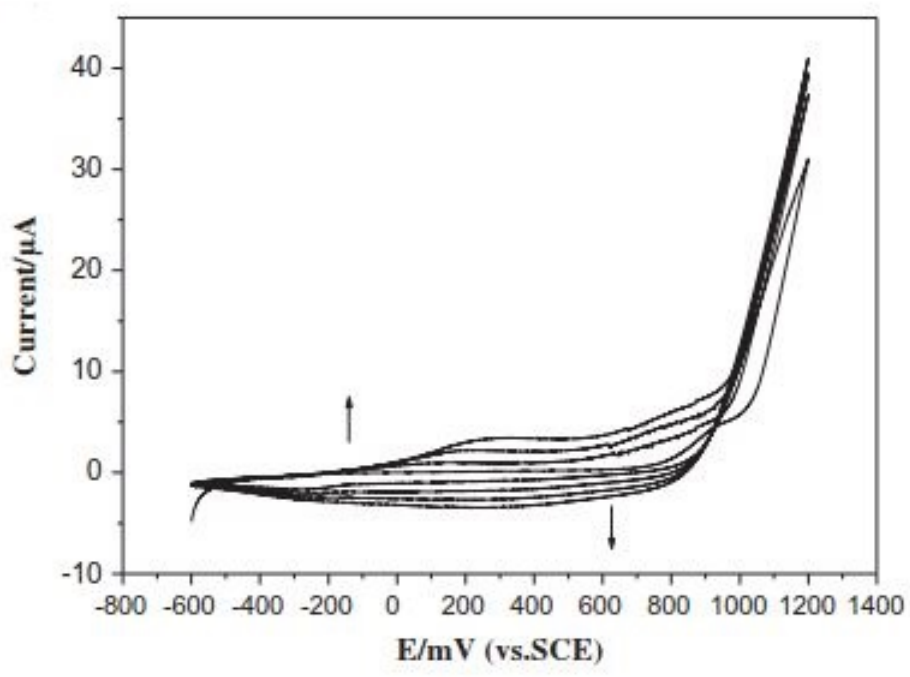

Figure 12 – Voltammogram of the electrodeposition of pyrrole. [54]

Functional PPy layers have also been deposited with amperometry. Deposition potential is set above + 0.85 (vs. Ag/AgCl) while the deposition time may differ from 15 s to 1000 s.[43, 46, 54]

Like in the case of polyaniline the electrical properties of the PPy film can be modified by over-oxidation of the polymer. The polymer film is highly electrically conducting in non-oxidized form and in over-oxidized form the polymer gets nonconductive and becomes an ion-exchange membrane. The over-oxidation can be done by chronoamperometry after the deposition of the polymer layer. The potential is kept at a constant value of +850 mV vs. Ag/AgCl in 0.1 M PBS (pH 7.4) for six hours [43]. During the over-oxidation process a carbonyl group is added into the carbon backbone of the polymer. Carbonyl groups hinder the anions in the solution due to the high electron density of the functional group.[5, 6, 46, 53]

The selectivity of the PPy membrane is greatly influenced by the film thickness, which can be controlled by the deposition time. The thickness also affects the sensitivity towards H_2O_2.[46] Ammam et al. did a study where the sensitivity towards H_2O_2 and the ability to block different interferents was determined. The dependence of the sensitivity towards H_2O_2 and AA to the layer deposition time is presented in Table 3.

Table 3 – Sensitivity to hydrogen peroxide and ascorbic acid with polypyrrole (PPy) covered platinum electrode [46]

PPy deposition time (s)	**Response to 250 uM H_2O_2 (nA)**	**Response to 250 uM AA (nA)**
0	1878.3	1050.3
200	388.1	35.2
400	274.6	13.7
1000	241.1	0
1500	184.2	0

According to the test results a deposition time of 1000 s resulted in a layer thick enough to block all of the AA, but still thin enough to let H_2O_2 through. Though with GlOx immobilized onto the electrode the 1000 s layer was not sufficient to block all of the AA, instead a layer of 1500 s was needed. Ammam et al. used electrodeposition as immobilization technique to GlOx.[46] This technique might result to PPy layer diffusion during the immobilization process, with a different immobilization technique a 1000 s layer of PPy might be sufficient.

3.3 Nafion as a protective layer

Nafion is widely used in amperometric biosensors as a protective layer. It has a sulfonated tetrafuorethylen (i.e. Teflon) backbone as can be seen in the structural formula presented in Figure 13. The teflon backbone structure gives Nafion excellent mechanical and thermal stability and the sulfonic acid group makes the membrane negatively charged. The polymer repels interfering species by its negative charge but also by its complex porous structure. The pores formed in the membrane are hydrophilic [55]. It has been reported to give an excellent barrier especially towards ascorbate acid. Due to the negative charge of the membrane Nafion is poorly selective against positively charged species like dopamine. Nafion is a nonconductive polymer.[5] According to several studies Nafion has improved the biocompatibility of the sensor during *in vivo* -applications[6, 55].

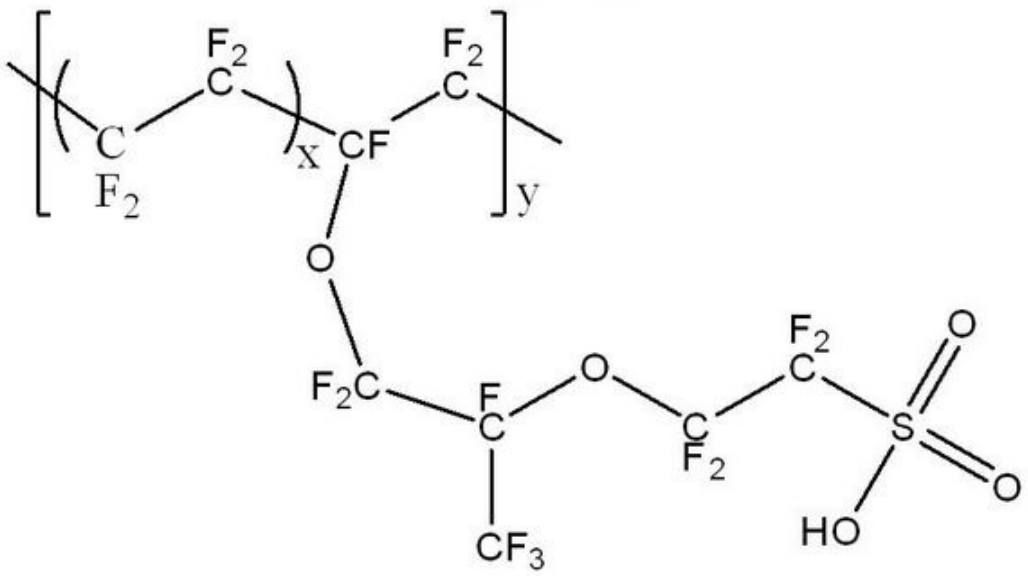

Figure 13 – The structural formula of Nafion. [55]

Nafion can be deposited onto the electrode by dipping the electrode to the Nafion solution. Different dipping times and concentrations of Nafion will affect the thickness and the structure of the polymer and hence the stability and permeability of the protective layer. After the polymer has dried it is usually annealed at high temperatures (e.g. 175°C) for few minutes. Annealing gives Nafion a more crystal-like structure which reduces the permeability of the membrane.[5, 6]

Nafion was the first polymer layer to be used in amperometric biosensors as a protective layer and it is still widely used in several applications [5, 6, 43]. One reason for its popularity is most likely the easy deposition method compared to other polymer layers, even though Nafion has not showed as good selectivity towards the electroactive species as many other polymers have e.g. PPy or PPD [6, 43].

3.4 Phenylenediamine as a protective layer

Phenylenediamine (PPD) has two amine groups attached to its phenyl group as presented in Figure 14. PPD can be deposited onto the electrode electrochemically either by chronoamperometry or by cyclic voltammetry. Also UV irradiation has been tried [56]. The polymerized structure of PPD is presented in Figure 14.

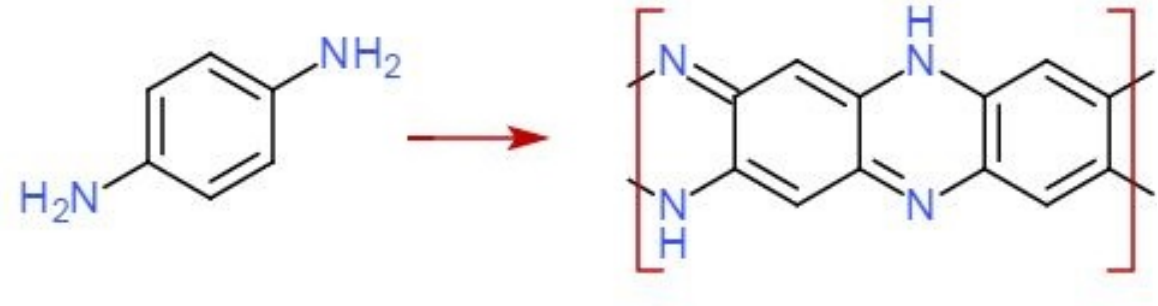

Figure 14 – Structural formulas of PPD monomer and polymer.

According to some studies cyclic voltammetry would result in more compact and orderly packed polymer and hence more selective membranes[6, 57]. A typical voltammogram of PPD deposition onto a platinum electrode in phosphate buffer solution is presented in Figure 15.

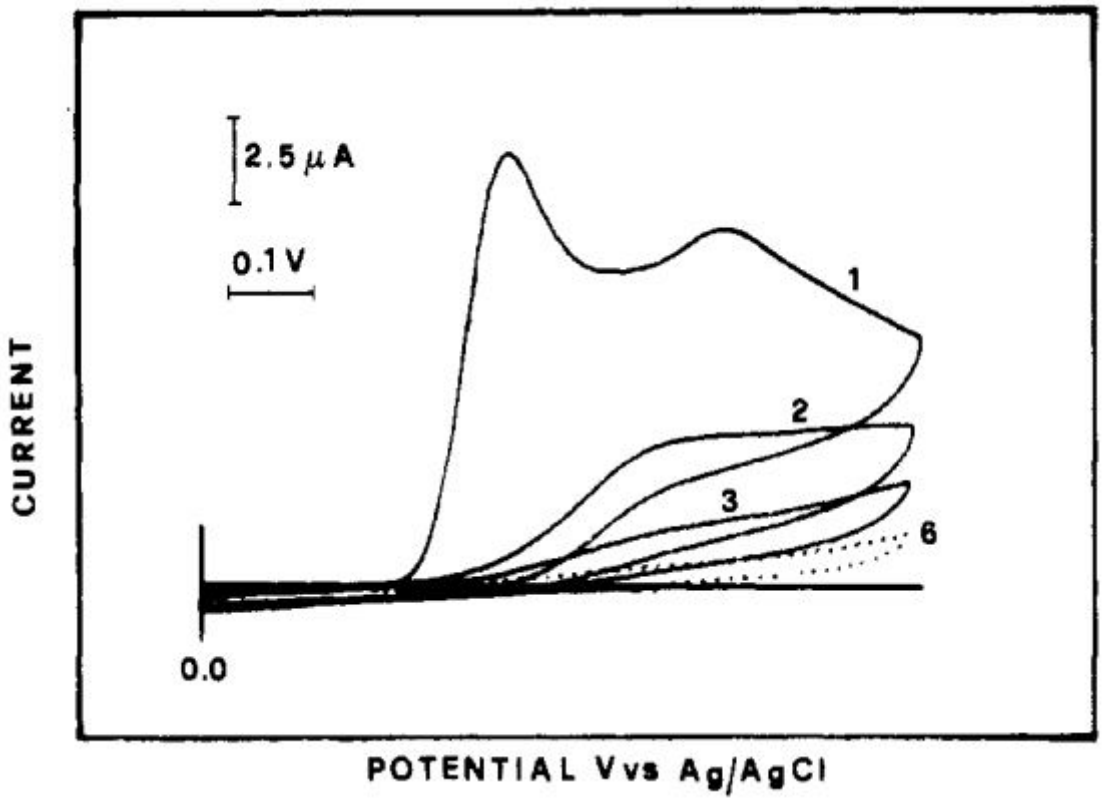

Figure 15 – Voltammogram of PPD deposition in phosphate buffer (pH 7.0) solution at platinum electrode. The concentration of PPD is 5 mM. Scan rate is 50 mV/s. Curve 1 refers to the first cycle, curve 2 to the second and so on. [57]

Clear oxidation peak is shown only in the first cycle, after that the current drops during each cycle until no current is detected. The current seen is caused by the

oxidation of monomers onto the electrode. The oxidation results in radical cation formation which then reacts either with another radical cation or with a neutral monomer forming a dimer and finally after more oxidation steps a tight polymer layer is formed onto the electrode. The reason for that no current is eventually detected is that the polymer layer becomes compact enough to block the access of new monomers to the electrode surface.[57]

PPD membranes have shown high selectivity, especially against dopamine. According to a study conducted by Wahono et al. PPD was superior to all other protective polymer layers tested *in vitro* for the selectivity towards AA, DA, DOPAC and UA.[6]

3.5 Summary of permselective polymers as protective layers

A general way of blocking electrochemically active interferents and preventing electrode fouling is the deposition of permselective polymer layers onto the electrode. They usually limit the access to the surface of the electrode by their porous structure letting only smaller particles through. Some of them have a charge on top of the complex structure which enables charge exclusion. Four different polymers were presented in this chapter: PANI, PPy, Nafion and PPD. Their qualities concerning their suitability for glutamate sensors are summarized in Table 4.

Table 4 – Summary of the properties of different polymer layers used in amperometric sensors for glutamate.

Polymer	**Working mechanism**	**Advantages**	**Disadvanteges**	**Source**
Polyaniline (PANI)	Size of the pores	Conductivity can be controlled by oxidation. Environmentally stable.	Blocks H_2O_2 significantly. Not selective enough towards dopamine	[6, 43]
Polypyrrole (PPy)	Size of the pores, charge exclusion (repels anions)	Conductivity can be controlled by oxidation.		[5, 6]
Nafion	Size of the pores, charge exclusion (repels anions)	Improves biocompatibility during *in vivo* implantation. Deposition easy.	Not selective enough towards dopamine	[5, 6]
Phenylenediamine (PPD)	Size of pores. In some cases also charge exclusion (repels anions)	Highly selective.		[6]

Most of the polymer layers can be deposited by chemical or electrochemical oxidative deposition, only Nafion is deposited by dipping the electrode into Nafion solution. In the oxidative electrochemical deposition process the electrode is cycled in a solution with a desired concentration of the monomer. At high anodic potentials the monomers will be oxidized forming radical cations which will then react with another radical cation or a monomer and thus form a dimer. The oxidative process will continue and the polymer is eventually formed onto the electrode.

According to the literature review PPD and PPy would seem to be the most attractive options as permselective layers for glutamate sensors. They have shown the best selectivity against interferents with the best sensitivity towards H_2O_2. The possibility to control the conductivity of PPy could also prove out to be a useful feature to a biosensor working in the brain. The fact that Nafion has showed to increase biocompatibility of the sensor in *in vivo* applications is an advantage that should not be forgotten while choosing the best option for the protective layer.

4 Enzyme immobilization

Due to the electrochemically inactive nature of glutamate and its high oxidation potential the detection is generally done by utilizing an enzyme, usually glutamate oxidase (GlOx). The enzymatic reaction of GlOx is presented in formula (3).

$$L\text{-}glutamate + O_2 + H_2O \rightleftharpoons 2\text{-}oxoglutarate + NH_3 + H_2O_2. \quad (3)$$

Glutamate, oxygen and water is consumed in the enzymatic reaction which produces H_2O_2 with ammonium and 2-oxoglutarate. The H_2O_2 is oxidized at the electrode and O_2 is produced. In some cases the reduction of oxygen can be seen at low potentials of the voltammogram (e.g. at -650 mV vs. Ag/AgCl).[5]

GlOx is composed of two protomers, each containing three fragments (α, β and γ) and a bound FAD (*flavin adenine dinucleotide*, a redox cofactor). The structure is presented in Figure 16. The protomers are in a head-to-tail orientation compared to each others, the substrate-binding site facing outwards (Fig 16A). The enzyme has two entrances leading to the active-site buried deep within the enzyme (Fig 16B). The size of the enzyme is 12.4 x 12.4 x 16.9 nm. [58]

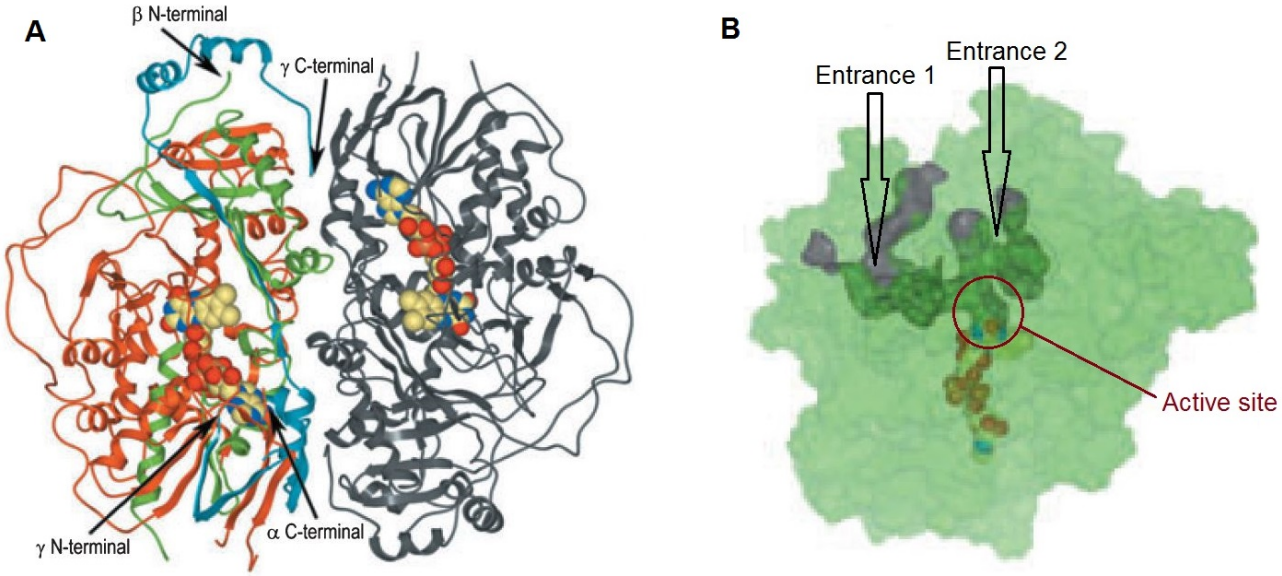

Figure 16 – The overall structures of GlOx. (A) The two protomers from an oligomeric dimer (the structures of the left dimer is color coded and the right dimer is gray). Each protomer is composed of three fragments α (orange), β (green) and γ (blue) and FAD, which can be seen in both fragments. The chains of each fragments are entangled with other chains. (B) shows the place of the funnels leading to the active site of the enzyme. Modified from [58].

Even though there are several ways of applying the enzyme layer onto the electrode surface (e.g. drop coating, dip coating or spray coating) achieving a stable and lasting enzyme layer is quite difficult. Greatest problem concerning the immobilization of the enzyme is that too hard techniques will lead to structural changes and denaturation of the enzyme. On the other hand too weakly immobilized enzymes will end up leaking to the surrounding from the enzyme layer.[5, 48] Several methods have been tried with glutamate oxidase, for example cross-linking or covalently linking GlOx to the surface of the electrode, or by entrapping the enzyme. These methods are presented in more detail in the following chapters.

4.1 Cross-linking as an immobilization method

Cross-linking is a method were the enzymes are linked to each other and to the surface with bifunctional agents. There may also be a functionally inert protein to stabilize the structure. Glutaraldehyde is the most often used cross-linker, other options include for example hexamethylenediamine and glyoxal. Bovine serum albumine (BSA) is the most commonly used enzyme stabilizer in immobilization done by cross-linking. The method is widely used due to its simplicity. Cross-linking results also to strong chemical bonds so leaking should not be a problem. The drawback of this strong bond is the possible conformations and chemical alterations of the active site of the enzyme, which might lead up to enzyme denaturation.[5, 48, 59] Glutaraldehyde has two aldehyde groups in the end of the backbone of five carbons. The molecular structure can be seen in Figure 17.

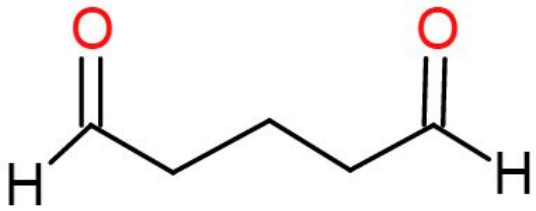

Figure 17 – Structural formula of glutaraldehyde.

The aldehyde groups react with amino groups linking the enzymes and the stabilizing proteins either to each other or to the surface. Glutaraldehyde can also polymerize with itself.[5, 59] Polymerization is not desired because the size and structure of the polymer is unknown and hence the reproducibility of the reaction is often low. The amount of polymerized glutaraldehyde in the solution is proportional to the age of the solution, therefore aged solutions will not yield same results as fresh solutions.[59]

4.2 Covalent immobilization techniques

Covalent immobilization is a method frequently used in the manufacturing of glutamate biosensors [5]. In this method covalent bonds are formed between the functional groups of the enzyme and the functional groups of the surface. GlOx has several amino and carboxyl groups on its surface of which the immobilization can occur, the surface of the electrode on the other hand needs often to be functionalized. This can be done by several different methods. Especially self-assembled monolayer (SAM) coatings are used due to their reproductibility and stability [48]. Photochemical functionalization is also a suitable method for functionalizing different types of surfaces. In the technique the surface is covered with suitable alkenes and irradiated by UV-light. The alkene bond will break and form bonds with the hydrogen terminated surface.[60, 61] Also polymers used in the protective layer might have free functional groups on the surface [48].

The reaction between the functional groups might happen spontaneously or it can be enhanced with the help of different reagents. For instance a carbodiimide called 1-Ethyl-3-(3-dimethylaminopropyl)carbodiimide (EDC) is frequently used. EDC is a zero-length cross-linker i.e. there will be no additional molecules or atoms in the bond formed. It can be used to conjugate an amino group from the enzyme to a carboxylic group from the surface or vice versa. The reaction between the functional groups is presented in Figure 18.

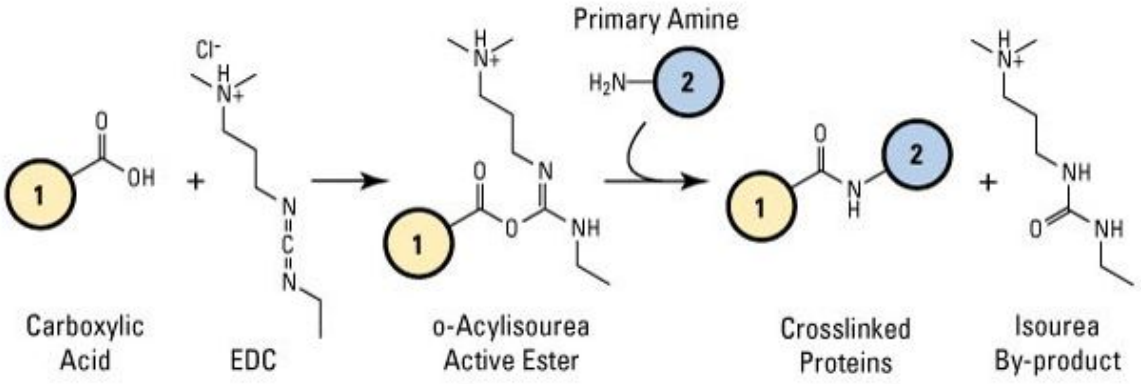

Figure 18 – The formation of a covalent bond between the electrode surface (1) and the enzyme (2) enhaced with EDC. [62]

EDC reacts with a carboxyl group forming a reactive and short-lived compound called o-acylisourea, which will then react with a nucleophile. When the nucleophile is a primary amine an amide bond will be formed.[59] Besides reacting with a primary amine the o-acylisourea might get hydrolyzed in the presence of water. This will result in the reformation of the carboxylic group preventing the formation of an amide bond. To prevent this from happening the EDC-conjugation can be intensified by sulfo-N-hydroxysuccinimide (sulfo-NHS). Sulfo-NHS is an organic molecule which reacts with o-acylisourea forming a hydrofilic, amine-reactive sulfo-NHS ester. This

will react with an amine resulting in a covalent bond with the molecules.[59] The possible reaction paths of the bioconjugation with EDC and NHS are presented in Figure 19.

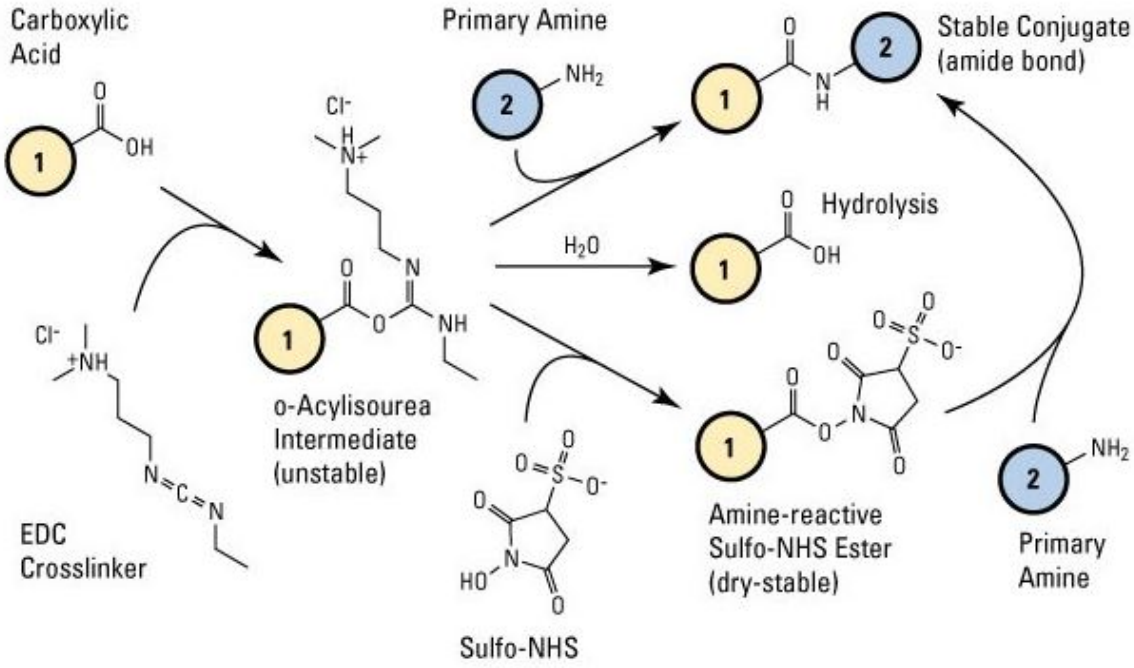

Figure 19 – The three possible reaction paths of the compound formed by a carboxylic group and EDC. First is the reaction presented in Figure 18 resulting in the formation of an amide bond. Second possibility is the hydrolization of o-acylisourea resulting in the reformation of the carboxylic group. Third reaction pathway presents the reaction between the unstable o-acylisourea and sulfo-NHS. This results in the formation of a sulfo-NHS ester that will react with an amine producing the amide bond.[62]

If the enzyme has both carboxylic and amine functional groups the conjugation with EDC and NHS might lead to self-polymerization of the enzyme. This can be prevented by activating the surface before the enzyme is brought onto it.[59]

Glutaraldehyde can also be used as an activator for amine groups in the surface and in the enzyme. First a Schiff-base reaction will occur between one of the aldehyde groups of glutaraldehyde and an amine group of the surface attaching the glutaraldehyde to the surface. Afterwards the free aldehyde group will react with an amine group of an enzyme.[48, 59] Unlike EDC and NHS glutaraldehyde is not a zero-length linker, instead the molecule will remain as a part of the formed bond.[59] This will increase the distance between the enzyme and the electrode by the length of the molecule and at least in theory it will lengthen the response time of the sensor. Because glutaraldehyde is so commonly used and the lenght of the molecule is relatively short compared to the size of the enzyme this should not be a major problem. But this aspect should also be considered while choosing the best alternative for GlOx immobilization.

Covalent immobilization binds the enzymes tightly to the surface resulting to a stable enzyme layer. The bonds will not break easily but there are some downsides to this method as well. Even though the enzymes are immobilized through functional groups that are not essential to their catalytic activity, some chemical alterations may happen in the active site of the enzyme as well. This decreases the catalytic activity of the enzyme layer.[48, 59]

4.3 Entrapment of enzymes

Entrapment is considered to be a gentle technique for enzyme immobilization. The enzyme can be trapped in several different types of three dimensional matrices. For instance polymer films, hydrogels or carbon pastes have been used [48]. The enzyme can be immobilized during the electropolymerization process of the protective layer. For instance PANI and PPy have been used to form functional biosensors with different enzymes such as glucose oxidase (GOD) immobilized into the polymer. The method is easy but requires relatively high concentrations of the monomer (0.05-0.5 M) and the enzyme (0.2-3.5 mg/ml).[5, 48, 63] Due to the expensiveness of GlOx electropolymerization is not used with glutamate biosensors.

Carbon pastes are also tempting matrices for enzyme entrapment in amperometric biosensors due to the good electrical properties of the paste. The paste is a mixture of graphite powder and a binder liquid. Stable and versatile matrices have been made with carbon paste. A relatively new method forming a porous matrix for the enzymes is the sol-gel process. It is based on the hydrolysis of labile precursors (e.g. polysilicic acid or esters of silicic) under acidic conditions followed by condensation of the hydroxylated units. This leads to a porous gel of solid metal or semi-metal oxides. The structure is both chemically and thermally stable, but may undergo deformation during drying.[48]

The general drawbacks of entrapment matrices are the possibility of enzyme leakage from the layer and the inevitable formation of a diffusion barrier by the matrix. This lengthens the response time.[5, 48, 63]. Due to the quick variations in glutamate concentrations in the brain an extra diffusion barrier will not be desirable for glutamate sensors.

4.4 Adsorption as an immobilization technique

Adsorption is a simple and easy technique for enzyme immobilization. The electrode is immersed to an enzyme solution where the enzymes will attach to the surface by weak bonds (e.g. Van der Waal's, electrostatic, hydrophobic interactions or a combination of the previous). After incubation the unadsorbed enzymes will be washed carefully away and the immobilization is ready. The process may also be aided electrochemically. In a solution where the pH is higher than the isoelectric point of the enzyme the enzymes will be negatively charged and get adsorbed to a

positively charged surface. The advantage of the process is that no functionalization or modification of the surface or the enzyme is needed. The process will not alter the structure of the enzyme so the activity of the enzyme is retained. Unfortunately the bonds formed are not that strong and the enzymes will desorb easily. This leads to a poor storage and operational stability.[48]

Adsorption can also be combined with entrapment to improve both methods. The enzymes can be pre-immobilized by adsorption to small positively charged beads which will then be entrapped in a porous matrix. The beads will not leak from the matrix as easily and the matrix will protect the adsorbed enzymes.[48]

4.5 Summary of immobilization techniques

Most of the amperometric glutamate sensors today are utilizing enzymes for detecting glutamate, glutamate oxidase (GlOx) being the enzyme most frequently used. Glutamate, oxygen and water are consumed in the enzymatic reaction by GlOx producing H_2O_2 with ammonium and 2-oxoglutarate. H_2O_2 is later on detected at the electrode.

Enzyme immobilization is the part which affects the stability of the sensors most. There are several methods to do it and four of them were presented in this thesis: cross-linking, covalent immobilization, entrapment and adsorption. Cross-linking is a method where the enzymes are linked to each other and to the surface with a linker molecule (for instance glutaraldehyde). In covalent immobilization technique the surface of the electrode is functionalized with suitable groups, which form covalent bonds with the funtional groups on the surface of the enzyme. The immobilization can be enhanced with different reagents for instance EDC with or without NHS. Both of the immobilization methods result in strong bonds making the enzyme layer stable which is a desirable feature in implantable sensors. Drawbacks include the possible denaturation of the enzymes.

In entrapment the enzymes are traped in a complex 3D matrix (e.g. polymer or carbon paste may be used). In adsorption the enzymes are merely adsorbed on the surface. Both methods are gentle towards the enzymes but the immobilization is not as stable as with cross-linking or covalent immobilization. Therefore the greatest problem with them is the possible leaking of the enzymes to the surroundings.

Both cross-linking and covalent immobilization have lead to functional sensors despite the possible inactivation of the enzymes. Comparing possible denaturation and possible leakage of the enzymes to the surroundings, denaturation would seem a better alternative for an implantable sensor. The features of the immobilization techniques are summarized in Table 5.

Table 5 – Summary of different enzyme immobilization methods.

Method	**Advantages**	**Disadvantages**	**Source**
Cross-linking	Simple and easy method. Strong bonds.	Possible activity loss of the enzymes due to denaturation.	[48, 64]
Covalent immobilization	No diffusion layer. Strong bonds.	Possible activity loss of the enzymes due to denaturation.	[48, 65]
Entrapment	No deformations to the enzyme. Different enzymes may be immobilized simultaneously.	Enzyme leakage from the layer. Requires a greater concentration of the enzyme. Formation of a diffusion layer.	[48, 64, 65]
Adsorption	Extremely easy and simple method. No deformations to the enzyme.	Desorption of the enzymes.	[48, 65]

5 Material and methods

The experimental part of this thesis is presented in this chapter. Three types of electrodes were used in the measurements: platinum alloyed DLC (CPt), platinum, and gold nanoparticle deposited onto DLC (AuNP). Also gold electrodes were manufactured but the adhesion between the gold layer and the substrate was not appropriate and the layer was delaminated during the measurements. After the electrochemical characterization in H_2SO_4 and PBS the sensitivity for H_2O_2 was determined by cyclic voltammetry. Two types of protective layers were tested on the electrodes: polyaniline (PANI) and polypyrrole (PPy). The results of polymer covered samples were compared to electrodes with a self-assembled monolayer (SAM) deposited onto them. The sample types which had the highest sensitivity towards H_2O_2 had GlOx immobilized onto them and were later used in measurements for glutamate detection. The work flow for the sample types is presented in Figure 20.

Some preparations needed to be done before the sample manufacturing and measurements. Self-made phosphate buffered saline (PBS) was used in all of the electrochemical measurements. It was prepared 10 liters at time by dissolving 80.0 g of sodium chloride (NaCl, VWR, Leuven, Belgium), 2.0 g of potassium chloride (KCl, J.T. Baker Deventer, Holland), 14.4 g di-Sodium hydrogen phosphate anhydrous (Na_2HPO_4, Merck, Darmstadt, Germany), and 2.4 g potassium dihydrogen phosphate (KH_2PO_4, Merck) to 1 liter of DI-water. The pH of the 1 M PBS was adjusted with 1 M HCl or NaOH -solution to 6.8 before diluting the volume to 10 liters. The final concentrations of the salts were 0.14 M of NaCl, 0.0027 M of KCl, 0.01 M of Na_2HPO_4 and 0.002 M of KH_2PO_4. Final pH of the solution was 7.4.

Salt bridges were prepared for the gold nanoparticle and polymer layer depositions. A saturated solution of ammonium nitrate (NH_4NO_3, Merck) was prepared in DI-water. Agar powder (Oriola, Espoo, Finland) was dissolved to the freshly prepared saline solution and heated up to 60°C until all of the agar was dissolved. The concentration of Agar was 1.5 - 3% depending of the badge. The solution was sucked into a thin tube. After the agar solution had solidified the tube was cut into about 10 cm long pieces. The salt bridges were stored in 3M KCl-solution at 4°C when not used.

Before electrochemical deposition or measurements the sample chips were contacted by scratching the back of the sample by a diamond pen and by a piece of copper. The chip was then taped on a FR4 copper circuit board with PTFE-tape (Irpola, Salo, Finland). A hole was made to the tape before contacting. Depending on the sample size the hole was either 3.5 mm (for 5x5 mm samples) or 6 mm (for 10x10 mm samples). The hole diameters correspond to surface areas of 0.2827 cm^2 and 0.0962 cm^2 accordingly.

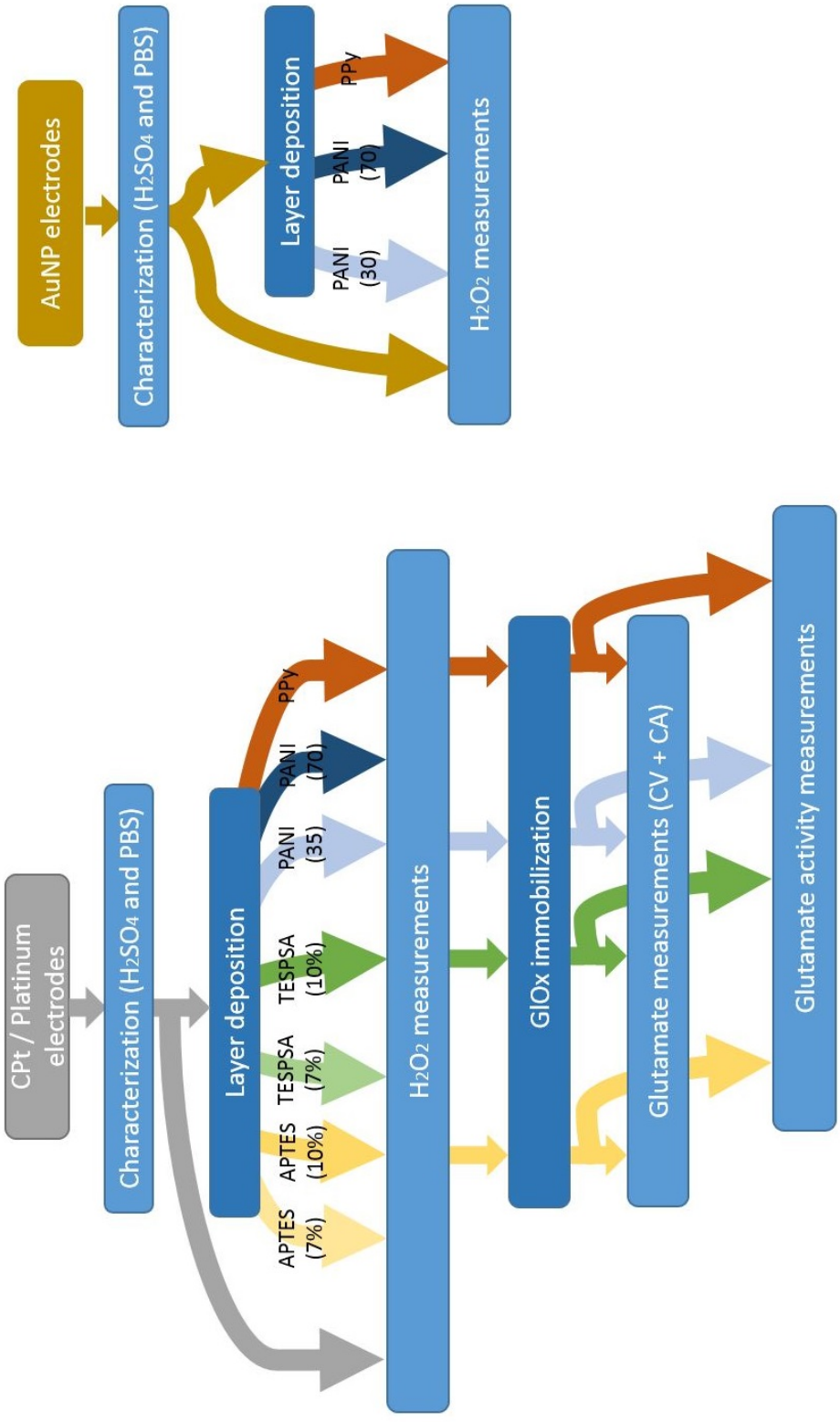

Figure 20 – Work flow for the samples used in this thesis.

5.1 Electrode manufacturing

5.1.1 Manufacturing of CPt and platinum electrodes and substrates for AuNP electrodes

The platinum based electrodes were obtained from the department of Material Science and Engineering, Aalto University. Substrate for the samples was RCA cleaned highly conducting (0.001-0.002 Ωcm) p-type (100) Si wafers (Ultrasil, USA). On top of that a 20 nm thick titanium layer was deposited as an adhesion layer. The deposition was done by direct current magnetron sputtering (DC-MS) with following parameters: discharge power was fixed at 100 W, total pressure was 0.67 Pa, temperature during deposition was close to room temperature, and deposition time was 350 seconds. The procedure was conducted under Argon gas flow with the flow rate of 28 sccm. The magnetron sputtering source was circular and water-cooled and had a 2 inch titanium target.

For CPt samples a 7 nm thick layer of platinum doped DLC was deposited on the adhesion layer with a method in which the concentration of platinum gradually increases layer by layer. The deposition was done with individual carbon and platinum cathodes, the triggering of these cathodes was controlled with a computer. To achieve a platinum doped ta-C film with increasing Pt content with increasing thickness, second order polynomial functions of $1\text{-}0.5x^2$ for carbon and $1+0.5x^2$ for Pt were used. The x denotes number of cycles and was stepped from values 1 to 10 resulting in a total number of 360 pulses of carbon and 155 pulses of platinum.

For pure platinum and pure DLC layers a separate platinum and graphite cathodes were utilized. The layers deposited were 8 nm thick on the adhesion layer. Platinum alloyed DLC, pure platinum and pure DLC layers were done by dual filtered cathodic vacuum arc (FCVA) deposition (Lawrence Berkley National Laboratory, USA). The arc current pulses had an aplitude of 0.7 kA and a pulse width of 0.6 ms with the triggering frequency of 1 Hz. The 2.6 mF capacitor bank was charged to 400 V. The total number of pulses was 1440 for platinum and 360 for combined cathodes and carbon. The pressure during the deposition process was above 0.13 mPa. The samples were placed in a rotating holder with the rotational velocity of 20 rpm. For reduction of macroparticle contamination the system was equipped with a 60° bent magnetic filter with the distance of 20 cm from the sample holder. Both of the deposition systems were installed in one chamber.

After the layer deposition wafers were cut into rectangular 5 x 5 mm or 10 x 10 mm chips with an automated dicing saw and stored dry at room temperature.

5.1.2 Gold nanoparticle deposition

The electrodeposition of gold nanoparticles on DLC samples were done either with QuadStat potentiostat (eDAQ Pty Ltd, Denistone East, Australia) and Echem software (ADInstruments Pty ltd, Castle Hill, Australia) or with Gamry Reference

600 potentiostat and Gamry Framework software (Gamry Instruments, Warminster, PA, USA) by using cyclic voltammetry. The deposition was done in a two-cell setup presented in Figure 21. The two-cell system protected the reference electrode from gold nanoparticle contamination. The volume of the cells were about 10 ml, small cells reduces the amount of solutions needed.

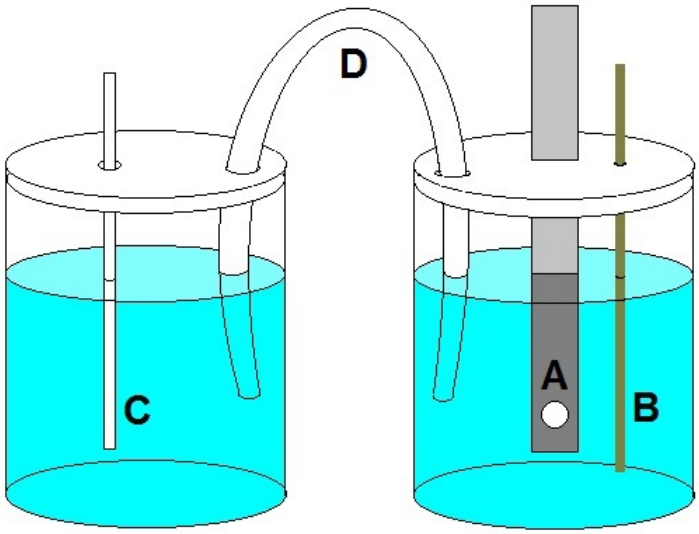

Figure 21 – Setup for electrodeposition of AuNP and the polymer layers. Sample as working electrode (A), platinum wire (B) was used as counter electrode and Ag/AgCl wire (Sarissa Biomedical Ltd, Coventry, UK) as reference electrode (C). The reference electrode was in 3 M KCl solution connected with a salt bridge (D) to the other cell.

Before the electrodeposition the samples were cleaned by cycling them 100 cycles in 0.5 M H_2SO_4 between -0.4 – 1.0V with scan rate of 1000 mV/s.

Two methods (a and b) were used in the electrodeposition of gold nanoparticles. The potential in both methods was sweeped between -0.5 V and +0.9 V (vs. Ag/AgCl wire in 3 M KCl) other parameters are presented in Table 6.

Table 6 – AuNP electrodeposition methods

Method	**NP size (nm)**	**$HAuCl_4$ (mM)**	**H_2SO_4 (M)**	**Cycles**	**Scan rate (mV/s)**	**Deposition time (s)**
a	14	1	0.5	2	20	140
b	40	2	1	15	50	420

The samples are referred as AuNP(a) and AuNP(b) according to the deposition method.

5.1.3 Manufacturing of gold electrodes

The silicon used in the gold samples (Au) was RCA-washed p-type (100) silicon. First batch of the gold samples were done by sputtering with Bal-Tec SCD 050 Sputter Coater (Los Angeles, CA, USA) a 100–200 nm thick layer of gold directly over the silicon chips (10 x 10 mm). The coating was not durable enough and got peeled easily from the samples. Next batch was done by sputtering first a 50 nm thick layer of titanium before the ca. 100 nm thick layer of gold. The gold layer of the second batch did not last either. The Au samples could not be used in the electrochemical layer depositions or measurements.

5.2 Polymer layer deposition

The deposition of polyaniline (Sigma Aldrich) and polypyrrole (Sigma Aldrich) was done with eDAQ or with Gamry with a similar set-up as used in the AuNP deposition presented in Figure 21. Deposition of PANI was done with cyclic voltammetry and deposition of PPy with chronoamperometry. Aniline and pyrrole was stored in +4°C when not used. Color of the liquid was supposed to be clear. If the color had started to change towards brown the liquid was vacuum distilled before use. With pyrrole this had to be done every time before it was used.

The platinum electrodes were pre-cleaned before polymer deposition by cycling them 100 cycles between -0.2 V – +1.3 V in 0.15 M sulfuric acid with the scan rate of 1000 mV/s.

5.2.1 Deposition of polyaniline

A solution with 0.1 M concentration of aniline and 0.3 M concentration of Camphor Sulfonic acid (CAS, Sigma Aldrich) was prepared in DI-water. 8 ml of the solution was used in each deposition.The potential was sweeped between -0.2 – +0.9 V, starting and finishing at 0 V with the scan rate of 100 mV/s. Two different layer thickness was prepared. For platinum based electrodes 35 and 70 cycles and for AuNP electrodes 30 and 70 cycles was used. The thinner layer thickness was determined so that the characteristic peaks of polyaniline deposition presented in Figure 10 had just started to show in the voltammogram.

5.2.2 Deposition of polypyrrole

Two different methods were tried in the polymerization of pyrrole. First method was from Ammam et al. [46] and the second one was from Maouche et al. [54].

Method 1: A 0.087 M solution of pyrrole was prepared by dissolving 0.21 ml of pyrrole to PBS. 8 ml of solution was used in each deposition. Amplitude of the pulse

was +1.1 V (vs. Ag/AgCl wire in 3M KCl). For pulse duration 500 s and 1000 s was used.

Method 2: A 0.1 M solution lithium perchlorate ($ClLiO_4$, Sigma Aldrich) was prepared to DI-water. The $ClLiO_4$ worked as a supporting electrolyte. Pyrrole was dissolved to the electrolyte solution so that the final concentration of pyrrole was 0.01 M. Amplitude of the pulse was 1.039 V (vs. Ag/AgCl wire in 3M KCl) and the duration 16 s.

In the original paper the amplitude was 1 V (vs. SCE) [54]. This was converted to the corresponding potential vs. Ag/AgCl (in 3 M KCl) according to Table 1.

The parameters of PPy deposition is summarized in Table 7.

Table 7 – PPy electrodeposition methods

Method	**Solvent**	**Concentration of PPy (M)**	**Potential step (V)**	**Pulse duration (s)**
1	PBS	0.087	+ 1.1	500 / 1000
2	0.1 M $ClLiO_4$	0.01	+1.039	16

5.3 Self-assembled monolayer deposition

The samples with SAM-layer deposited onto them were used as 'reference samples' for the polymer layer covered samples. The PTFE-tape was removed from AuNP samples prior to SAM-layer deposition.

5.3.1 APTES deposition

7 % and 10 % APTES (3-aminopropyltriethoxysilane) solutions were prepared in dry toluene (Merck). The samples were immersed to the solution and incubated for one hour at room temperature. After the incubation the samples were immersed first to dry toluene for five minutes and then to acetone for five minutes. After the acetone the samples were sonicated in DI-water for ten minutes and dried with compressed air. The samples were stored dry at room temperature.

The chemical structure of an APTES molecule is presented in Figure 22. The attachment to the surface will happen via the silicon atom leaving the rest of the molecule outwards and hence functionalizing the surface with amino groups. The formed layer will about 0.9 nm thick [66].

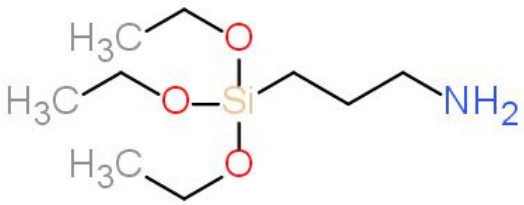

Figure 22 – The molecular structure of an APTES molecule.

5.3.2 TESPSA deposition

7 % and 10 % TESPSA (3-triethoxysilylpropyl succinic anhydride) solutions were prepared to dry toluene (Merck). The samples were immersed to the solution and incubated for one hour at room temperature. After the incubation the samples were immersed first to dry toluene for five minutes and then to acetone for another five minutes. After the acetone incubation the samples were sonicated in DI-water for ten minutes and dried with compressed air. Thereafter the samples were hydrolyzed by immersing them to 10 mM HCl solution for one hour. Finally the samples were sonicated in DI-water for ten minutes and dried with compressed air. The samples were stored dry at room temperature.

The chemical structure of an TESPSA molecule is presented in Figure 23. The molecules forms a 0.9 nm thick layer over the surface [66].

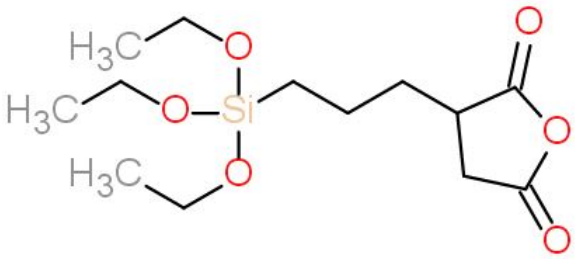

Figure 23 – The molecular structure of an TESPSA molecule.

5.4 Electrochemical measurements

Cyclic voltammetry and amperometry with Gamry was used in the measurements. The measurements were either conducted in a glass cell (setup presented in Figure 24) or a plastic cell (setup presented in Figure 25). An Ag/AgCl wire reference electrode used with the plastic cell will be destroyed faster in solutions not containing chloride ions (in this thesis meaning the measurements in H_2SO_4). With the glass cell a

different type of reference electrode was used, the Ag/AgCl electrode was immersed to a saturated KCl solution protecting the reference from other solutions. The reference electrodes used with glass cells were purchased from Radiometer analytical (Villeurbanne cedex, France).

Rest of the measurements would also be possible to perform in the glass cell. Unfortunately the setup is much harder to construct and clean between measurements. Hence measurement series with H_2O_2 and glutamate were performed in the plastic cell.

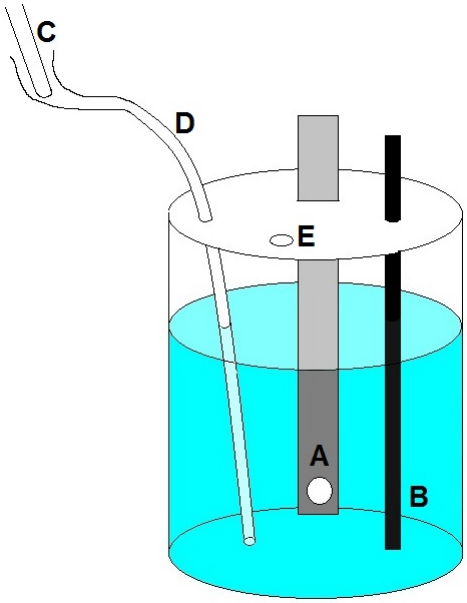

Figure 24 – Glass cell used in measurements with H_2SO_4. Sample as the working electrode (A), glassy carbon rod (B) was used as counter electrode and Ag/AgCl (KCl sat.) as reference electrode (C). The reference was connected with Luggin capillary (D) to rest of the cell. The measurements were conducted under constant nitrogen flow with a tube immersed to the sealed cell from the hole (E).

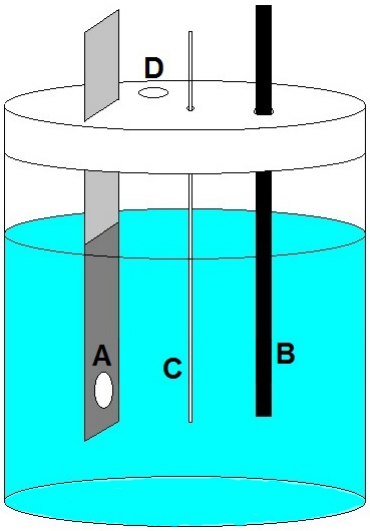

Figure 25 – Plastic cell used in measurements in liquids containing chloride ions (in this thesis measurements in PBS). Sample as the working electrode (A), glassy carbon rod (B) was used as counter electrode and Ag/AgCl wire as reference electrode (C). Measurements with H_2O_2 were conducted under nitrogen flow with a tube placed in the hole (D).

5.4.1 Characterization of the electrode materials

All the sample types were characterized by cycling them in 0.15 M H_2SO_4. The purpose of this was to see whether the voltammograms showed any characteristic features of platinum or gold (depending of the sample type). Also the water window was defined. All measurements in H_2SO_4 were conduted in the glass cell against Ag/AgCl (in KCl sat.) reference.

All platinum samples were cleaned before measurements by cycling them 100 cycles in 0.15M H_2SO_4 with the scan rate of 1000 mV/s between -0.2 – +1.0V or -0.2 – +1.3V. The H_2SO_4 used in the cleaning and measurements was deoxygenated with nitrogen bubbling for 10 minutes before the measurements, also the measurements were conducted under nitrogen atmosphere.

After the H_2SO_4 characterization the sample types were also characterized in PBS in order to determine the scan limits for H_2O_2 measurements.

5.4.2 Measurements with hydrogen peroxide

After the samples were characterized and if the presence of platinum or gold (depending on the sample type) was confirmed the detection limit for H_2O_2 could be determined with the sample type. This was done by cyclic voltammetry measurements in H_2O_2 solutions of different molarity. 100 mM solution of H_2O_2 was prepared by adding 0.103 ml of 30% stock solution to 10 ml of PBS. This was then diluted

to 10 mM, 1 mM, 500 µM, 200 µM, 100 µM, 50 µM, 20 µM, 10 µM and 1 µM concentrations of H_2O_2 in PBS. 100 mM and 10 mM solutions were not used in the measurements due to too big currents. The concentration of 100 mM would also be irrelevant to the glutamate sensor development because the solubility of glutamate allows only about 50 mM solutions to be made. The measurements were conducted from the weakest solution to the strongest. Before and after the measurements in H_2O_2, the samples were cycled in PBS in order to deteremine the baseline for the measurements.

The measurements with CPt and platinum samples were done between -0.5 – +1.2 V and -0.5 – +0.8 V and measurements with AuNP samples were done between -0.4 – +0.8 V with the scan rate of 50 mV/s. Starting point for all measurements was 0 V. The scan limits were determined by PBS characterization. The upper scan limit for platinum based samples were lowered from 1.2V to 0.8V when the voltammograms suggested that the higher potentials resulted in oxide and oxygen formation which could disturb the detection limit determination.

Amperometry was performed with an AuNP(a) sample. The measurement was conducted in the plastic cell (Fig. 25) with the potential of +0.7 V (vs. Ag/AgCl) and step duration of 180 seconds. The measurement was repeated with PBS and each concentration of H_2O_2.

Cyclic voltammetry measurements with H_2O_2 were repeated with the same parameters after the polymer and SAM coatings. To determine if the PANI layer deposited onto the electrode forms an diffusion barriere, one injection amperometry was conducted with a CPt/PANI(35) -sample.

The measurement was conducted in the plastic cell (Fig. 25) with an initial volume of 27 ml of PBS. The pre-step voltage of 0.0 V was held for 10 seconds, after that the potential was stepped to +0.7 V in total of 1200 seconds. At the time point of 300 seconds 1.0 ml of 10 mM H_2O_2 solution was added to the cell. After that 0.5 ml of 10 mM H_2O_2 was injected to the cell every 120 seconds. The progress of the measurement is presented in Table 8.

Table 8 – Injection amperometry with CPt/PANI(35) sample

Time (s)	**Initial volume (ml)**	**Volume of the injection (ml)**	**Final concentration (mM)**
0	27	0	0
300	27	1.0	0.357
420	28	0.5	0.526
540	28.5	0.5	0.699
660	29	0.5	0.847
780	29.5	0.5	1
900	30	0.5	1.148
1020	30.5	0.5	1.29

5.4.3 Measurements with glutamate

Sample types that could detect H_2O_2 got GlOx immobilized onto them (the methods for immobilization are described in chapter 5.5). With GlOx samples both cyclic voltammetry and amperometry was utilized. The measurements were conducted in the plastic cell (Fig. 25). In cyclic voltammetry the parameters were the same as used in the H_2O_2 measurements (scan rate of 50 mV/s and scan limits for platinum based samples: -0.5 – +1.2V or -0.5 – +0.8 V and for AuNP samples: -0.4 – +0.8 V). In amperometry the potential of 0.65 V (vs Ag/AgCl wire) was held for 180 seconds for each concentration.

A 10 mM glutamate solution was prepared by dissolving L-glutamate (Sigma Aldrich) to PBS. The solution was diluted to 1 mM, 500 µM, 200 µM, 100 µM, 50 µM, 20 µM, 10 µM and 1 µM concentrations of glutamate. The PBS used had been warmed up to 37°C before the solutions were prepared to optimize the environment for enzyme activity and also to make it resemble more of the environment the biosensor is intended to be used in.

Like with the H_2O_2 measurments, the measurements with glutamate were conducted from the weakest solution to the strongest. Before and after the measurements the sample was cycled in PBS in order to deteremine the baseline.

5.5 Enzyme immobilization

All of the samples were sonicated in DI-water for ten minutes prior to the immobilization in order to get rid of possible impurities. After the sonication the samples were dried with a compressed air.

After the immobilization the samples were stored in PBS at +4°C. The PBS used in enzyme immobilization was purchased from Merck.

5.5.1 Enzyme immobilization onto a surface functionalized with amino groups

A solution of 0.1 U/ml GlOx (Cosmo Bio Co., Ltd., Tokyo, Japan) was prepared in PBS. The samples were covered by droplets of the GlOx solution. The size of the droplet varied depending of the size of the sample. A 100 µl droplet was used to samples with diameter of 6 mm and 30 µl droplet was used to samples with the diameter of 3.5 mm. The GlOx covered samples were incubated for four hours at room temperature. After the immobilization the solution was blotted away and samples were washed three times with PBS.

5.5.2 Enzyme immobilization onto a surface functionalized with carboxyl groups and on unfunctionalized CPt sample

The immobilization of GlOx on samples functionalized with TESPSA were done by EDC conjugation in the pressence of NHS. Also GlOx immobilization onto a CPt sample with no surface functionalization was done with the same method.

Solution of 0.2 M of EDC (Sigma Aldrich) and 0.2 M of NHS (Sigma Aldrich) was prepared. The solvent used was DI-water. The sample was covered by a droplet of the EDC-NHS solution and incubated for two hours at room temperature.

After EDC-NHS incubation was done the droplet was absorbed from the sample. GlOx solution was diluted to 0.1 U/ml in PBS. The sample was promptly covered by a droplet of GlOx solution and incubated for two hours at room temperature. After the immobilization the droplet was blotted away and washed three times with PBS.

5.5.3 Enzyme immobilization on polymer layers

The immobilization onto the polymer samples were done by glutaraldehyde conjugation. A solution of 0.2 M Na_2HPO_4 and 0.1 M citric acid (Sigma Aldrich) was prepared by diluting the substaces to DI-water. Glutaraldehyde (VWR) was added to the solution so that the final concentration of glutaraldehyde was 2.5%. A drop of the solution was put on the samples and incubated for two hours at room temperature.

After the incubation was over the droplets were blotted away and the samples were covered by a droplet of 0.1 U/ml GlOx solution. The samples were incubated for four hours at room temperature. After the immobilization the droplets were blotted away from the samples and washed three times with PBS.

5.6 Activity measurements of glutamate oxidase

The activity measurements were done by Glutamate Oxidase Assay Kit (ab138885, Abcam, Cambridge, UK) according to the instructions. An indicator solution was made by dissolving 4 µl Ab red colourant, 2.5 µl glutamate, and 2.5 µl horse radish peroxide (HRP) to 1 ml of buffer solution.

Standard series was done by diluting 10 mU/ml GlOx solution from the kit to 3 mU/ml, 1 mU/ml, 0.3 mU/ml, 0.1 mU/ml, 0.03 mU/ml, and 0.01 mU/ml concentrations. Also blank reference was used. Prior to the measurement the samples were washed three times with PBS and blotted as dry as possible. After that 50 µl of PBS and 50 µl indicator solution was pipeted on the samples. The first standard (10 mU/ml) had a volume of 100 µl and the rest of them including blank had the volume of 50 µl. Equal amount of indicator solution was pipeted to the standars. The samples were covered from the light and incubated for 40 minutes at room temperature.

After the incubation an 80 µl droplet was collected from the samples and standard solutions and analyzed with a microplate reader (FLUOstar Optima, Ortenberg, Germany). An excitation wavelength of 544 nm and an emission wavelength of 590 nm was used for analyzing.

5.7 Sample characterization with scanning electron microscopy

The morphology of some of the sample types were characterized by scanning electron microscopy (SEM, Hitachi-4700, Hitachi Ltd, Tokyo, Japan). Prior to imaging the sample chips were mounted on chromium stubs with silver glue (Agar Scientific Ldt, Essex, UK). Samples with a polymer layer deposited onto them were made conducting with chromium sputtering (Bal-Tec SCD 050 Sputter Coater) prior to the imaging. Magnification of 20, 100, 500, 2000, 5000, 15000, and 30000 were obtained. To determine the size of the gold nanoparticles a 60000 magnification was also obtained from some AuNP samples.

5.8 Sample characterization with light microscopy

Before the chromium sputtering and after the sample characterization with SEM some of the samples were imagined with light microscopy (Olympus BX51M, Tokyo, Japan). This was done because no layer could be seen in the first PANI sample imagined with SEM and it was speculated that the layer had detached during the chromium sputtering. Magnification of 20 was used.

6 Results and discussion

The results are presented in this chapter and they are compared to results of similar kind of measurements found in the literature. The suitability of the sample types for detecting glutamate in amperometric biosensors is discussed.

6.1 Sample manufacturing

CPt and platinum samples and the DLC substrate for AuNP depositions were received prepared. AuNPs and the polymer layers were deposited electrochemically and the surfaces were analyzed with light microscope and SEM.

6.1.1 Electrodeposition of gold nanoparticles

Two different methods were tried with the deposition of gold nanoparticles, method a and method b, presented in Table 6. After the deposition a yellow layer was visible on the samples. The layer was noticeably darker with AuNP(b) samples than with the AuNP(a) samples. Unfortunately notable variations between samples of the same method were also visible, especially with the AuNP(b) samples. Some micrographs of the samples are presented in Figure 26. Figure 26A shows the surface of an AuNP(a) and B the surface of an AuNP(b) sample. The distribution of the gold nanoparticles were mostly even on AuNP(a) samples, whereas AuNP(b) samples had some areas with fewer particles. The areas were visible even to the naked eye and are presented in Figure 26C.

Figures 26E and F present a 60 000x magnification of the surfaces of AuNP(a) and AuNP(b) samples respectively. The smallest particles produced with method a are approximately 20 nm in diameter, which is close to the intended diameter of 14 nm. Unfortunately most of the particles are clearly bigger, roughly estimated to be about 80 nm in diameter. The probable reason for this is that in the original experiment resulting in 14 nm nanoparticles, glassy carbon was used as the substrate. The carbon atoms in glassy carbon are mostly sp^2 hybridized in contrary to DLC which has more sp^3 hybridized carbons. Due to these differences glassy carbon is more conducting and not as inert as DLC [40, 67]. It is also possible that the bigger particles seen in Figure 26E are agglomerates of the smaller particles. The particle size with method b was approximated to be about 60 nm in diameter, which is quite close to the intended diameter of 40 nm. Figure 26F was taken at an area with fewer particles, nanoparticles shown at Figure 26B are aggregated and form strands on the surface.

According to Liu et al. the size of the gold nanoparticles can be controlled by the electrodeposition time. Shorter deposition times resulted in smaller particles, also size variation between the particles was smaller. With their set-up (cyclic voltammetry with the scan rate of 20 mV/s, between -0.05 V – +0.85 V vs SCE) deposition time

of 20 s resulted in gold nanoparticles with the average diameter of 50.1 nm while the deposition time of 720 s resulted in gold nanoparticles with the average diameter of 90.1 nm. They also noticed that longer deposition times enhanced the formation of agglomerates. Liu et al. used DLC as the substrate in their studies.[30] This time depency was not noticed in the samples produced for this thesis. This suggest that the concentration of $HAuCl_4$ and H_2SO_4 and the scan rate also affects the size of the gold nanoparticles. Slower scan rates gives usually more time for the electrochemical reactions to happen, which might explain why the particles with method a (scan rate of 20 mV/s) are bigger than the particles produced by method b (scan rate of 50 mV/s). With a shorter deposition time or with a faster scan rate the fabrication of smaller nanoparticles should be possible.

Like mentioned in chapter 2.3, gold nanoparticles enable the immobilization of biomolecules like enzymes directly onto them [36, 37]. The size of the GlOx enzyme is 12.4 nm x 12.4 nm x 16.9 nm [58] i.e. approximately the same size as the nanoparticles intended with method a. This would mean that only one or few enzymes would be able to attach onto the surface of one nanoparticle. Even though the total surface area increases when the size of the nanoparticles decreases, the surface area allowing the attachment of enzymes decreases after some point. The bigger nanoparticles would allow more enzymes to be immobilized onto them and still provide the positive qualities of nanoparticles. The optimal size of the gold nanoparticles for GlOx immobilization remains yet to be determined.

The greatest problem with the AuNP samples manufactured for this thesis was the detachment of the nanoparticles from the surface. Figure 26D shows the surface of an AuNP(b) sample. Several of the samples were scratched remarkably even though they were handled with care. Neither did the AuNP samples withstand the sonication in DI-water, which is a part of the SAM layer deposition. This is also an indication of the poor attachment of the nanoparticles onto the surface. The poor attachment is most likely caused by the antifouling and anti-adhesion properties of DLC [10].

Most of the sensors based on gold nanoparticles found in the literature did not have the nanoparticles deposited directly onto the electrode. Instead they were either linked to a SAM layer deposited onto the electrode [37, 68] or deposited with a polymer [69, 70, 71]. The stability of these types of sensors was reported to be good. Polymer layer deposition onto the nanoparticles should also reduce the detachment of them. In this type of structure the enzymes would not be directly in contact with the nanoparticles. It would probably also decrease the significance of the size of the nanoparticles. At least the success of immobilization onto the electrode would not be as directly dependent on it.

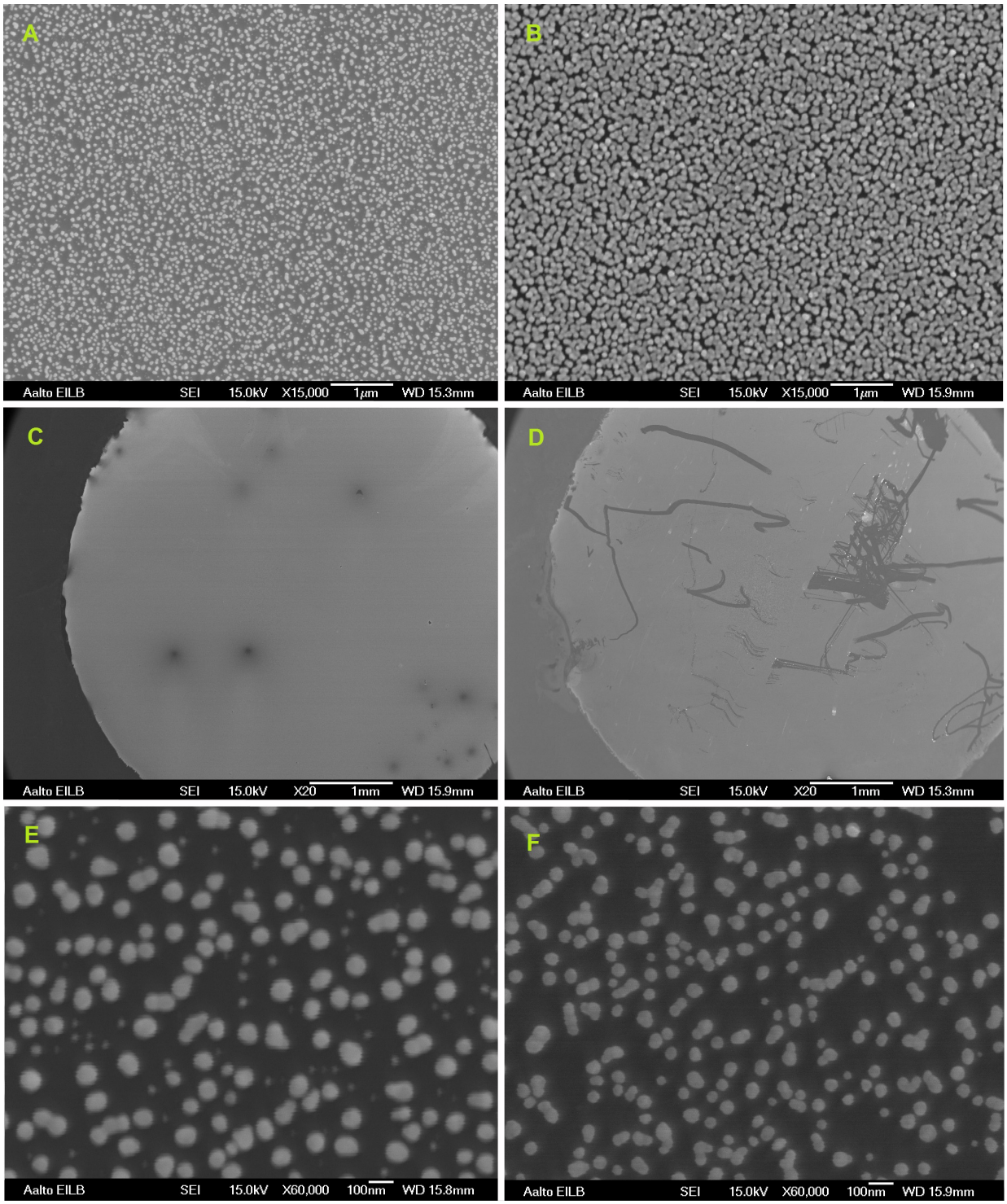

Figure 26 – SEM micrographs of AuNP sample surfaces. (A) represents the surface of an AuNP(a) sample and (B) the surface of an AuNP(b) sample. (C) displays the uneven distribution of gold nanoparticles on the surface of an AuNP(b) sample. Most of the samples were also severely scratched (D) indicating of poor attachment of the particles. The size of the particles was bigger than intended, (E) shows the size distribution of an AuNP(a) sample and (F) the size distribution of an AuNP(b) sample.

6.1.2 Electrodeposition of polyaniline

Two different layer thicknesses were tried with the PANI samples. The thin one was determined so that the characteristic peaks of the deposition had started to show (35 cycles for the CPt and platinum samples and 30 for the AuNP samples). The thicker layer was done with 70 cycles and the characteristic peaks showing clearly in the voltammograms.

The voltammograms of PANI depositions onto two AuNP(a) samples are presented in Figure 27. They resemble the one found in the literature presented in the theoretical part of this thesis in Figure 10. The membrane growth is indicated by the peak b and peak a represents the insertion of anions to the membrane.

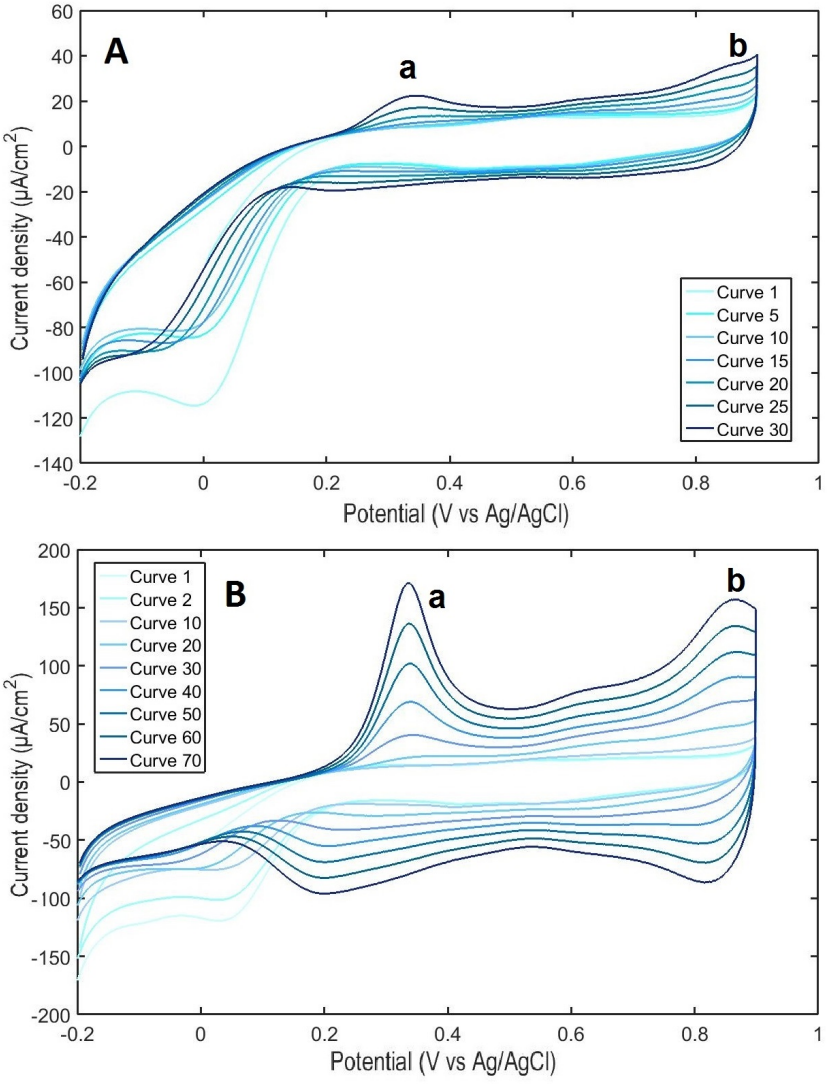

Figure 27 – Electrodeposition cycles of PANI on AuNP -samples. 30 cycles on the top (A) and 70 cycles on the bottom (B). Scan rate of 100 mV/s was used during the deposition.

After the layer depositions no changes on the electrode surfaces could be detected with naked eye. Imagining with the light microscope and SEM revealed that PANI deposition on CPt samples was not successful. Figure 28A is a 20x magnification of the surface of a CPt sample with a thin layer of PANI deposited onto it. The layer was partially uniform but most of it was clearly damaged and torn. The adhesion between the polymer layer and surface of the CPt sample was clearly insufficient. As can be seen in Figure 28C the whole layer had detached during the chromium sputtering. This might be caused by the antifouling properties of DLC [10]. Pretreatments to the surface may help to turn the surface more favorable towards PANI deposition.

PANI deposited onto the platinum samples looked completely different compared to the layer seen on CPt samples. Imaging with light microscope and SEM revealed that a cracked layer had formed on top of the samples. The layer looked the same regardless of the layer thickness. Figure 28B is a 20x magnification of the surface of a platinum sample with a thin layer of PANI deposited onto it. The same structures are still visible in the micrograph presented in Figure 28D. Adhesion of the layer was deficient on the platinum surface. Some of the flakes formed by the cracks had detached and some scratches were visible on the surface as well.

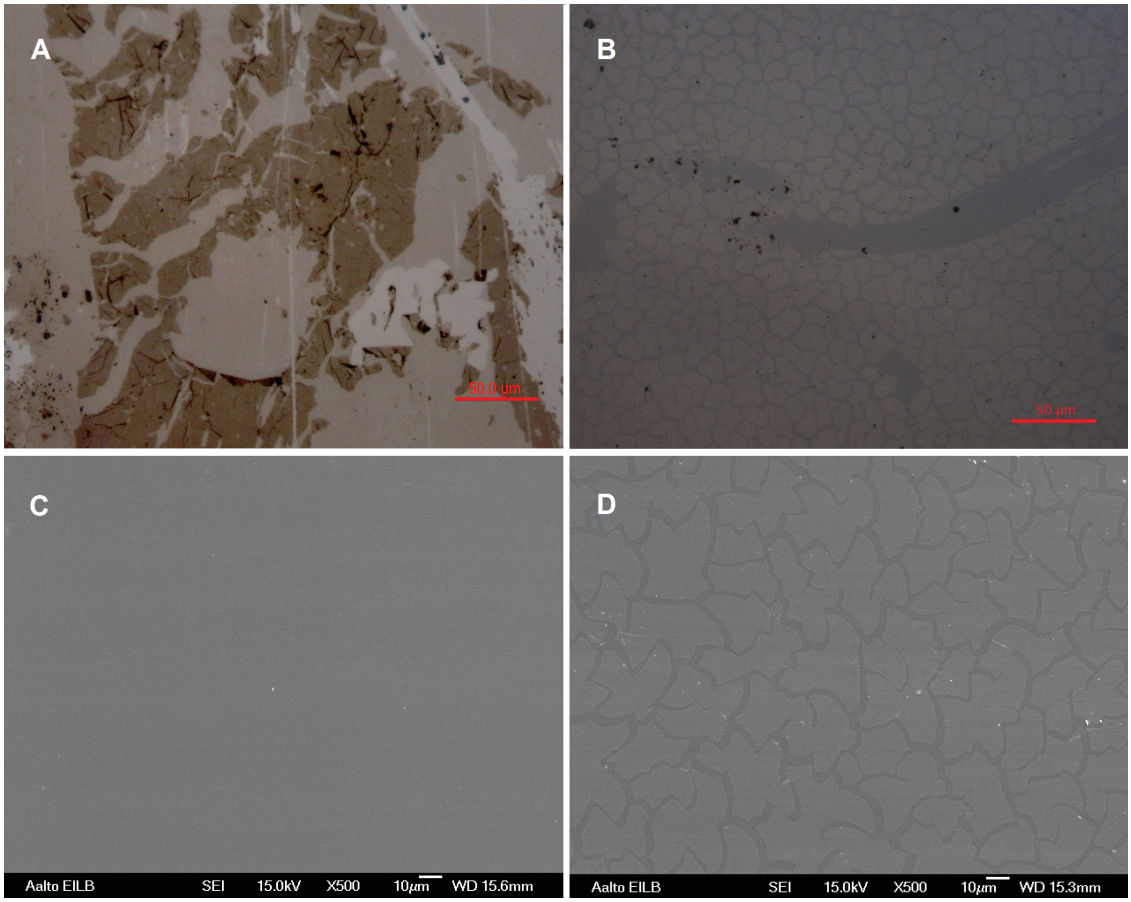

Figure 28 – Light microscope images of the surfaces (A) CPt/PANI(35) and (B) Pt/PANI(35) samples. SEM micrographs of the same samples (C) CPt/PANI(35) and (D) Pt/PANI(35).

The cracked surface would suggest that the polymer had shrinked during drying. According to the literature the layer should stay stable both under air and water exposure [47]. Even though the problem might be solved by having the electrode immersed after the deposition, the unstability towards the environmental changes indicates that the deposition did not succeed.

The depostion of PANI onto the AuNP samples did not reveal any visible changes on the electrodes. Even the SEM micrograph presented in Figure 29 appeared to look like the AuNP samples without any layers deposited onto them. One unprobable explanation to this might be that the adhesion between the formed layer and the surface was not sufficient and the layer got detached during the chromium sputtering like with the CPt samples. Though it would be likely that at least some of the gold nanoparticles would have detached during this process as well. Another possible explanation could be that the thin PANI layer does not have visible structures when formed onto the AuNP surface.

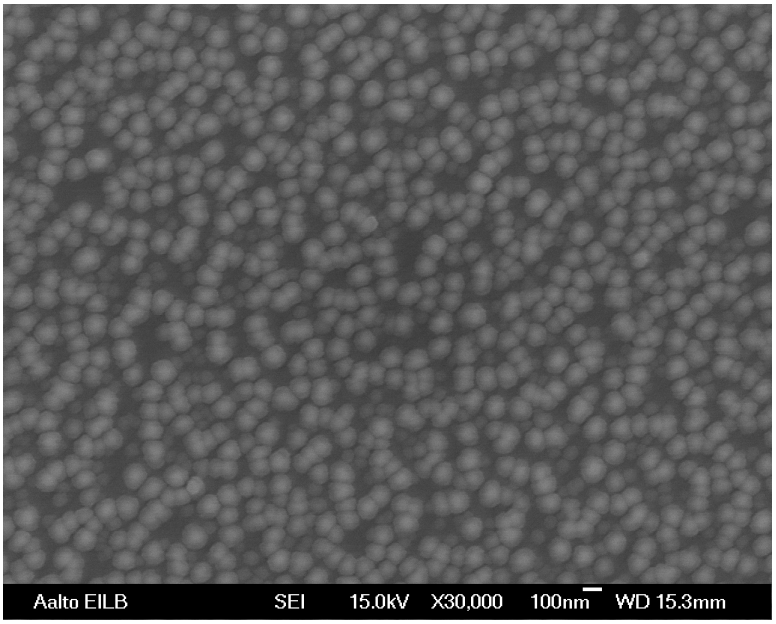

Figure 29 – A SEM micrograph of the surface of an AuNP(b)/PANI(30) sample.

6.1.3 Electrodeposition of polypyrrole

The deposition of PPy turned out to be more complicated than presented in the literature review. Firstly the monomer dispersion needed to be distilled every time before use. Secondly the layers deposited did not always resemble those described in the literature. According to Ammam et al. a light brown or yellowish layer should be visible on the electrode after PPy deposition [46]. Electrodes manufactured by the first method, presented in the article by Ammam et al., got a thick and uneven black polymer layer onto them like presented in Figure 30A. The layer delaminated also easily. The substrate used in the article was platinum wire with the active area of

0.78 mm^2. The size of the active surface should not have an effect on the success of the deposition. According to the article the only preparation made to the electrode before the deposition was cleaning it by dipping it into a mixture of nitric acid (7 %) and H_2O_2 (30 %) for a few seconds. CPt and platinum samples were cleaned with H_2SO_4 cycling prior to deposition. The electrodes manufactured by this method did not perform well in the electrochemical measurements and no measurements were able to be conducted with them. Consequently the method was not used with the AuNP samples.

PPy layers deposited onto CPt samples with the second method, presented in the article by Maouche et al., had a visible brown layer on them, though the layers were not even. Pt samples did not get any visible layers on them and the layer on AuNP(b) sample presented in Figure 30B was more purple or orange than brown. Maouche et al. used glassy carbon as substrate in their electrodes. This might explain why the method seemed more suitable for DLC layers compared to platinum layers.

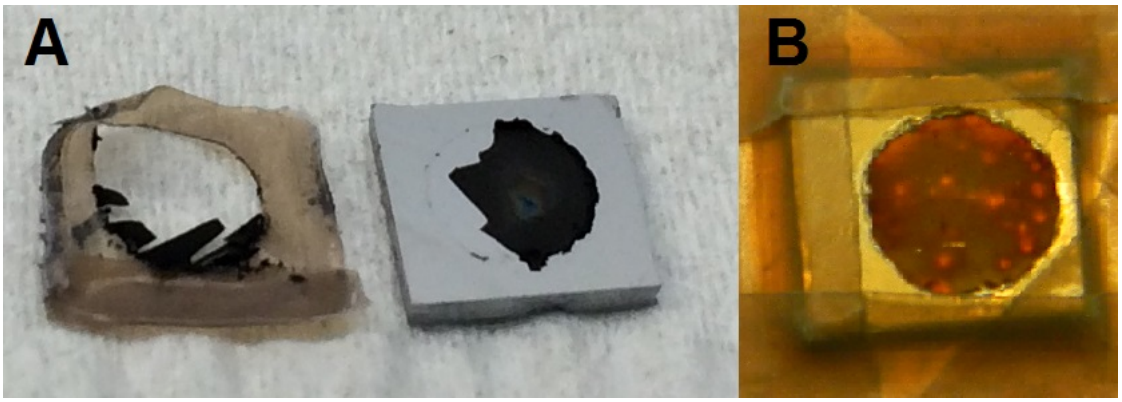

Figure 30 – Pictures of PPy samples. A shows a Pt/PPy(1) sample. The layer formed by method 1 resulted in thick, uneven black layers. Part of the layer got peeled off with the removal of the teflon tape. B shows an AuNP(b)/PPy(2) sample.

Closer view of the surface revealed that even though the surface of CPt/PPy samples deposited by the second method seemed proper the layer was not homogenous or even. Figure 31 shows PPy layers deposited onto the surface of CPt and Pt samples. Figures 31A and B are pictures from light microscope and the rest of them are SEM micrographs. Figure 31A shows the surface of a Pt/PPy sample. The layers were deposited with the second method. Adhesion between the layer and the surface was insufficient. Only few flakes of the polymer layer could be seen on the sample prior to the chromium sputtering and even less in the SEM micrographs. What is left of the polymer layer's edge deposited by the first method is shown in Figure 31B. Nothing could be seen with the light microscope in the middle of the sample.

Figures 31C-E are micrographs of a CPt sample covered by a PPy layer deposited by the second method. As can be seen in the figures the layer is not homogenous. Holes with the size varying from a couple to several hundreds of micrometers are seen on the surface. Also half of the samples had only patches of the layer. This type of

layer structure was not present in the platinum samples deposited by second method. Figure 31F is a 30 000x magnification of middle of a Pt/PPy sample deposited by the first method. Similar kinds of spherical structures as seen in Figure 31E can also be seen in Figure 31F. This might suggest that by shortening the deposition time of the first method a decent layer may be deposited.

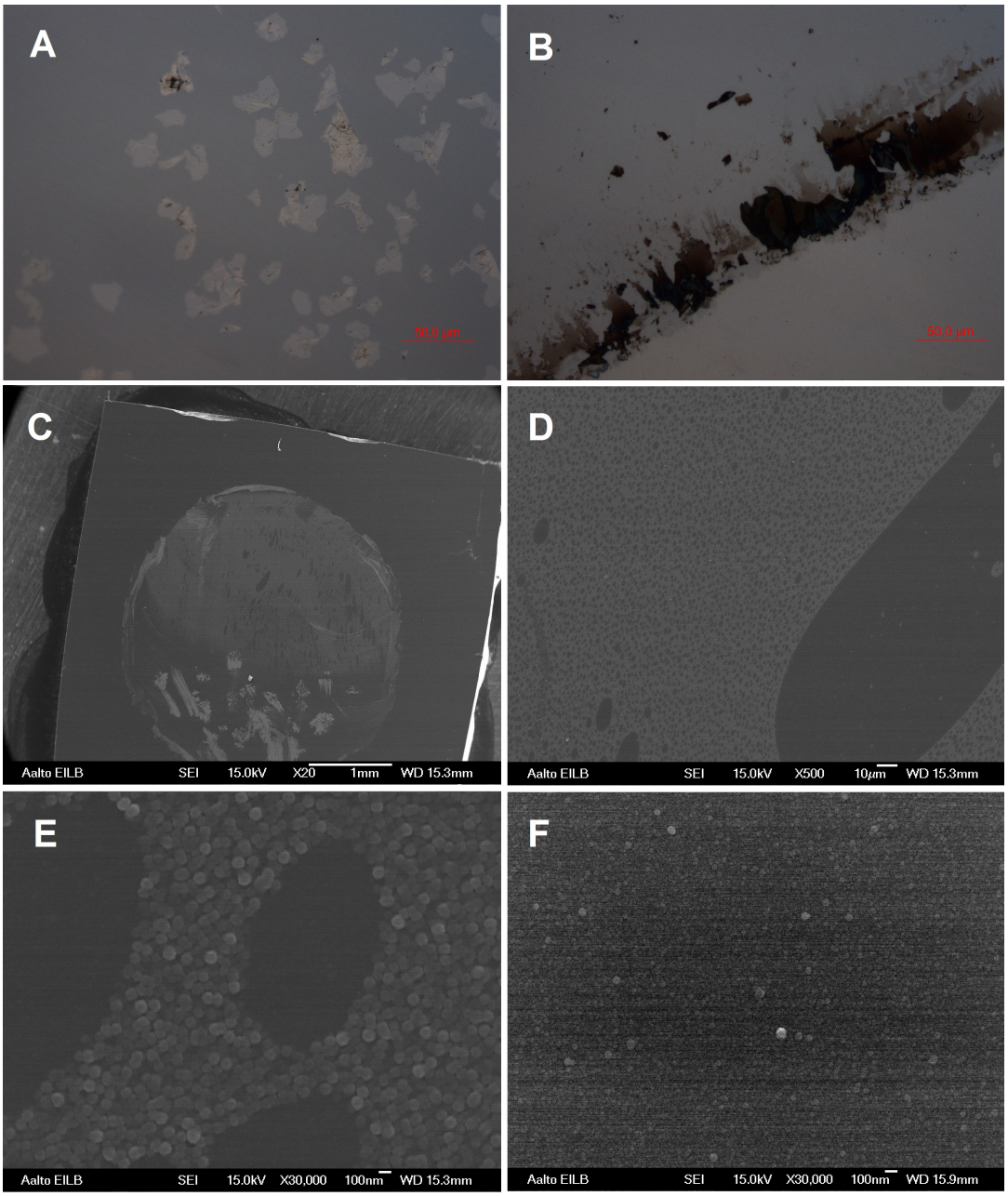

Figure 31 – Light microscope images of Pt/PPy samples (A) and (B), and SEM micrographs of CPt/PPy samples (C)-(F).

The greatest challenge with both of the polymer layers seems to be the insufficient adhesion between the layer and the substrate. The adhesion may be improved by surface pretreatments. For instance etching the surface of DLC with hydrogen plasma would leave the surface hydrogen terminated. Because the PPy layer with the first method was succesfully deposited onto a glassy carbon electrode [46], the plasma etching might improve the adhesion between the CPt electrode and PPy layer. Glassy carbon has also been used with PANI layers [72, 73, 74].

6.2 Electrochemical measurements

6.2.1 Characterization of samples

The characteristic peaks of platinum were visible in the H_2SO_4 and PBS measurements. Figure 32A is the voltammogram of H_2SO_4 characterization for a CPt sample and Figure 32B is a voltammogram found in the literature [19] for H_2SO_4 characterization of a platinum electrode. Peaks for hydrogen desorption (a) and oxide reduction (b) are present in both voltammograms. Also peaks for hydrogen and oxygen evolutions are about at the same potentials for both samples.

Figure 32C presents the voltammogram of PBS characterization for a CPt sample and Figure 32D is a voltammogram found in the literature [19] for PBS characterization of a platinum electrode. Peaks for hydrogen desorption (c) and oxide reduction (d) are present in both voltammograms like they were in the characterization in H_2SO_4 (Figures 32A and B). Peak e is the reduction peak of the phosphate group like mentioned earlier in chapter 2.2. The safe potential window for the H_2O_2 and glutamate measurements were determined from Figure 32C to be between -0.5 V and +1.2 V.

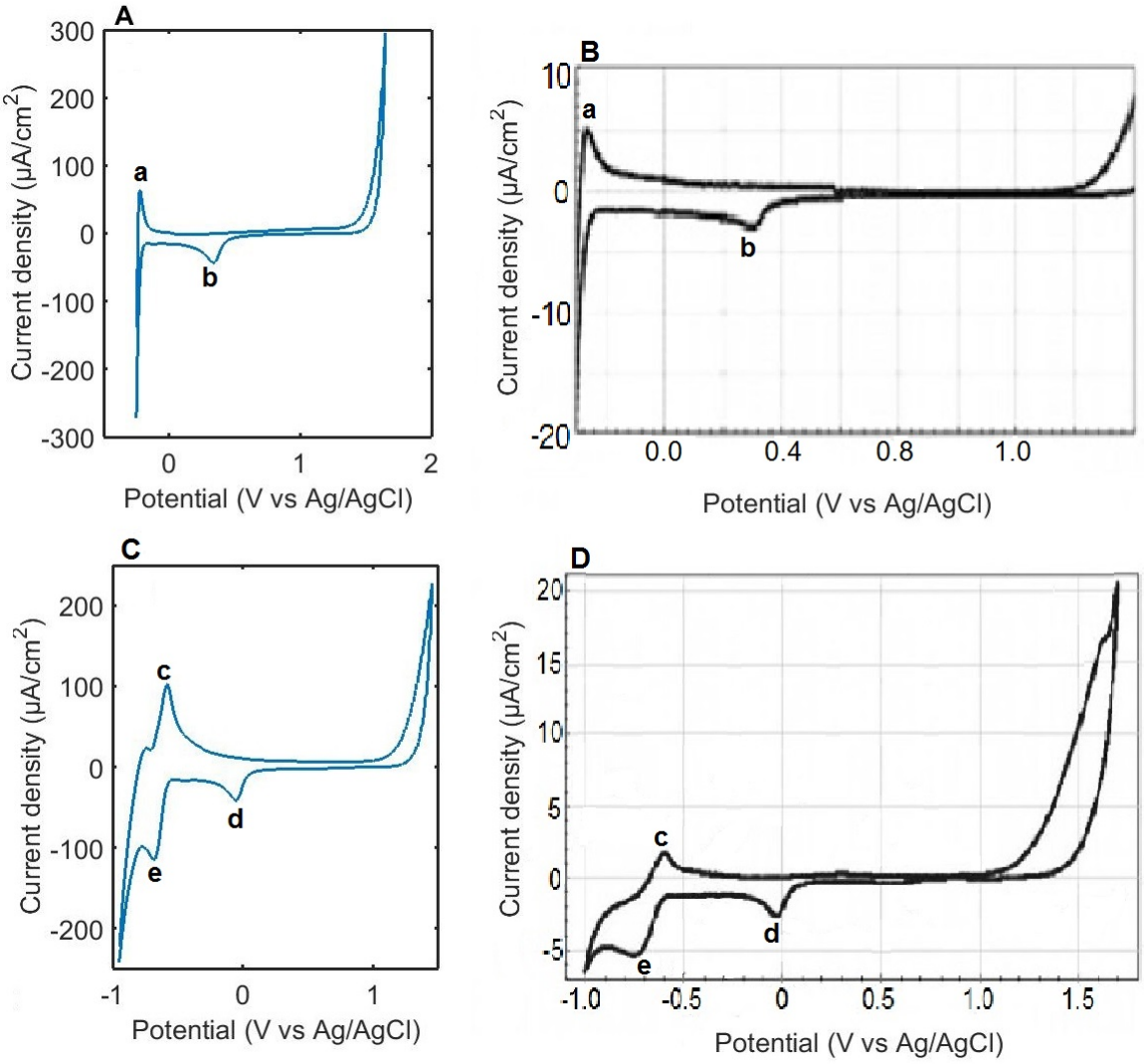

Figure 32 – Water window of CPt samples in 0,15 M H_2SO_4 (A) and in PBS (C). Measured with the scan rate of 50 mV/s. Water window for Pt samples in H_2SO_4 (B) and PBS (D). B and D are modified from [19].

All of the CPt samples were cleaned by H_2SO_4 cycling before electrochemical measurements or polymer layer deposition. This was also a way to certify that the electrode in question presented the characteristic peaks of platinum. If the peaks did not emerge the sample was not used in the measurements.

The voltammogram of an AuNP(a) sample in H_2SO_4 seen in Figure 33A presented the characteristic peaks of gold also seen in Figure 7. Peaks for oxide formation (a) and reduction (c) as well the evolution peaks for oxygen (b) and hydrogen (d) are clearly present. In the PBS measurement presented in Figure 33B the evolution peaks for hydrogen (g) and oxygen (e) as well as the oxide reduction peak (f) are present. A safe potential window for the H_2O_2 measurements was determined to be between -0.4 – + 0.8 V. Which is in line with corresponding measurements of H_2O_2 with gold and AuNP electrodes found in the literature [30, 31].

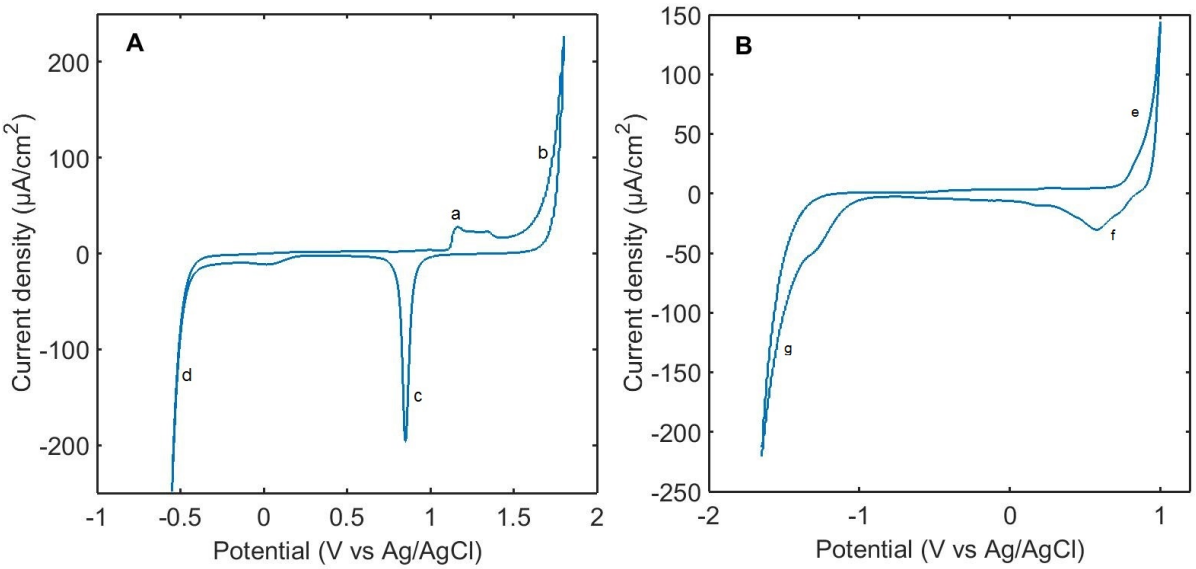

Figure 33 – Water window for AuNP samples in 0.15 M H_2SO_4 (A) and in PBS (B) with the scan rate of 50 mV/s. These cycles present the voltammograms of AuNP(a) samples. The measurements with AuNP(b) resulted in similar voltammograms.

6.2.2 Hydrogen peroxide measurements

During the measurements the samples were cycled three times in each concentration. The voltammograms presented in this chapter show only the first complete cycle of the relevant curves to determine the detection limit. This is done in order to make the figures more clear. Complete voltammograms are found in the appendix.

The term 'detection limit' may be used for signifying two different features of the performance of the electrode. It can be used for describing the signal-to-noise ratio like in the article of Liu et al.[30] or it may indicate the lowest concentration of the analyte in which a detectable signal is received. The latter definition of the term is used in this thesis.

Prior to the H_2O_2 series the samples were cycled 6-9 cycles in PBS with the same parameters than in the actual measurements. This was done in order to stabilize the surface of the sample and determine the 'baseline' for the measurments. One of these stabilized PBS curves is presented as PBS1 in the voltammograms. After the last H_2O_2 concentration the samples were cycled once again in PBS in total of 9 cycles to determine if some unreversible changes had happened to the sample during the measurements. One of these curves is also presented in the voltammograms as PBS2.

Hydrogen peroxide detection with CPt electrodes

Voltammogram of the H_2O_2 measurements of a CPt sample is presented in Figure 34. Clear peaks are seen at -0.3 V and +0.4 V (vs Ag/AgCl), which increase correspondent to the concentration of H_2O_2. According to literature the detection peaks for H_2O_2

on a platinum electrode should be at 0.7 - 0.8 V (vs Ag/AgCl) [8, 24]. One reason for the lower detection potential is that nanoparticles and clusters offer more binding sites compared to bulk electrodes which loweres the reaction potential [75].

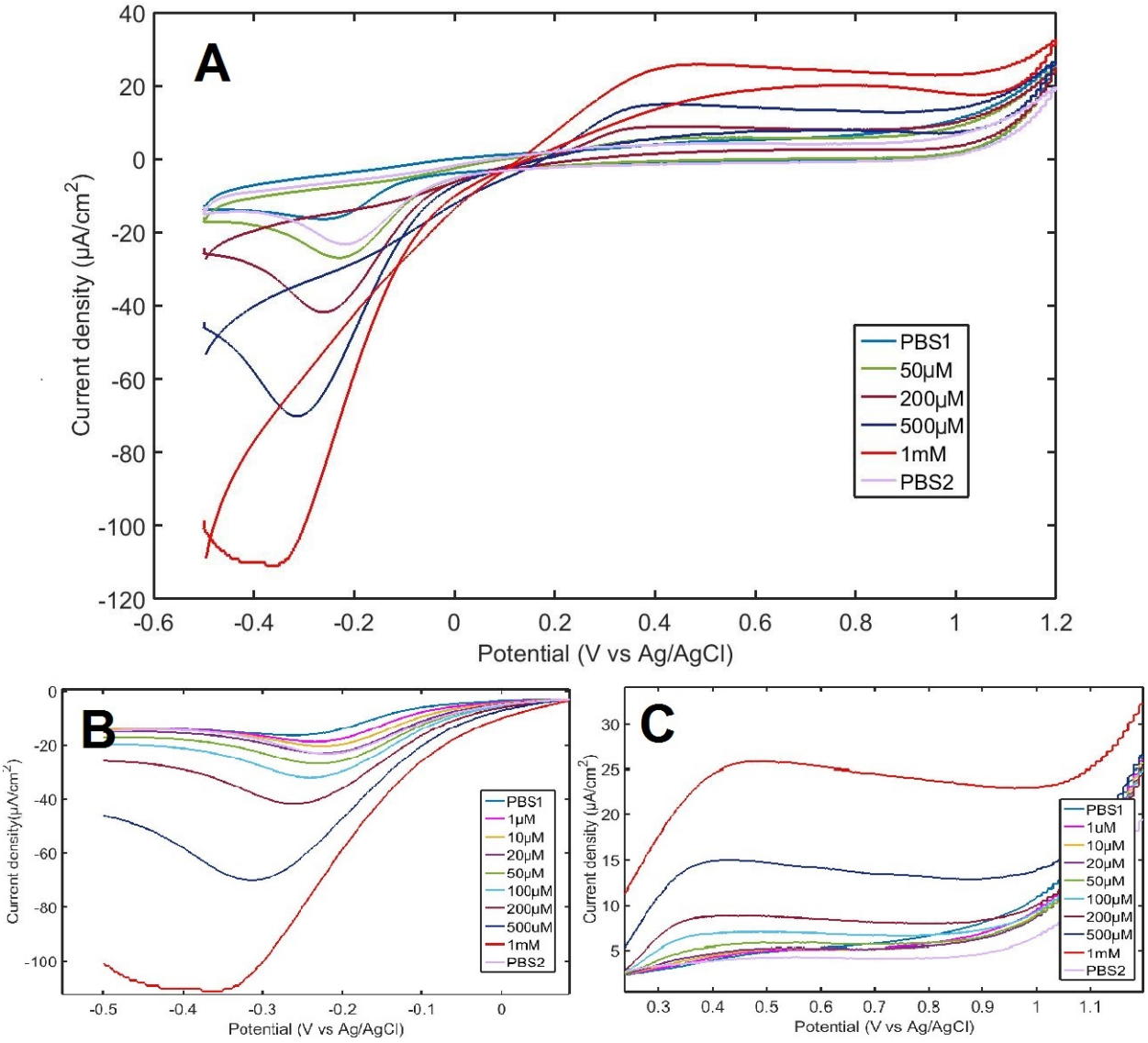

Figure 34 – H_2O_2 measurements with a CPt sample. The measurements were done between -0.5 – +1.2 V vs. Ag/AgCl wire in different concentrations of H_2O_2 with the scan rate of 50 mV/s. The electrode was cleaned by cycling in 0.15 M sulfuric acid prior to the measurements. Figure B is a close-up of the hydrogen end of the figure and C a close-up from the oxygen end.

The other reason for the potential difference is most likely caused by the measurement set-up. The Ag/AgCl wire used as the reference electrode is placed directly into the solution like presented in Figure 25 instead of connecting it with a salt bridge or Luggin carillary to the measurement solution. This will make the reference electrode

unstable over time which might lead to potential shifts. The results are still usable though it should be remembered while interpreting the data and comparing it to measurements conducted with a different setup.

The peak starting at -0.2 V is a combination of the reduction reactions of H_2O_2, oxygen and oxide groups. Even though the measurements were done in a nitrogen purged solution in order to get rid of the excess oxygen, cycling the sample to high anodic potentials will lead to oxygen formation, which is also catalyzed by the presence of H_2O_2. This makes it more difficult or even impossible to determine the detection of H_2O_2 by its reduction. By lowering the upper scan limit to +0.8 V the excess formation of unnecessary oxygen can be minimized still allowing the detection of H_2O_2 to occur. The smallest concentration of H_2O_2 that was detected by oxidation during the measurements with CPt was 50 µM, in other words it is the detection limit for the CPt samples.

Another approach for H_2O_2 detection would be by using only the reduction of the analyte instead of the oxidation. Meaning that in cyclic voltammetry the potential would stay below the oxide formation region, e.g. below +0.2 V (vs Ag/AgCl), during the whole measurement. This would also prevent the oxygen formation making it possible to use the reduction peak for H_2O_2 detection. An advantage of this approach would also be that the interfering species present in the brain do not show any electrochemical activity at this potential region [44].

Hydrogen peroxide detection with platinum electrodes

The H_2O_2 measurements with a platinum electrode is presented in Figure 35. Two clear peaks are seen, the first one at -0.4 V (vs Ag/AgCl) and the second one at +0.6 V (vs Ag/AgCl). The peaks increase in size correspondent to the concentration of H_2O_2. A shoulder at 0 V is also noticeable in the curves. The first peak is once again most likely the combination of oxygen and H_2O_2 reduction reactions and the shoulder might be the oxides reducing from the surface of the electrode. Like with the CPt electrode this peak may not be used for determining the detection of H_2O_2 because of the difficulty of separating these peaks from each other.

The second peak at +0.6 V (vs Ag/AgCl) is the detection of H_2O_2 after its oxidation. The detection limit appears to be 100 µM. This is greater than the detection limit for CPt electrodes. A possible reason for this might be that the platinum electrodes contaminate more easily compared to the CPt samples. A result like this is peculiar, in a study conducted by Pleskov et al. they compared platinum electrodes with platinum alloyed DLC electrodes. According to their study the pure platinum electrodes detected H_2O_2 better than the alloyed ones.[11].

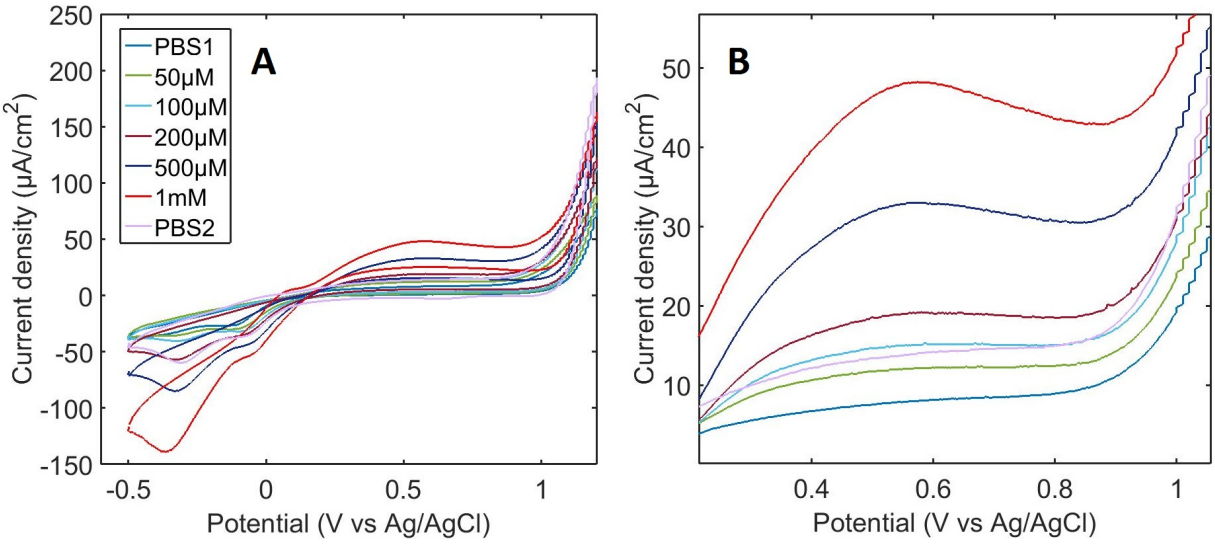

Figure 35 – H_2O_2 measurements with a platinum sample (A) with the scan rate of 50mV/s. (B) is the close-up from the oxygen end of the voltammogram.

In the close-up of the oxygen end of the voltammogram (Figure 35B) it can be seen that in the PBS cycling after the H_2O_2 measurements the background current was greater compared to the PBS curve before the measurements. This usually indicates that some changes have happened on the surface of the electrode. In this case it is most likely caused by oxides accumulating onto the surface, but it may also indicate some analyte left-overs or impurities that have adsorbed onto the surface.

Hydrogen peroxide detection with AuNP electrodes

The H_2O_2 measurements with AuNP samples are presented in Figure 36 for method a and in Figure 37 for method b. The voltammograms of the electrodes are very similar to each other. The oxidation of H_2O_2 causes a peak at +0.5 V (vs Ag/AgCl) and the detection limit for AuNP(a) is 200 µM and for AuNP(b) 50 µM.

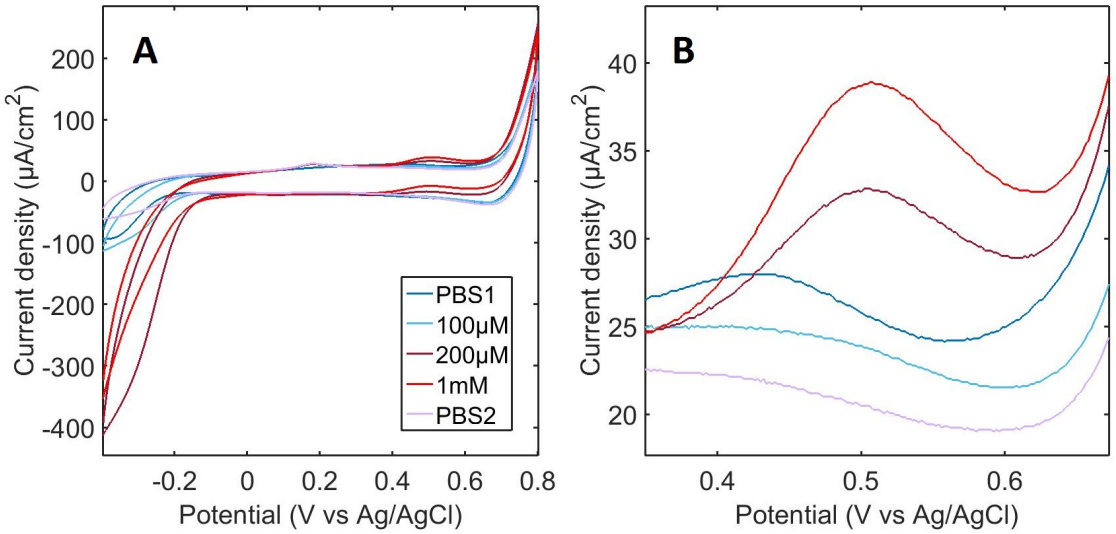

Figure 36 – H_2O_2 measurements with AuNP(a) (A). Scan rate of 50mV/s was used during the measurements. (B) is the close-up of the H_2O_2 detection.

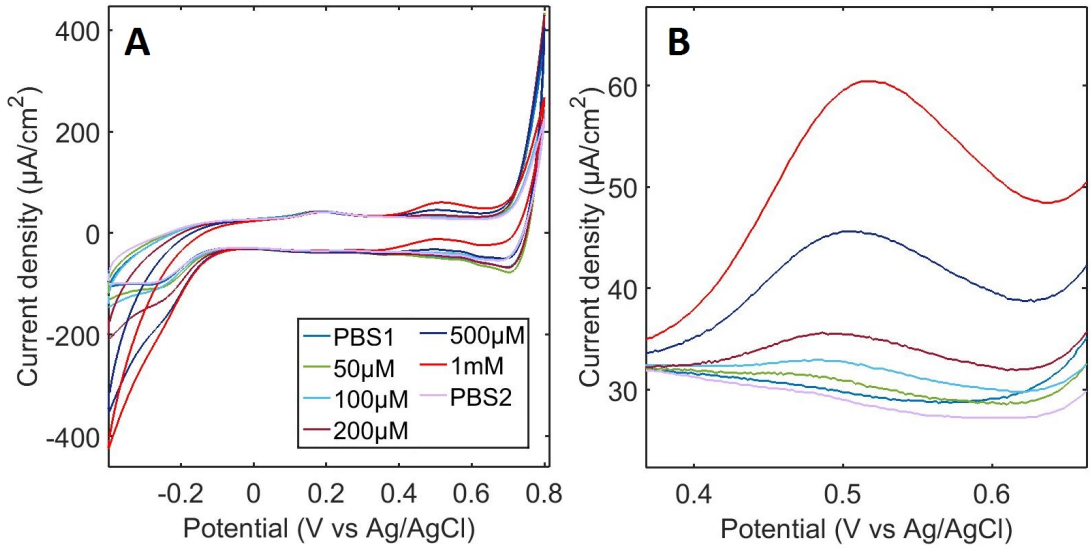

Figure 37 – H_2O_2 measurements with AuNP(b) (A). Scan rate of 50mV/s was used during the measurements. (B) is the close-up of the H_2O_2 detection.

The combined peak for oxygen reduction and hydrogen evolution (at -0.2 V) grew quite big with the larger concentrations of H_2O_2. Also the peak for oxygen evolution was quite big compared to the detection peak of H_2O_2. For future studies it might be good to reconsider the upper scan limit of the measurements in order to avoid the interference of excess oxygen in the solutions.

A major problem with the AuNP samples was that the surface was not stable. The color of the sample changed after the electrochemical measurements which would indicate detachment of the nanoparticles from the surface. Amperometry might be

more gentle towards the surface compared to cyclic voltammetry and hence it was used with an AuNP(a) sample. The results of the measurement are presented in Figure 38.

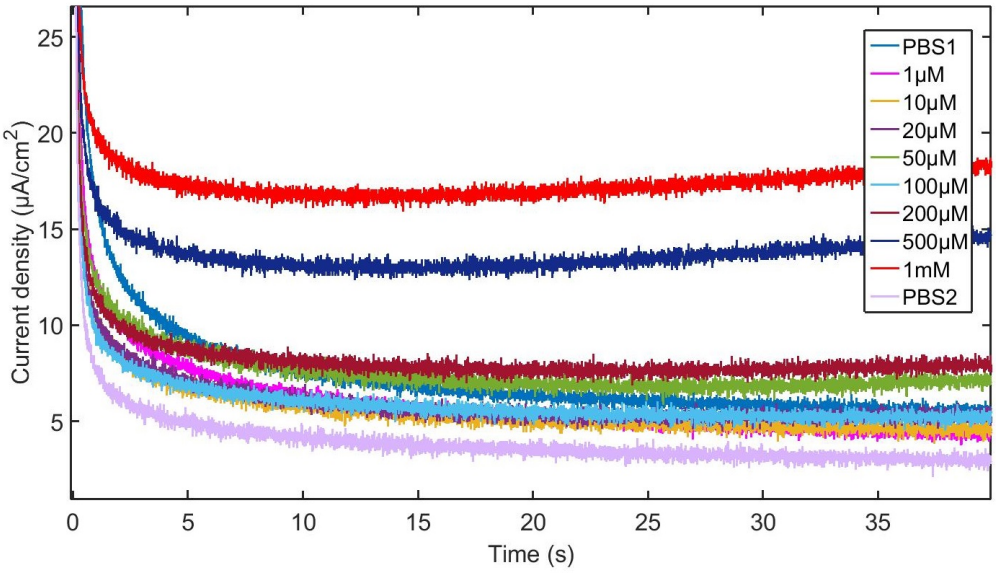

Figure 38 – Amperometry with an AuNP(a) sample in different concentrations of H_2O_2. The potential was held at +0.7 V (vs. Ag/AgCl) for 180 s.

The detection limit according to the amperometric measurements would be 500 μM. The potential during the measurement was held constant at +0.7 V (vs. Ag/AgCl) which might have been a bit too high because the current increased with time. Figure 38 presents only the first 40 seconds of the measurement, the whole figure can be seen in the appendix. The increasing current most likely indicates oxide formation on the surface. The sensitivity (change of current density per unit concentration of H_2O_2) was calculated to be 10.5 nA/cm^2·μM (R=0.9907). This was lower comparing to the AuNP sensor (composed of gold nanoparticles electrodeposited onto the surface of an DLC electrode) fabricated by Liu et al. which had the sensitivity of 48.4 nA/cm^2·μM [30]. The linearity of sample can not be evaluated properly with this few data points.

The detachment of the particles was confirmed with SEM imaging, the micrographs are presented in Figure 39. Figure 39A presents an AuNP(a) sample before any measurements were conducted with it. Figure 39B shows the surface of an AuNP(a) sample after the characterization in H_2SO_4. The amount of gold nanoparticles has clearly decreased. The deposition of the nanoparticles was made in a solution of H_2SO_4, which could explain the detachment of the particles in the H_2SO_4 characterization. Of course considering the final application, measurements in H_2SO_4 are not that relevant. Cycling in acids has been used for sample cleaning though. Figure 39B shows that this is not the best choice for the AuNP samples.

Figures 39C and 39D are micrographs of AuNP surfaces after cyclic voltammetry and amperometry measurements in H_2O_2 respectively. The total amount of the

nanoparticles seems to have decreased, also some of the particles have increased in size. This aggregation of the particles is most likely caused by the same phenomenon as the aggregation of the particles during longer deposition times. Due to the high surface energy of nanoparticles they tend to aggregate. During electrochemical measurements some of the gold nanoparticles might have detached and fused into other particles nearby. The smaller particles present on the surface are probably gold nanoparticles with better attachment and therefore not affected by the electrochemical measurements as much. Amperometry would seem to be more gentle towards the surface judging by the figures. Which is good considering the final application. Still detachment of the gold nanoparticles during measurements would lead up them leaching to the surrounding and decreasing the biocompatibility of the sensor remarkably.

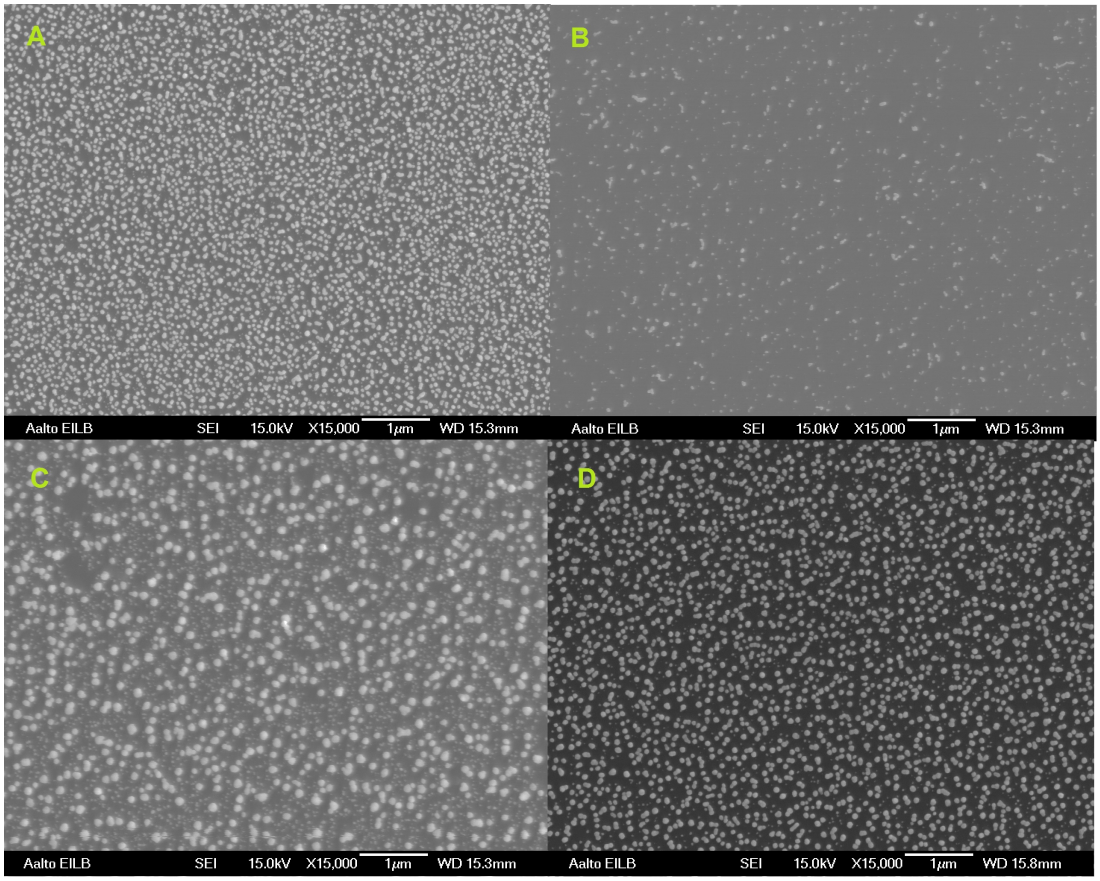

Figure 39 – SEM micrographs of AuNP(a) samples (A) before and (B-D) after electrochemical measurements. (B) is the surface of an AuNP(a) sample after cyclic voltammetry in 0.15 M H_2SO_4. (C) represents the surface after cylic voltammetry in H_2O_2 and (D) after amperometry in H_2O_2.

H_2O_2 detection with CPt and platinum samples after layer depositions

After the SAM and polymer layer depositions the measurements with H_2O_2 were repeated with the same set-up and parameters as earlier except the upper scan limit

was lowered from 1.2 V to 0.8 V (with the exception of Pt/TESPSA and PANI samples where the upper scan limit remained 1.2 V).

Two types of layers were used with both of the SAM layers. The first one was made from 7% solution and the second one was made from 10% solution. The 10% samples were either better or as good as the 7% samples in H_2O_2 detection. Therefore the sample types with 10% SAM layer deposited onto them were chosen for the glutamate measurements. APTES layer will functionalize the surface with amino groups and TESPSA with carboxyl groups.

With PANI layers also two different thicknesses were tried, a thin layer (35 cycles for platinum based samples and 30 cycles for AuNP samples) and a thick layer (70 cycles). For CPt/PANI the detection limit for the thin layer was 100 µM and 500 µM for the thick layer. For Pt/PANI samples the detection limit was 1mM for the thin layer and no detection for the thick one. Like mentioned earlier the deposition of PPy succeeded only with the second method. After the layer deposition the detection limit for CPt/PPy and Pt/PPy samples were 100 µM. The voltammograms of CPt and platinum samples with 10% SAM layers and polymer layers are presented in Figures 40 and 41 respectively.

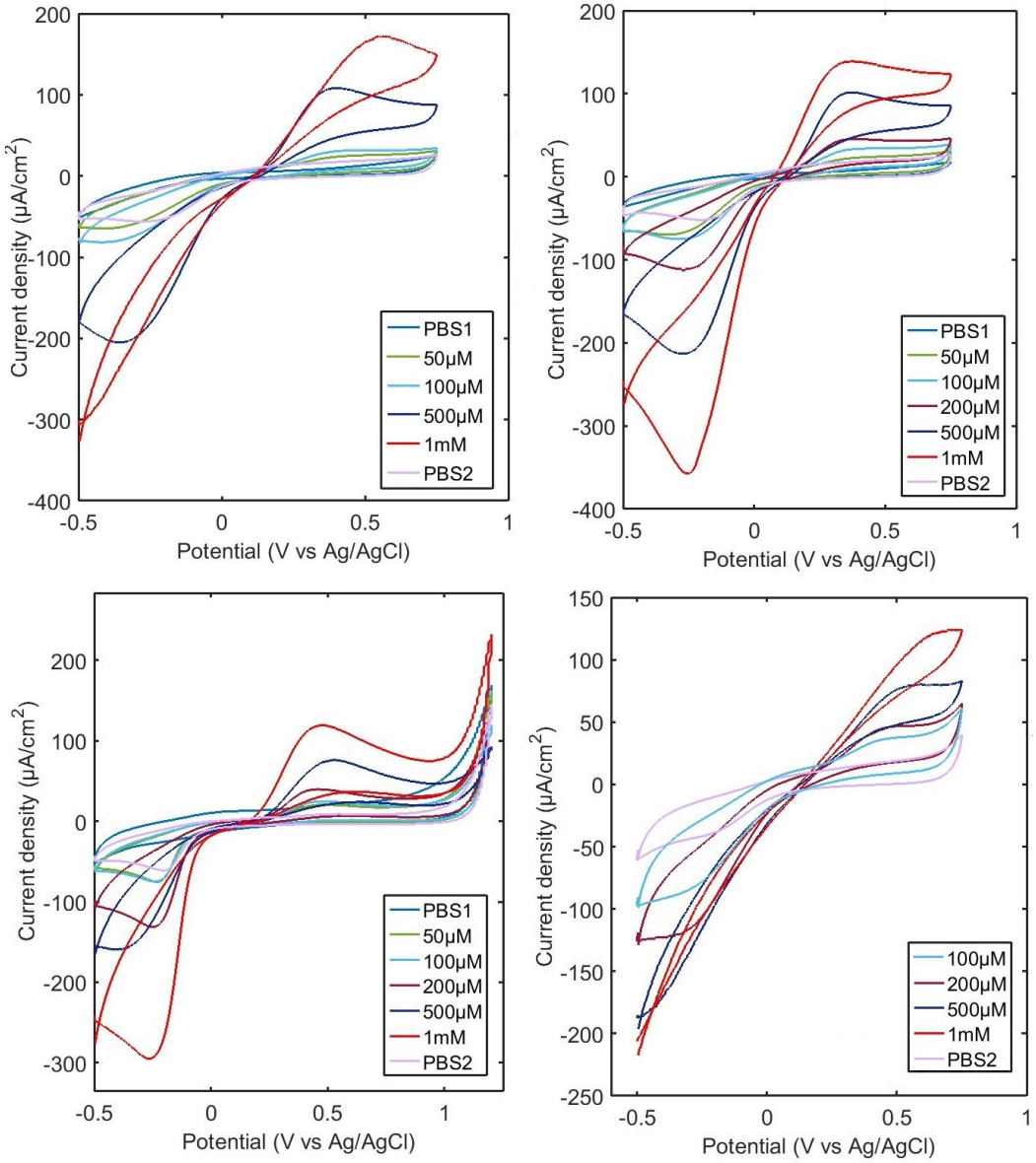

Figure 40 – H_2O_2 measurements conducted with (A) CPt/APTES (B) CPt/TESPSA (C) CPt/PANI(35) (D) CPt/PPy samples. The measurements were conducted under nitrogen atmosphere with the scan rate of 50 mV/s.

The oxidation of H_2O_2 is clearly visible on the anodic side of the curves. A cathodic peak which is the combination of H_2O_2 and O_2 reduction reactions is also present in all of the voltammograms presented in Figure 40. In the voltammogram of H_2O_2 measurements with CPt/PPy sample the first PBS curve is not presented.

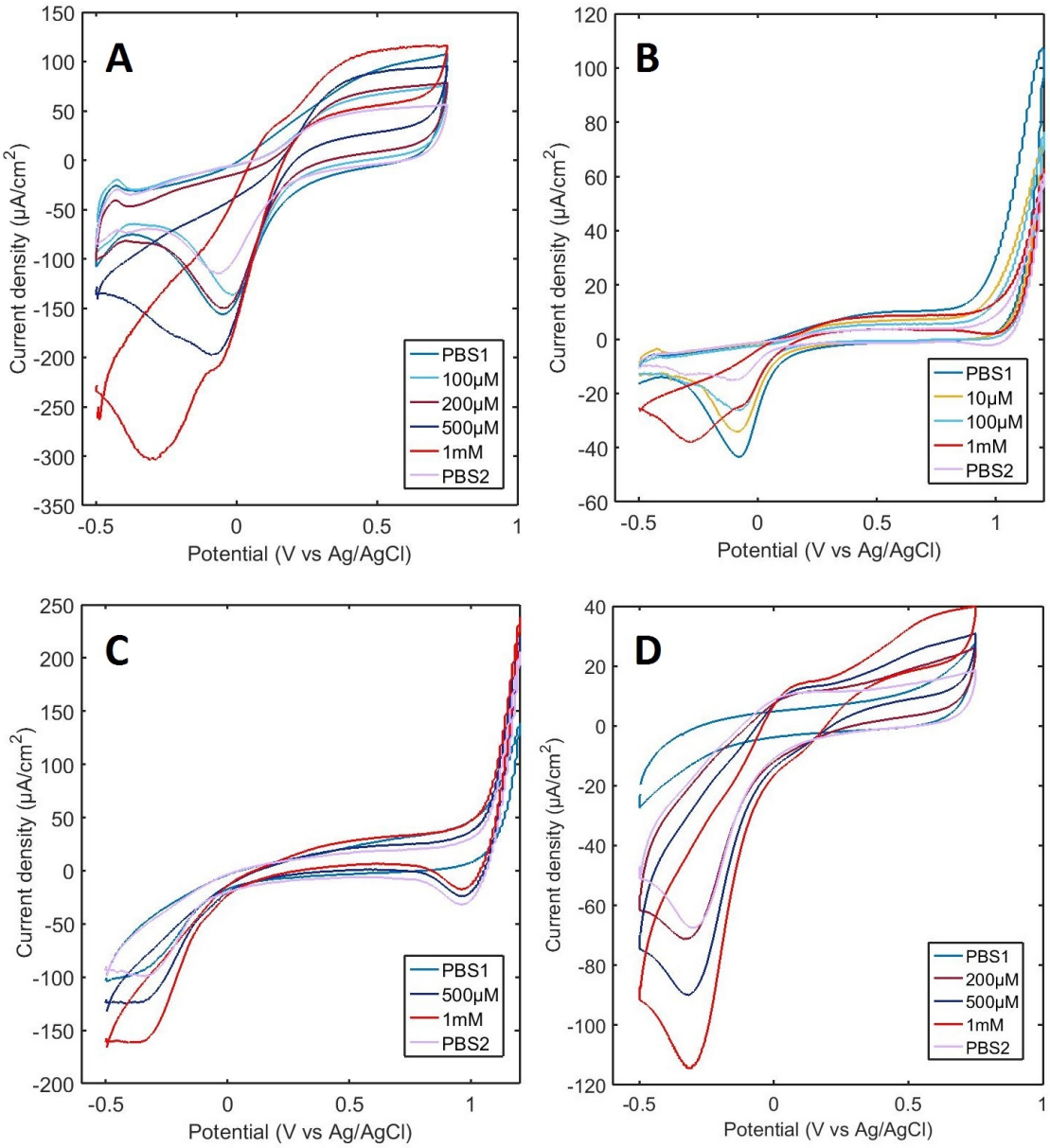

Figure 41 – H_2O_2 measurements conducted with (A) Pt/APTES (B) Pt/TESPSA (C) Pt/PANI(35) (D) Pt/PPy samples. The measurements were conducted under nitrogen atmosphere with the scan rate of 50 mV/s.

The measurements with platinum samples did not turn out to be what was expected. Firstly the platinum samples did not detect H_2O_2 nearly as good as it was originally assumed based on the literature review [8]. Secondly the voltammograms had some peculiar features.

Figure 41A is the voltammogram of Pt/APTES sample. The peak at 0 V represents the reduction of oxides which then combines with the reduction reaction of oxygen

in the bigger concentrations of H_2O_2. The effect of the excess oxygen presented in chapter 2.2 is visible with the curves 500 µM and 1 mM, the curves have shifted below the zero-current axis at potentials less than 0 V. This effect is also present in the other voltammograms (Figure 41B-D). Also the peak for hydrogen desorption is visible in the voltammogram of Pt/APTES. As clear characteristic features are not present even in the H_2O_2 measurements of the platinum sample in Figure 35. Despite the clear presence of platinum the Pt/APTES sample does not detect H_2O_2 at satisfactory levels.

The oxidation peak for H_2O_2 is not present in the voltammogram for Pt/TESPSA in Figure 41B. Pt/PANI(35) in Figure 41C showed a slight detection with the concentration of 1mM and Pt/PPy in Figure 41D seemed to detect H_2O_2 at the concentration of 100 µM.

An injection chronoamperometry measurement was also conducted on a CPt/PANI(35) sample presented in Figure 42. The red arrows mark the injection of 10 mM H_2O_2 solution to the cell. After 700 s the current starts to decrease after the increase caused by the H_2O_2 injections. This might be an indication of delamination of the PANI layer.

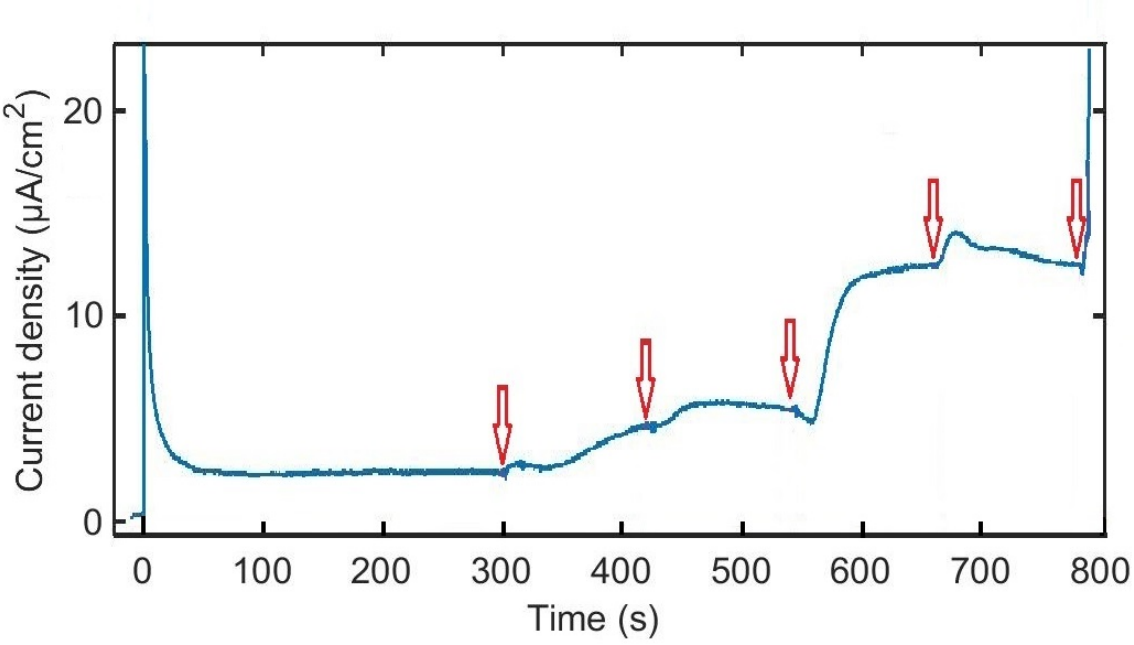

Figure 42 – H_2O_2 injection amperometry for a CPt/PANI(35) sample.

The result of the chronoamperometry measurement does not answer the question whether the polymer layer works as a diffusion barrier or not. Firstly of course the PANI layer formed was not proper and most likely got delaminated at least partially in the end of the experiment. Secondly no stirring was used during the measurement, which made the reaction diffusion limited. This is also detectable in the curve, the current response to the injections of 10 mM H_2O_2 is relatively erratic compared to the results of similar kind of measurements found in the literature [30, 76]. For future

experiments the measurement set-up should be improved either by using stirring or by using a rotating working electrode in order to control the mass transport process.

H_2O_2 detection with AuNP samples after polymer layer depositions

Like mentioned earlier the gold nanoparticles detached from the surface of AuNP samples during the sonication in DI-water and hence SAM layer deposition was not able to be performed with them.

The voltammograms of H_2O_2 measurements for AuNP(a)/PANI(30) and AuNP(b)/PANI(30) are presented in Figure 43A and B respectively. As can be seen in the figures the samples did not detect H_2O_2 and neither did the samples with the thick PANI layer (figures not shown). Therefore the AuNP/PANI samples were not used in glutamate measurements.

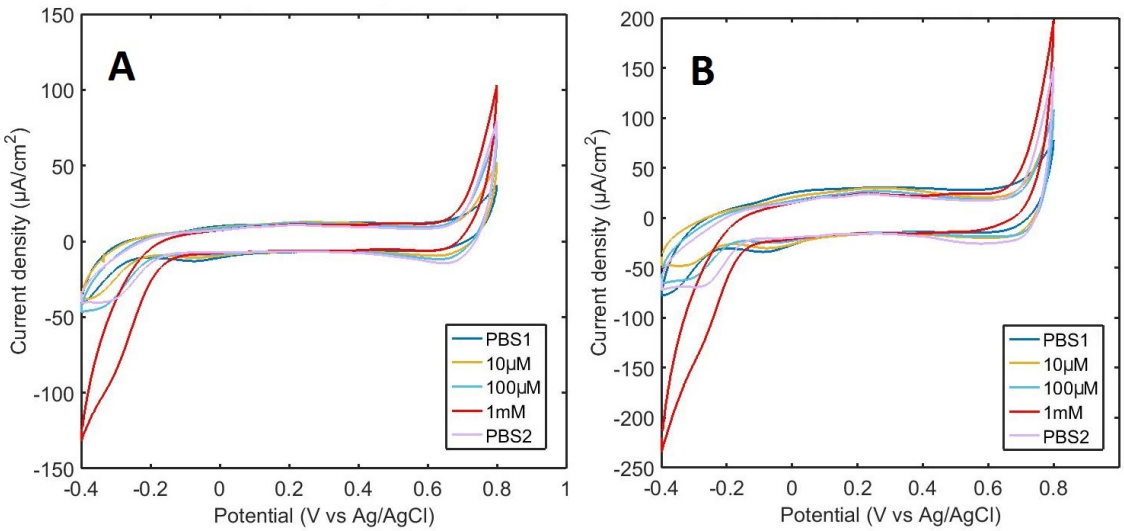

Figure 43 – H_2O_2 measurements conducted with AuNP/PANI samples. (A) AuNP(a) with the thin PANI layer deposited onto it and (B) AuNP(b) sample also with the thin PANI layer.

The voltammograms with AuNP/PPy samples seemed bizarre. Some curves from the measurements with AuNP(b)/PPy is presented in Figure 44. The current decreased with each curve until it stabilized to a curve which resembled the characteristic curve of a pure DLC electrode presented in the theoretical part of this thesis in Figure 8. This would suggest that the layer got peeled off during the measurements and with the AuNP samples the gold nanoparticles with it.

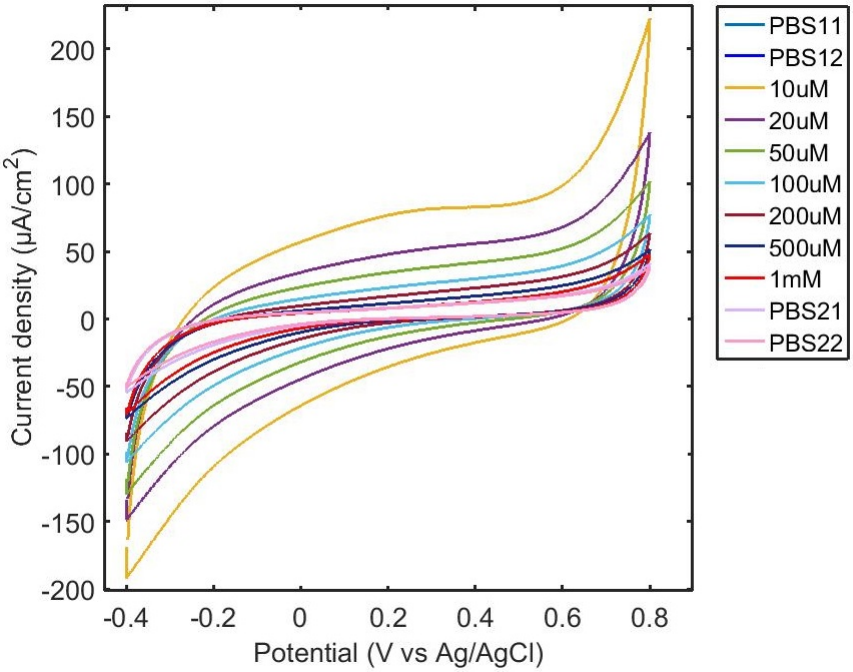

Figure 44 – The voltammogram of the H_2O_2 measurements conducted with an AuNP(b)/PPy sample. It is clearly visible how the current gets smaller and smaller during each measurement.

The delamination of the PPy layer was later on confirmed with SEM images of a CPt/PPy sample presented in Figure 45. It presents the surface of a CPt/PPy sample prior to the measurements (Figure 45A) and after them (Figure 45B). It is clearly visible that there are only traces left of the PPy layer on the sample after H_2O_2 measurements.

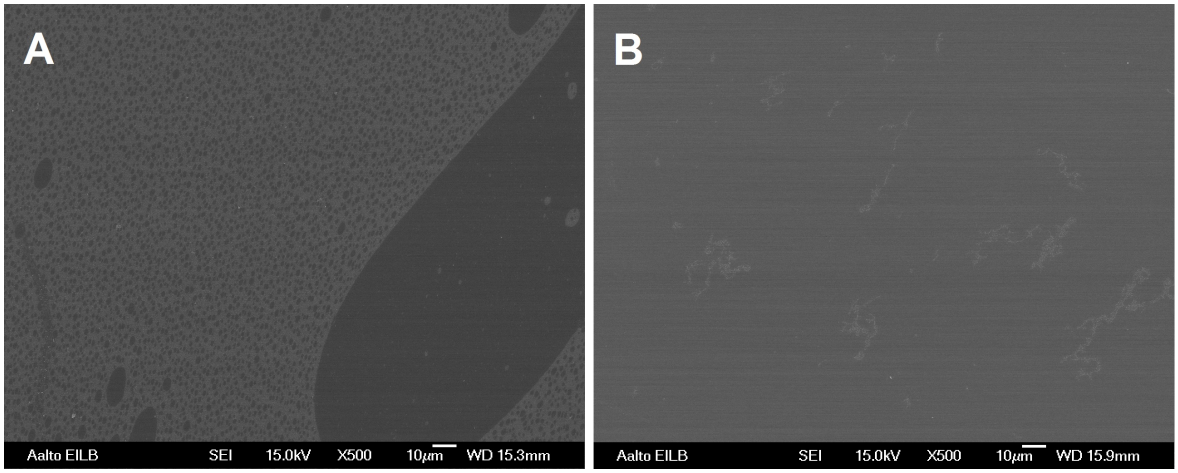

Figure 45 – (A) is the micrograph of a CPt/PPy sample surface presented also earlier in this thesis. (B) is a micrograph of a CPt/PPy sample after H_2O_2 measurements.

A summary of the detection limits for H_2O_2 of the different sample types is presented in Table 9. For polymer layers these results should be interpreted with caution because no uniform proper polymer layers were manufactured. The detection limit might be the 'real' detection limit of the layer deposited or give out the point where the layer was peeled off enough to let H_2O_2 properly through.

Table 9 – Detection limits for H_2O_2 of different sample types.

Sample type	**No layer**	**APTES (7%)**	**APTES (10%)**	**TESPSA (7%)**	**TESPSA (10%)**	**PANI (thin)**	**PANI (thick)**	**PPy**
CPt	50 µM	50 µM	50 µM	50 µM	20 µM	100 µM	500 µM	100 µM
Platinum	100 µM	200 µM	100 µM	1 mM	1 mM	1 mM	-	100 µM
AuNP(a)	200 µM	-	-	-	-	-	-	-
AuNP(b)	50 µM	-	-	-	-	-	-	-

6.2.3 Measurements with glutamate

Like in the previous chapters only the relevant curves are presented in the figures, the complete voltammograms can be found in the appendix. The results for CPt/PPy/GlOx and Pt/PPy/GlOx samples are not presented because the detachment of the PPy layer during the measurements.

Some peculiar and disappointing results were obtained with the GlOx samples. None of them seemed to detect any glutamate during the measurements with cyclic voltammetry, voltammograms are presented in Figures 46 and 47 for CPt and platinum samples respectively. This was unexpected specially with the CPt samples which performed well in the H_2O_2 measurements presented in Figure 40.

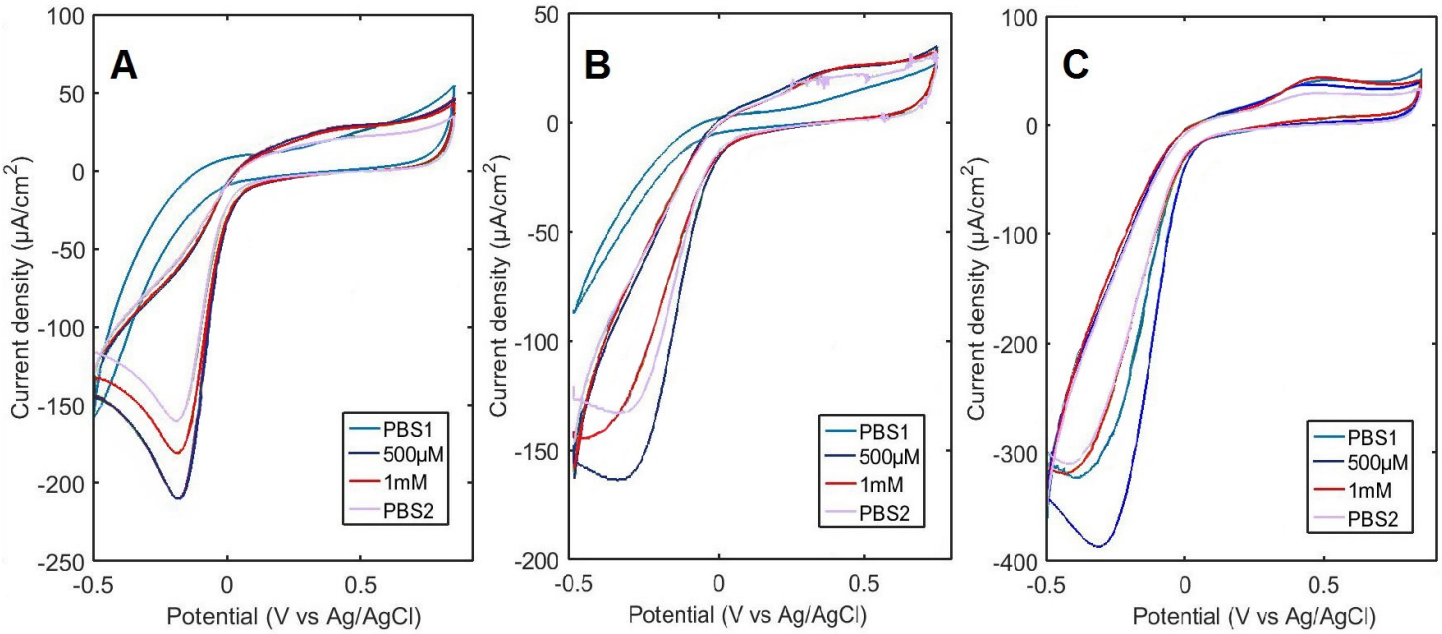

Figure 46 – Glutamate measurements with (A) CPt/APTES/GlOx (B) CPt/TESPSA/GlOx and (C) CPt/PANI(35)/GlOx samples with the scan rate of 50 mV/s.

The fact that CPt/APTES/GlOx sample did not detect any glutamate was disappointing. Previous studies of the group have lead to a functional CPt/APTES/GlOx sensor with the detection limit of 10 µM of glutamate and storage stability up to 7 weeks (in +4 °C) [12]. One possible reason for the unsuccessful sensor manufactured for this thesis could be that CPt electrodes were manufactured with slightly different methods. The one used by Kaivosoja et al. had a constant concentration of platinum throughout the DLC layer [12]. This could affect the surface of the CPt sample and thereby have an effect on the APTES layer formation. Inadequate APTES layer may still let H_2O_2 through, but inhibit the immobilization of GlOx. This would also explain the inconsistency between the H_2O_2 and glutamate measurements. The suitability for glutamate detection with CPt/APTES samples would need futher investigation.

The solutions were not deoxygenized prior to the measurements because oxygen is needed in the enzymatic reaction of GlOx. The effect of excess oxygen can be seen in the hydrogen end in all of the CPt voltammograms. The curves have shifted clearly below the zero-current axis. The same shift is also present in the voltammograms of Pt/APTES/GlOx and Pt/PANI(35)/GlOx in Figures 47A and C.

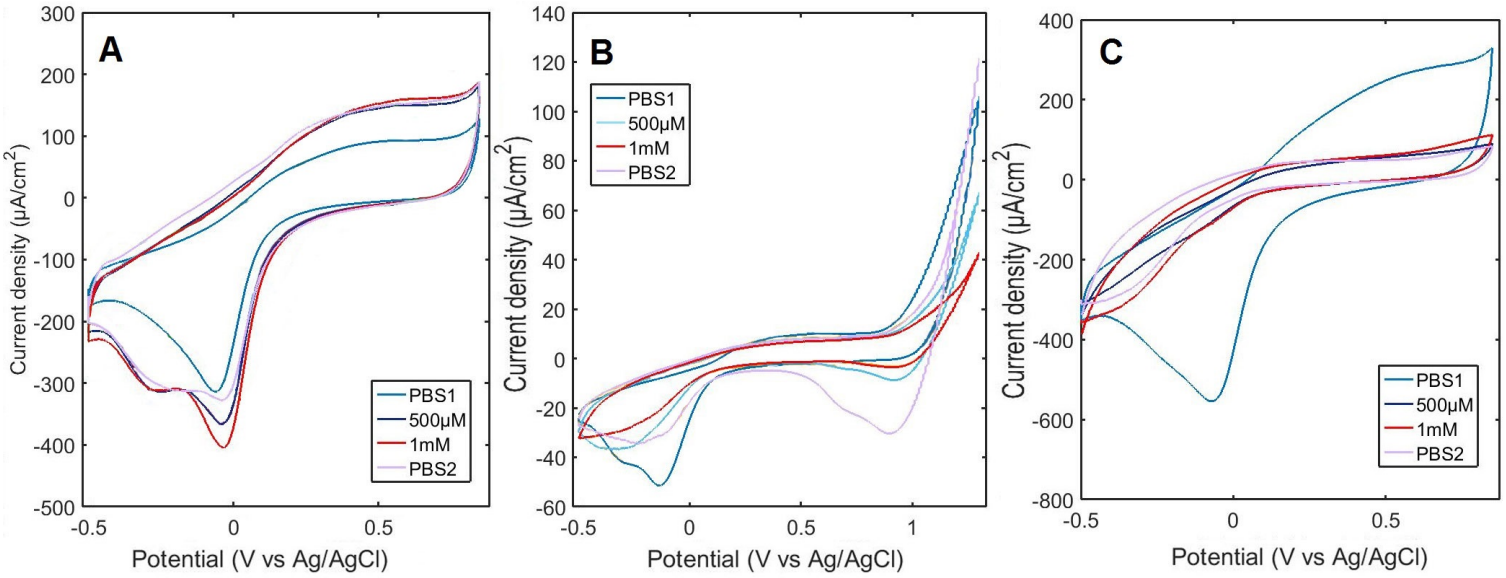

Figure 47 – Glutamate measurements with (A) Pt/APTES/GlOx (B) Pt/TESPSA/GlOx and (C) Pt/PANI(35)/GlOx samples with the the scan rate of 50 mV/s.

Some characteristic features of platinum are present in the voltammograms presented in Figure 47, like the sharp cathodic peak of oxide and oxygen reduction reactions at about 0 V. For some reason this peak disappears after the first PBS measurements with Pt/TESPSA/GlOx and Pt/PANI(35)/GlOx samples.

In addition to the poor performance in the glutamate measurements the storage stability of the GlOx samples was unsatisfactory. The first disturbances in the curves were seen already in the first measurements with CPt/TESPSA/GlOx sample in the Figure 46B. The samples had been submerged for one day in PBS (at +4 °C). The poor storage stability had not been a problem in the previous studies of the group. All of the GlOx samples prepared for this thesis were destroyed within two weeks. The reason for this was the taping method. In the previous samples the Teflon tape was not deposited on itself. The experiment demonstrated that the adhesion between the tapes was not sufficient which lead to PBS leaking underneath it and destroying the samples. The taping method used for the samples in this thesis is presented in Figure 48A and the technique used in the previous experiments is presented in Figure 48B. The new method was adopted due to the tape breaking in the sharp edges of the sample corners. It is functional in short-term measurements but long-term immersion of the samples will lead to sample breakdown.

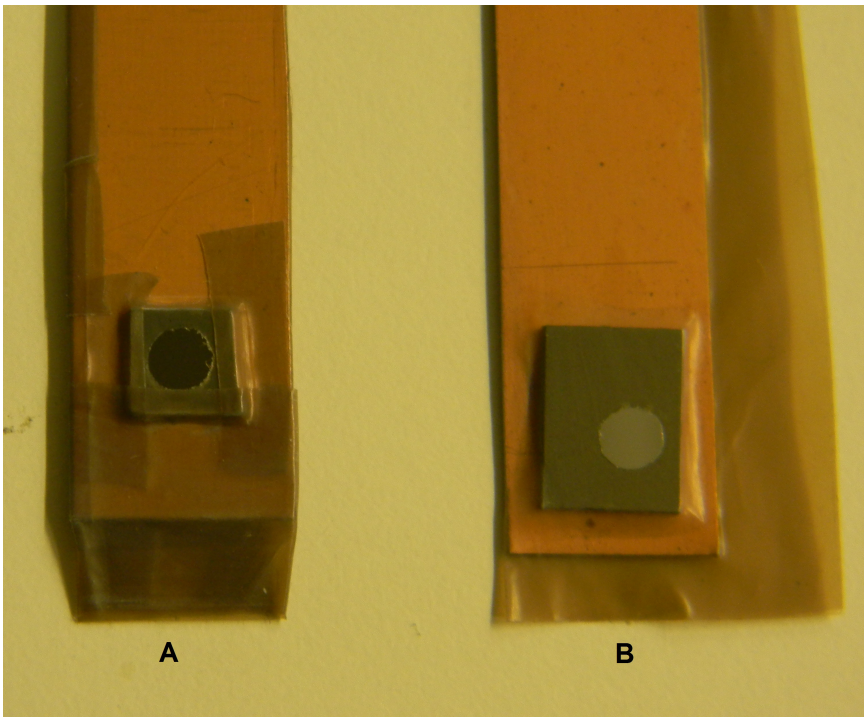

Figure 48 – In the newer taping technique (A) the corners of the samples are reinforced with multiple layers of tape. The poor adhesion between the tape layers leads to the measurement solution leaking between the layers and breaking the sample. In the older technique (B) only the adhesive surfaces of the once folded tape touch each other resulting in a more insulating structure.

Chronoamperometry measurements were also conducted with the GlOx samples eight days after the immobilization. CPt/APTES/GlOx, Pt/APTES/GlOx and Pt/TESPSA/GlOx samples were already destroyed at this point so no proper data was collected with them. The results from the rest of the samples are presented in Figure 49. CPt/TESPSA/GlOx in Figure 49A shows a slight detection with the 500 µM and 1 mM solutions, with the sensitivity of 0.8 nA/cm^2·µM (R=0.9643). CPt/PANI(35)/GlOx presented in Figure 49B has the detection limit of 100 µM, though for some reason the detection of 10 mM solution was not in line with the other solutions. The sensitivity of the sample was 1.1 nA/cm^2·µM (R=0.8525) if disregarding the measurement with the 10 mM solution. With the 10 mM solution the sensitivity would be 0.05 nA/cm^2·µM (R=0.1823). Figure 49C presents the results from the measurement with Pt/PANI(35)/GlOx and it is presented here merely to show that the sample could not detect any glutamate.

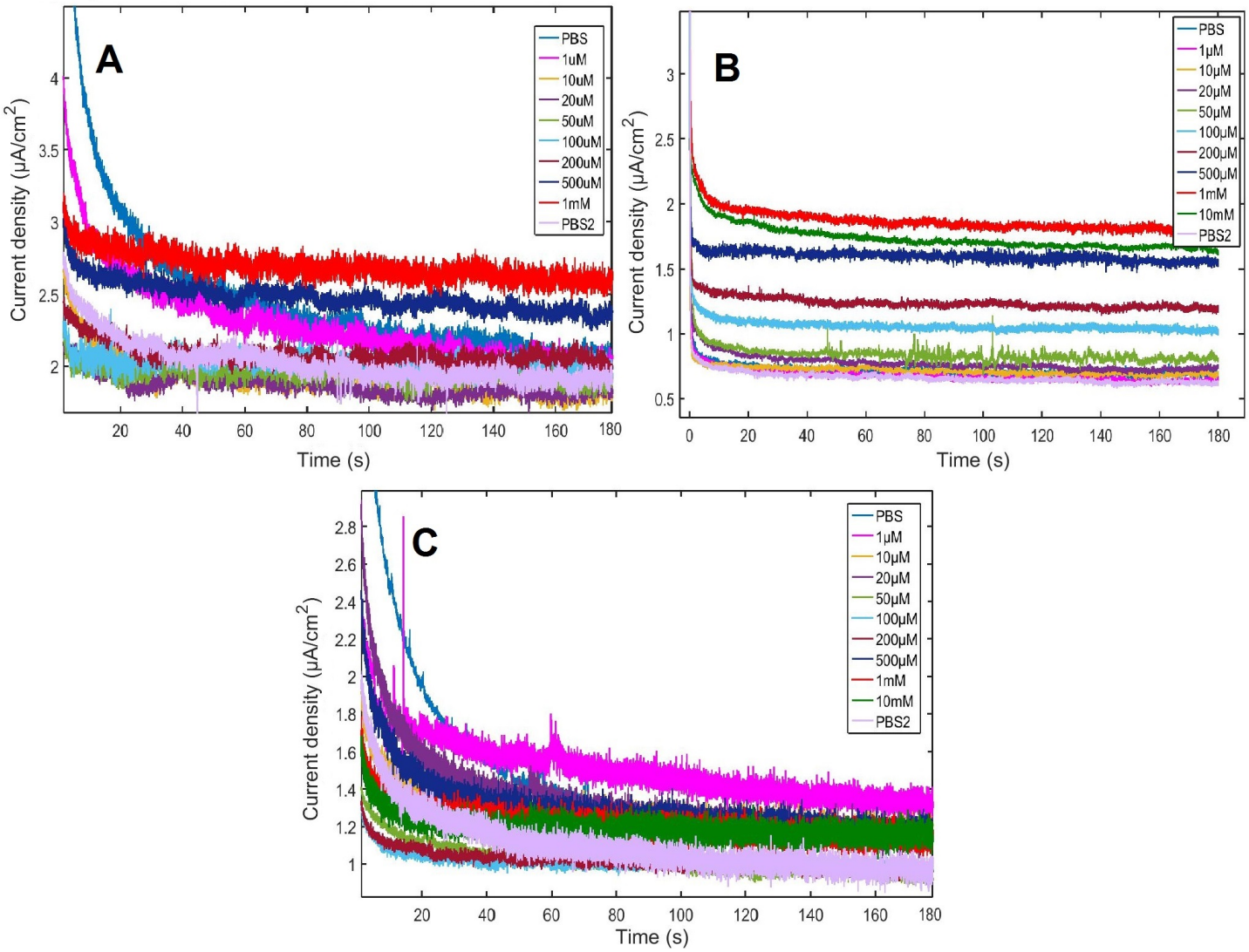

Figure 49 – Chronoamperometry with (A) CPt/TESPSA/GlOx, (B) CPt/PANI(35)/GlOx and (C) Pt/PANI(35)/GlOx. The potential was kept at +0.65 V (vs Ag/AgCl) for 180 s.

The taping problem does not explain the insensitivity for glutamate. The obvious reason would be a mistake made in the immobilization process. This is not likely though because the enzyme activity samples were immobilized at the same time with the same solutions. The immobilization on them was mostly successful as can be seen in chapter 6.3.

It was also suspected that the TESPSA solution was old and hence a proper SAM layer was not formed inhibiting the enzyme immobilization. The problem with the PANI samples could be a result of the poor adhesion between the layer and the surface, which resulted in a partial delamination of the polymer with the enzymes. One must also take into account that no doubles were used in this experiment. The use of parallel samples would lead to more reliable results. Unfortunately it was not possible within this time window. The results of the glutamate measurements are

summarized in Table 10.

Table 10 – The detection limit for glutamate for different sample types.

Sample type	APTES	TESPSA (CV/CA)	PANI (CV/CA)
CPt	-	- / 500µM	- / 100 µM
Platinum	-	-	-

6.3 Enzyme activity measurements

The results of the enzyme activity measurements are presented in Figures 50 and 51. Figure 50 presents the samples which were manufactured with the GlOx samples used in the electrochemical measurements. In addition of the sample types used in the electrochemical measurements, GlOx was also immobilized onto a gold sample with an APTES (10 %) layer deposited onto it (referred as Au/APTES). When handeled with care and not used in the electrochemical measurements, the gold film did not delaminate from the Au/APTES sample.

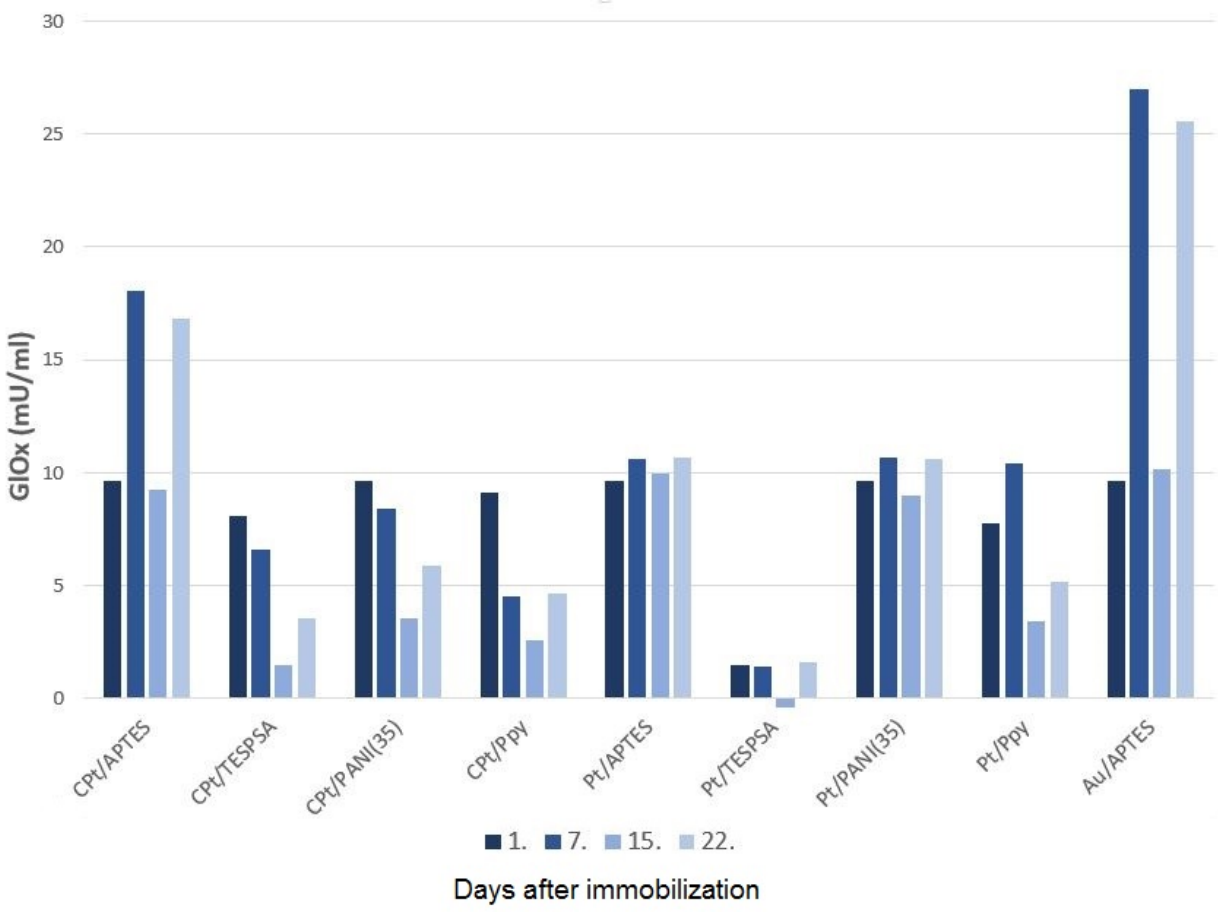

Figure 50 – Results of the enzyme activity measurements.

Apart from SiPt/TESPSA/GlOx the immobilization succeeded in all of the samples and they showed decent activity in the first activity measurement. Clear differences in the stability of the enzyme immobilization are noticeable in the results. The activity on APTES samples remained stable which is consistent with the literature [12]. TESPSA samples turned out to perform suprisingly poorly. This gives more reason to doubt that there was a problem with the TESPSA layer deposition or with the solution itself.

GlOx remained active immobilized onto the Pt/PANI sample, but not on the CPt/PANI sample. Like presented in chapter 6.1.2 the deposition of PANI was more successful on platinum compared to CPt. It is possible that the deposited PANI layer on CPt had delaminated with the immobilized enzymes. With PPy the layer seemed more stable on CPt than on platinum. This is not noticable in the activity measurements with the PPy samples, both of them seem to loose enzyme activity during the course of measurements.

The activity seems to fluctuate especially with the CPt/APTES/GlOx and SiAu/APTES/GlOx samples. This is most likely caused by the fact that their activity reached above the linearity range of the kit. The kit was reported to be linear up to 10 mU/ml of GlOx. For futher studies the linearity above this point could be evaluated by making a set of GlOx solutions with greater concentrations. The problem may also be solved by immobilizing less enzyme onto the samples and hence reducing the activity. This method would work with sample types that have shown good activity in previous experiments.

The smaller fluctuations present in the activity data of the samples are caused due to the differences of the activity kits used. The activity of the sample is always calculated from the standard line and small variations may occur between each set. The trend of the stability can still be evaluated.

The surface of DLC has been reported to have some carboxyl groups on it [77]. To evaluate if there would be enough of them for enzyme immobilization, GlOx was also immobilized directly onto a CPt sample. A CPt/TESPSA sample was used as a reference sample. The results of the activity measurements are presented in Figure 51.

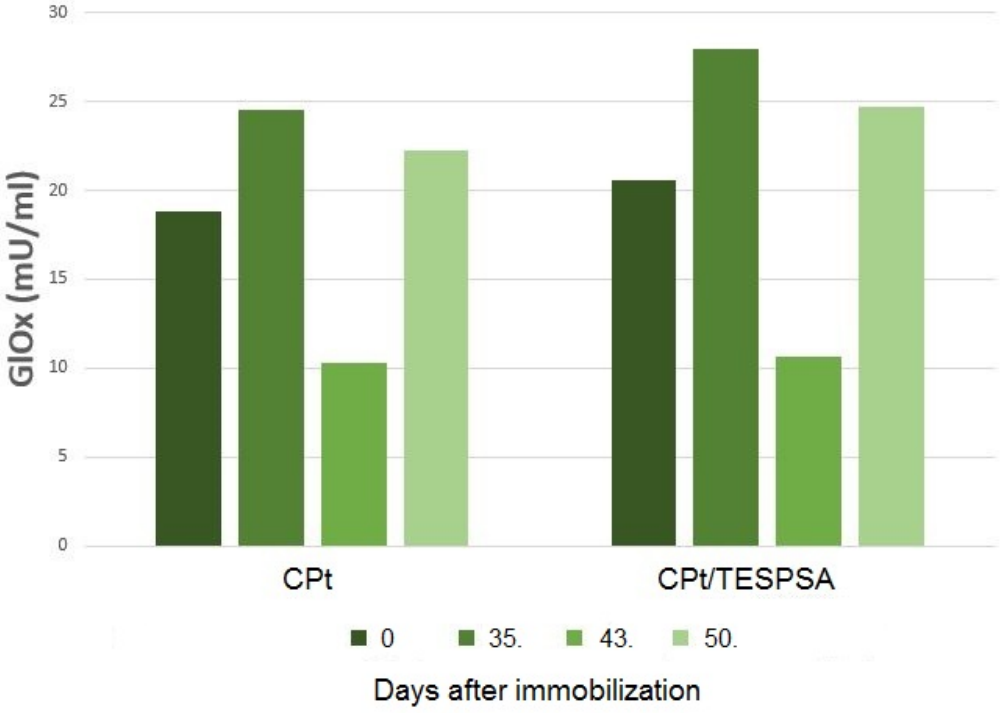

Figure 51 – Enzyme activity measurement results with CPt/GlOx and CPt/TESPSA/GlOx samples.

The activity of the enzymes seems to be above the linerity range once again which indicates a successful immobilization. The contradiction between the results of the CPt/TESPSA samples presented in Figures 50 and 51 may be caused by the agening of the TESPSA solution. Aged solutions may not give as repeatable results as fresher ones. It may also indicate that something went wrong in the TESPSA deposition for the other GlOx samples.

No doubles were used in the activity measurements. To minimize random errors during the process and thereby receiving more reliable data, replicates of the sample types should be used in future studies.

6.4 Summarized suitability evaluation of the sample types for an amperometric sensor.

The performance of CPt and platinum samples in the measurements conducted for this thesis is summarized and visualized in Table 11. The green color indicates promising results for an amperometric sensor, purple satisfactory and the red color indicates poor performance in the measurements. The white cells mean that the measurement was not performed with the sample type in question.

Table 11 – Summary of the measurement results conducted with CPt and platinum samples.

Sample type	Detection of H_2O_2	Detection of glutamate (CV/CA)	Enzyme activity
CPt	50 µM		Good
CPt/APTES	50 µM	-	Good
CPt/TESPSA	20 µM	- / 500 µM	Good
CPt/PANI(35)	100 µM	- / 100 µM	Poor
CPt/PPy	100 µM	-	Poor
Pt	100 µM		
Pt/APTES	100 µM	-	Good
Pt/TESPSA	1 mM	-	Poor
Pt/PANI(35)	1mM	- / -	Good
Pt/PPy	100 µM	-	Poor

CPt seems to be a promising electrode material for an amperometric sensor. It performed well in the H_2O_2 measurements with APTES and TESPSA layers. Also the enzymes seemed to remain stable after immobilization on the CPt/APTES sample. CPt/TESPSA performed poorly in the activity measurements presented in Figure 50 but the activity of the enzymes remained stable in the measurement presented in Figure 51. This may indicate that the TESPSA layer deposition did not succeed in the first experiment or it may suggest that the reproductibility of the TESPSA layer deposition is poor. Of course CPt/TESPSA was the only type that had a duplicate in the measurements, therefore no reproductibility evaluation can be made from the other sample types. The electrochemical measurements with glutamate were unsuccessful and hence it would require further studies for the proper evaluation of them.

The adhesion of the polymers was inadequate. This makes it difficult to assess the performance of the sample types with PANI and PPy. The layers got mostly delaminated from the samples used in the electrochemical measurements, still somehow the detection limit for glutamate in the amperometric measurement with CPt/PANI(35) was 100 µM. The sensitivity of the sample was poor though, 0.05 $nA/cm^2 \cdot \mu M$ (R=0.1823).

The performance of the uncoated CPt samples is also promising and specially intriguing when bearing in mind that the H_2O_2 could also be detected by its reduction. An inconsistency can be observed in the H_2O_2 measurements with uncoated CPt and CPt/TESPSA. The detection limit for CPt/TESPSA is lower than the detection

limit for the CPt sample. The upper scan limit was + 1.2 V with the CPt sample and +0.8 V with the CPt/TESPSA sample. The detection of H_2O_2 may be enhanced by lowering the upper scan limit for the CPt in the measurements.

Platinum samples did not perform well in the electrochemical measurements conducted for this thesis. The only promising results with the platinum samples were obtained from the enzyme activity samples with the APTES and PANI layers. The overall good performance of APTES samples in the enzyme activity measurements is in line with the prior studies of the group.

Like mentioned before the stability of the electrodeposited gold nanoparticle layer on the AuNP samples needs remarkable improvement until they can be used as an electrode in the electrochemical measurements. The results show nevertheless that the electrochemical activity of DLC can be improved by doping it with platinum or by deposition of gold nanoparticles onto it.

7 Conclusions

CPt seems to be a promising electrode material for glutamate detection. Oxidation was clearly detectable, though the detection limit was not low enough for *in vivo* applications. Clear peaks were also observed at the cathodic potentials with the samples. Even though the peaks observed in the measurements made for this thesis are a combination of H_2O_2 reduction and oxygen reduction reactions, it could be possible to use the H_2O_2 reduction for glutamate detection when using a smaller potential window in the measurements.

According to the literature review gold nanoparticles are an intriguing alternative for enhancing the electroactive features of DLC electrodes. In the experimental part of this thesis it was demonstrated that electrodeposition of gold nanoparticles directly onto the surface of DLC does not result in a durable structure. The gold nanoparticles will detach from the surface during the measurements reducing the biocompatibility of the electrode remarkably. A better deposition method needs to be developed before the suitability of AuNP electrodes for glutamate detection can be more accurately determined. Like mentioned earlier, linking gold nanoparticles with a SAM layer to the surface or depositing the particles with the polymer layer has proven to produce functional biosensors in other studies.

Deposition of PANI and PPy layers did not succeed in the experimental part of this thesis. The layer formation on CPt and platinum samples was quite different. On CPt the layer looked like it had not really even formed properly and the adhesion between the layer and the surface was weak. On platinum samples a layer had formed but it had cracked most likely during the drying phase after the deposition. No reference to similar observations was found during the literature review. Possible problems causing the insufficient adhesion between the polymer and the surface could be resolved by pre-treatment of the surface. The cracking after deposition might have been caused by the acid the polymerization was conducted in. Different deposition methods could also be tried to find a more suitable one.

The deposition of PPy layers was more successful on CPt samples than on platinum samples. An unhomogenous, holey layer was formed on the CPt samples. The layer endured the chromium sputtering process and imaging but got mostly peeled off during electrochemical measurements. The layer formation and most likely the adhesion between the polymer and platinum samples was inadequate. The images obtained from Pt/PPy surfaces showed only some remains of a layer. For future purposes different pre-treatments could be tried to modify the surface more applicable to PPy deposition.

Enzyme activity measurements gave probably a better view of the suitability of the polymer layers for GlOx immobilization than the electrochemical measurements with glutamate. According to those, glutaraldehyde conjugation on PANI layers gave promising results. Immobilization on PPy was not as enduring but the samples showed some activity nevertheless.

If the strategy for glutamate detection with CPt electrodes would be the reduction of H_2O_2 the electrode might not need a protective permselective layer at all. The enzyme immobilization could be done with the help of APTES or TESPSA layers or the enzyme could be immobilized directly onto the CPt surface without anything between the enzyme and the electrode. Currently the results on direct immobilization onto the surface are only preliminary but they show that the possibility should not be disregarded at this point.

References

[1] Smythies J. The neurochemical basis of learning and neurocomputation: the redox theory. Behavioural brain research 99: 1-6. 1999

[2] Meldrum, B. Glutamate as a neurotransmitter in the brain: review of physiology and pathology. The Journal of nutrition 130: 1007 -1015. 2000

[3] Danysz W., Parsons C., Bresink I., & Quack G. Glutamate in CNS Disorders. Drug News and Perspectives 261-277. 1995

[4] Platt S. The role of glutamate in central nervous system health and disease – A review. The Veterinary Journal 173: 278–286. 2007

[5] Qin S., van der Zeyden M., Oldenziel W., Cremers T., & Westerink B. Microsensor for in vivo Measurement of Glutamate in Brain Tissue. Sensors 8: 6860-6884. 2008

[6] Wahono N., Qin S., Oomen P., Cremers T., Vries M., & Westerink B. Evaluation of permselective membranes for optimization of intracerebral amperometric glutamate biosensors. Biosensors and Bioelectronics 33: 260-266. 2012

[7] Jamal M., Hasan M., Mathewson A., & Razeeb K. Disposable sensor based on enzyme-free Ni nanowire array electrode to detect glutamate. Biosensors and Bioelectronics 40: 213-218. 2013

[8] O'Neill R., Chang S-C., Lowry J., & McNeil C. Comparisons of platinum, gold, palladium and glassy carbon as electrode materials in the design of biosensors for glutamate. Biosensors & bioelectronics 19: 1521-1528. 2004

[9] Roy R. & Lee K-R. Biomedical Applications of Diamond-Like Carbon Coatings: A Review. Journal of Biomedical Materials Research Part B: Applied Biomaterials 72-85. 2007

[10] Suzuki M., Yamakawa K., & Saito T. Deposition Technology and Applications of DLC Films. JTEKT Engineering Journal 1008E. 2011

[11] Pleskov Y., Evstefeeva Y., Krotova M., Elkin V., Baranov A., & Dement'ev A. Electrochemical behavior of amorphous carbon films: kinetic and impedance-spectroscopy studies. Diamond and Related Materials 8:64-72. 1999

[12] Kaivosoja E., Tujunen N., Jokinen V., Protopopova V., Heinilehto S., Koskinen J., & Laurila T. Glutamate detection by amino functionalized tetradedral amorphous carbon surfaces. Talanta 141: 175-181. 2015

[13] Murtomäki L., Kallio T., Lahtinen R., & Kontturi K. Sähkökemia. Teknillinen korkeakoulu, 2nd edition. 2010. ISBN 978-952-60-3384-6

[14] Bard A. & Faulkner L. Electrochemical Methods: Fundamentals and applications. Wiley, 2nd edition, 2000. ISBN 978-0-471-04372-0

[15] http://www.gamry.com/products/accessories/reference-electrodes/ (14.8.2015)

[16] https://www.comsol.com/blogs/modeling-electroanalysis-cyclic-voltammetry/ (19.9.2015)

[17] https://en.wikipedia.org/wiki/Chronoamperometry (19.9.2015)

[18] Cowley A., & Woodward B. A Healthy Future: Platinum in Medical Applications. Platinum Metals Review 55: 98-107. 2011

[19] Hudak E., MortimerJ., & Martin H. Platinum for neural stimulation: voltammery considerations. Journal of Neural Engineering 7: 1741-2560. 2010

[20] Climent V. & Feliu J. Thirty years of platinum single crystal electrochemistry. Journal of Solid State Electrochemistry 15: 1297-1315. 2011

[21] Palomäki T. Electrochemical Measurement of Dopamine with Diamond-like Carbon/Pt Composite Electrodes. Master's Thesis, School of Electrical Engineering, Aalto University. 2013.

[22] Jerkiewicz G., Vatankhah G., Lessard J., Soriaga M., & Park Y.-S. Surface-oxide growth at platinum electrodes in aqueous H_2SO_4: Reexamination of its mechanism through combined cyclic-voltammetry, electrochemical quartz-crystal nanobalance, and Auger electron spectroscopy measurements. Electrochimica Acta 49: 1451-1459. 2004.

[23] Bohmer, A., Muller, A., Passarge, M., Liebs, P., Honeck, H., & Muller, H. A Novel L-Glutamate Oxidase from Streptomyces Endus. Purification and Properties. European Journal Biochemistry 182: 327-332. 1989

[24] Hall S., Khudaish E., & Hart A. Electrochemical oxidation of hydrogen peroxide at platinum electrodes. Part 1. An adsorption-controlled mechanism. Electrochimica Acta 43: 579-588. 1998

[25] Hall S., Khudaish E., & Hart A. Electrochemical oxidation of hydrogen peroxide at platinum electrodes. Part II: effect of potential. Electrochimica Acta 43: 2015-2024. 1998

[26] Hall S., Khudaish E., & Hart A. Electrochemical oxidation of hydrogen peroxide at platinum electrodes. Part V: Inhibition by chloride. Electrochimica Acta, 45:3573-3579. 2000

[27] Guo S. & Wang E. Synthesis and electrochemical applications of gold nanoparticles. Analytical Chimica Acta 598: 181-192. 2007

[28] Ma Y., Di J., Yan X., Zhao M., Lu Z. & Tu Y. Direct electrodeposition of gold nanoparticles on indium tin oxide surface and its application. Biosensors and Bioelectronics 24: 1480-1483. 2009

[29] Luo X., Xu J., Du Y. & Chen H. A glucose biosensor based on chitosan-glucose oxidase-gold nanoparticles biocomposite formed by one-step electrodeposition. Analytical Biochemistry 334: 284-289. 2004

[30] Liu A., Dong W., Liu E., Tang W., Zhu J., & Han J. Non-enzymatic hydrogen peroxide detection using gold nanocluster-modified phosphorus incorporated tetrahedral amorphous carbon electrodes. Electrochimica Acta 55: 1971-1977. 2010

[31] Gerlache M. Senturk Z., Quarin G., & Kauffmann J.-M. Electrochemical behavior of H_2O_2 on gold. Electroanalysis 9: 1088-1092. 1997

[32] Akbar S., Elliott J., Rittman M., & Squires A. Facile Production of Ordered 3D Platinum Nanowire Networks with "Single Diamond" Bicontinuous Cubic Morphology. Advanced Materials DOI: 10.1002/adma.201203395. 2012

[33] El-Deab M. & Ohsaka T. An extraordinary electrocatalytic reduction of oxygen on gold nanoparticles-electrodeposited gold electrodes. Electrochemistry Communications 4:288-292. 2002a

[34] El-Deab M., Okajima T., & Ohsaka T. Electrochemical Reduction of Oxygen on Gold Nanoparticle-Electrodeposited Glassy Carbon Electrodes. Journal of The Electrochemical Society 150: 851-857. 2003

[35] Zeis R., Lei T., Sieradzki., Snyder J., & Erlebacher J. Catalytic reduction of oxygen and hydrogen peroxide by nanoporous gold. Journal of Catalysis 253: 132-138. 2008

[36] Pingarrón J. Yáñes-Sedeño P., & González-Cortés A. Gold nanoparticle-based electrochemical biosensors. Electrochimica Acta 53: 5848-5866. 2008

[37] Xiao Y., J H-X., & Chen H-Y. Hydrogen peroxide sensor based on horseradish peroxidase-labeled Au colloids immobilized on gold electrode surface by cystemine monolayer. Analytical Chimica Acta 391: 73-82. 1999

[38] Fischer L., Tenje M., Heiskanen A., Masuda N., Castillo J., Bentien A., Émneus J., Jakobsen M., & Boisen A. Gold cleaning methods for electrochemical detection applications. Microelectronic Engineering 86: 1282-1285. 2009

[39] Hauert R. A review of modified DLC coatings for biological applications. Diamonds and related Materials 12: 583-589. 2003

[40] Robertson J. Diamond-like amorphous carbon. A Review Journal. Materials Science and Engineering R 37: 129-281. 2002

[41] Zeng A., Neto V., Gracio J., & Fan Q. Diamond-like carbon (DLC) films as electrochemical electrodes. Diamond and Related Materials. 43:12-22. 2014

[42] Laurila T., Protopopova V., Rhode S., Sainio S, Palomäki T., Moram M, Feliu J, & Koskinen J. New electrochemically improved tetrahedral amorphous carbon films for biological applications. Diamond and Related Materials. 2014. doi: 10.1016/j.diamond.2014.08.007

[43] Hamdi N., Wang J. & Monbouquette H. Polymer films as perselective coatings for H_2O_2-sensing electrodes. Journal of Electroanalytical Chemistry 581: 258-264. 2005

[44] Robinson D., Hermans A., Seipel A., & Wightman R. Monitoring Rapid Chemical Communication in the Brain. Chemical Reviews 108: 2554-2584. 2008

[45] MacDiarmid A. Polyanaline and polypyrrole: where are we headed? Synthetic Metals 84: 27-34

[46] Ammam M., & Fransaer J. Highly sensitive and selective glutamate microbiosensor based on cast polyurethane/AC-electrophoresis deposited multiwalled carbon nanotubes and the glutamate oxidase/electrosynthesized polypyrrole/ Pt electrode. Biosensors and Bioelectronics 25: 1597-1602. 2010

[47] Yang Y-L., Tseng T-F., Yeh J-M., Chen C-A., & Lou S-L. Performance characteristic studies of glucose biosensor modified by (3-mercaptopropyl)trimethoxysilane sol-gel and non-conducting polyaniline. Sensors and Actuators B 131: 533-540. 2008

[48] Sassolas A., Blum L., & Leca-Bouvier B. Immobilization strategies to develop enzymatic biosensors. Biotechnology Advances 30: 489-511. 2012

[49] Song E. & Choi J-W. Conducting Polyaniline Nanowire and Its Applications in Chemiresistive Sensing. Nanomaterials 3: 498-523. 2013

[50] Morita M., Miyazaki S., Ishikawa M., & Matsuda Y. Layered Polyaniline Composites with Cation-Exchanging Properties for Positive Electrodes of Rechargeable Lithium Batteries. Journal of the Electrochemical Society 142: 3-5. 1995

[51] Wang P., Li S., & Kan J. A hydrogen peroxide biosensor based on polyaniline/FTO. Sensors and actuators. B, Chemical 137: 662-668. 2009

[52] Cui S-Y. & Park S-M. Electrochemistry of conductive polymers XXIII: polyaniline growth studied by electrochemical quartz crystal microbalance measurements. Synthetic Metals 105: 91-98. 1999

[53] Batra B., Kumari S., & Pundir C. Construction of glutamate biosensor based on covalent immobilization of glutamate oxidase on polypyrrole nanoparticles/polyaniline modified gold electrode. Enzyme and Microbial Technology 57: 69-77. 2014

[54] Maouche N., Guergouri M., Gam-Derouich S., Jouini M., Nessark B., & Chehimi M. Molecularly imprinted polypyrrole films: Some key parameters for electrochemical picomolar detection of dopamine. Journal of Electroanalytical Chemistry 685: 21-27. 2012

[55] Wang X. & Uchiyama S. Polymers for Biosensor Construction. ISBN 978-953-51-1004-0

[56] Min Y-L., Wang T., Zhang Y-G., & Chen Y-C. Synthesis of poly(p-phenylenediamine) microstructures without oxidants and their effective adsorption of lead ions. Journal of Materials Chemistry 21: 6683-6689. 2011

[57] Malitesta C., Palmisano F., Torsi L., & Zambonin P. Glucose Fast-Response Amperometric Sensor Based on Glucose Oxidase Immobilized in an Electropolymerized Poly(o-phenylenediamine) Film. Analytical chemistry 62: 2735-2740. 1990

[58] Arima J., Sasaki C., Sakaguchi C., Mizuno H., Tamura T., Kashima A., Kusakabe H., Sugio S., & Inagaki K. Structural characterization of L-glutamate oxidase from Streptomyces sp. X-119-6. The FEBS Journal, 276: 3894–3903. 2009

[59] Hermanson G. Bioconjugate Techniques. Second edition. Elsvier Inc. ISBN: 978-0-12-370501-3. 2008

[60] Colavita P., Sun B., Wang X. & Hamers R. Influence of Surface Termination and Electronic Structure on the Photochemical Grafting of Alkenes to Carbon Surfaces. Journal of Physical Chemistry 113: 1526-1535. 2009

[61] Nichols B., Butler J., Russel J. & Hamers R. Photochemical Functionalization of Hydrogen-Terminated Diamond Surfaces: A Structural and Mechanical Study. Journal of Physical Chemistry B 109, 20938-20947. 2005

[62] https://www.lifetechnologies.com/fi/en/home/life-science/protein-biology/protein-biology-learning-center/protein-biology-resource-library/pierce-protein-methods/carbodiimide-crosslinker-chemistry.html (11.8.2015)

[63] Poitry S., Poitry-Yamate C., Innocent C., Cosnier S. & Tsacopoulos M. Detection of glutamate released by neurons with an enzyme-based microelectrode: applications and limitations. Electrochimica Acta 42: 3217-3223. 1997

[64] Park B., Yoon D., & Kim D. Recent progress in bio-sensing techniques with encapsulated enzymes. Biosensors and Bioelectronics, 26: 1 – 10, 2010

[65] Alvarez-Icaza M. & Bilitewski U. Mass Production of Biosensors. Analytical Chemistry, 65: 525-533, 1993

[66] Toworfe G., Composto R., Shapiro I. & Ducheyne P. Nucleation and growth of calcium phosphate on amine-, carboxyl- and hydroxyl-silane self-assembled monolayers. Biomaterials 27: 631-642. 2006

[67] Pesin L. Review: Structure and properties of glass-like carbon. Journal of Materials Science 37: 1-28. 2002

[68] Raj C., Okajima T., & Ohsaka T. Gold nanoparticle arrays for the voltammetric sensing of dopamine. Journal of Electroanalytical Chemistry 543: 127-133. 2003

[69] Yang W., Li Y., Bai Y., & Sun C. Hydrogen peroxide biosensor based on myoglobin/colloidal gold nanoparticles immobilized on glassy carbon electrode by Nafion film. Sensors and Actuators B 115: 42-48. 2006

[70] Chen W., Li C., Chen P., & Sun C. Electrosynthesis and characterization of polypyrrole/Au nanocomposite. Electrochimica Acta 52: 2845-2849. 2007

[71] Njagi J. & Andreescu S. Stable enzyme biosensors based on chemically synthesized Au-polypyrrole nanocomposites. Biosensors and Bioelectronics 23: 168-175. 2007

[72] Yin T., Wei W., & Zeng J. Selective detection of dopamine in the presence of ascorbic acid by use of glassy-carbon electrodes modified with both polyaniline film and multi-walled carbon nanotubes with incorporated β-cyclodextrin. Analytical Biochemistry 386:2087-2094. 2006

[73] Ivanov A., Lukachova L., Evtugyn G., Karyakina E., Kiseleva S., Budnikov H., Orlov A., Karpacheva G., & Karyakin A. Polyaniline-modified cholinesterase sensor for pesticide determination. Biochemistry 55: 75-77. 2002

[74] Evtugyn G., Stoikov I., Beljyakova S., Shamagsumova R., Stoikova E., Zhukov A., Antipin I., & Budnikov H. Ag selective electrode based on glassy carbon electrode covered with polyaniline and thiacalix[4]arene as neutral carrier. Talanta 71: 1720-1727. 2007

[75] Shao M., Peles A., & Shoemaker K. Electrocatalysis on Platinum Nanoparticles: Particle Size Effect on Oxygen Reduction Reaction Activity. Nano Letters 11:3714-3719. 2011

[76] Santhosh P., Manesh K., Gopalan A., & Lee K.-P. Fabrication of a new polyaniline grafted multi-wall carbon nanotube modified electrode and its application for electrochemical detection of hydrogen peroxide. Analytical Chimica Acta 575: 32-38. 2006

[77] Takabayashi S., Okamoto K., Motoyama H., Nakatani T., Sakaue H., & Takahagi T. X-ray photoelectron analysis of surface functional groups on diamon-like carbon films by gas-phase chemical derivatization method. Surface and Interface Analysis 42: 77-87. 2010

A Appendix

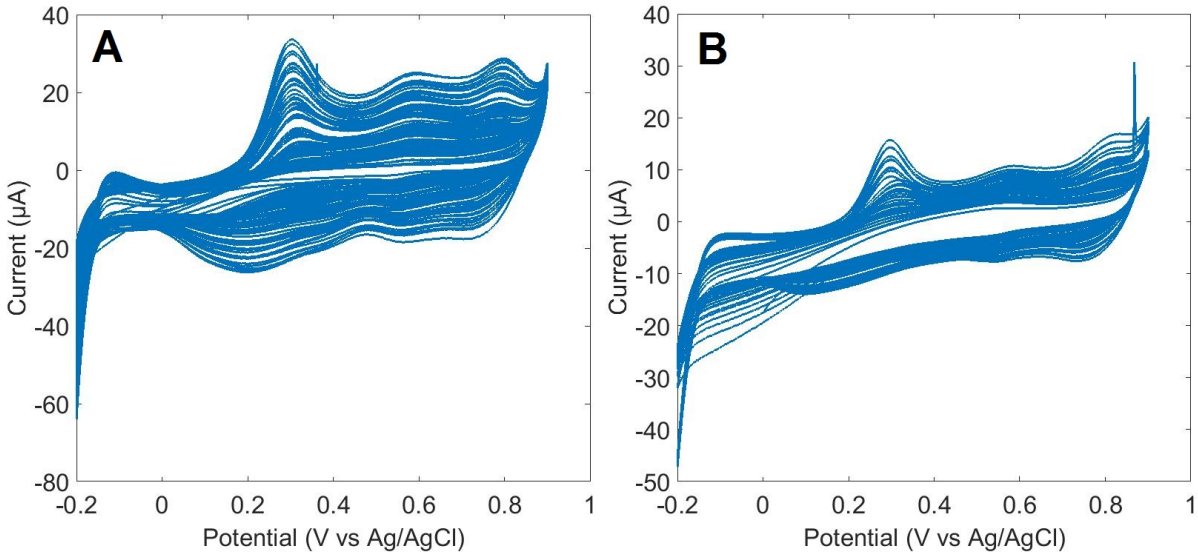

Figure A1 – PANI deposition on a CPt sample with the scan rate of 100 mV/s. (A) is the deposition curve of a CPt/PANI(70) and (B) the deposition curve of a CPt/PANI(35).

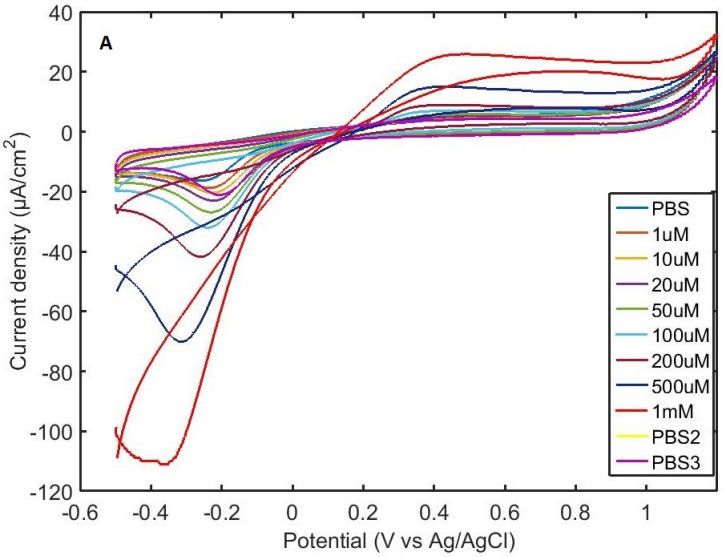

Figure A2 – H_2O_2 measurement with a CPt sample. Scan rate was 50 mV/s.

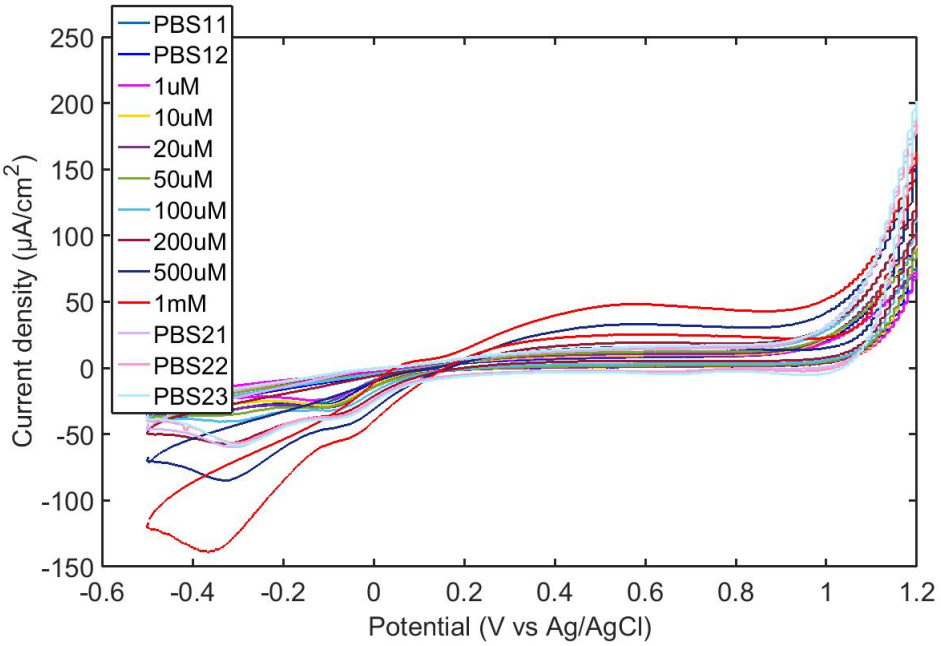

Figure A3 – H_2O_2 measurement with a platinum sample. Scan rate was 50 mV/s.

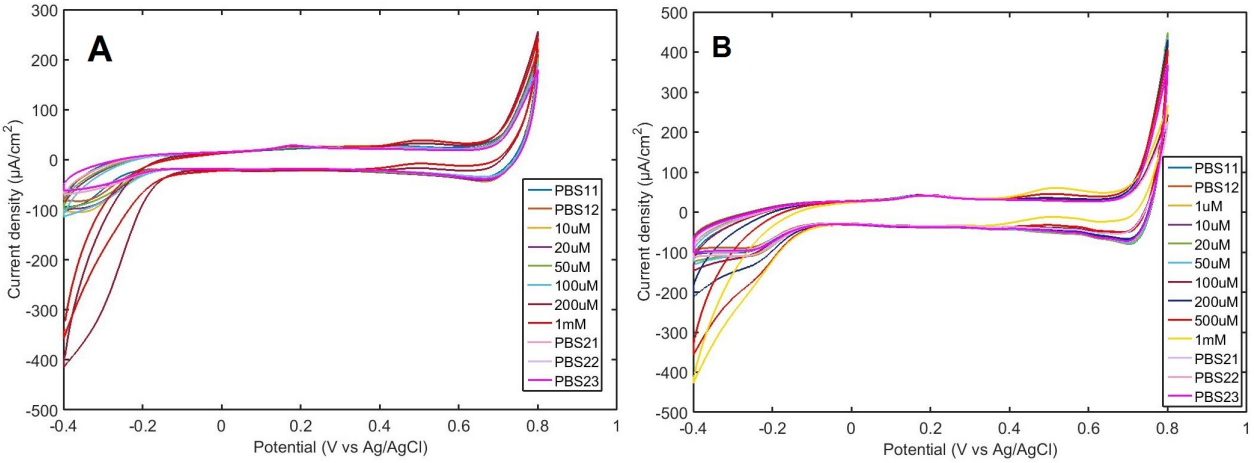

Figure A4 – H_2O_2 measurement with (A) AuNP(a) sample and (B) AuNP(b) sample. Scan rate was 50 mV/s.

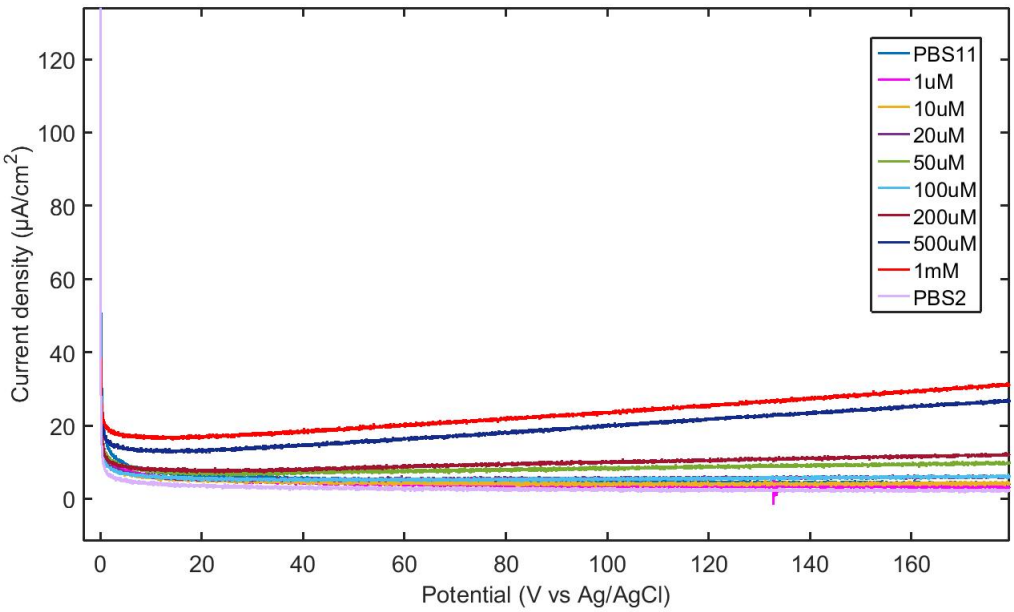

Figure A5 – CA with AuNP(a). Potential was +0.7 V (vs. Ag/AgCl) for 180s.

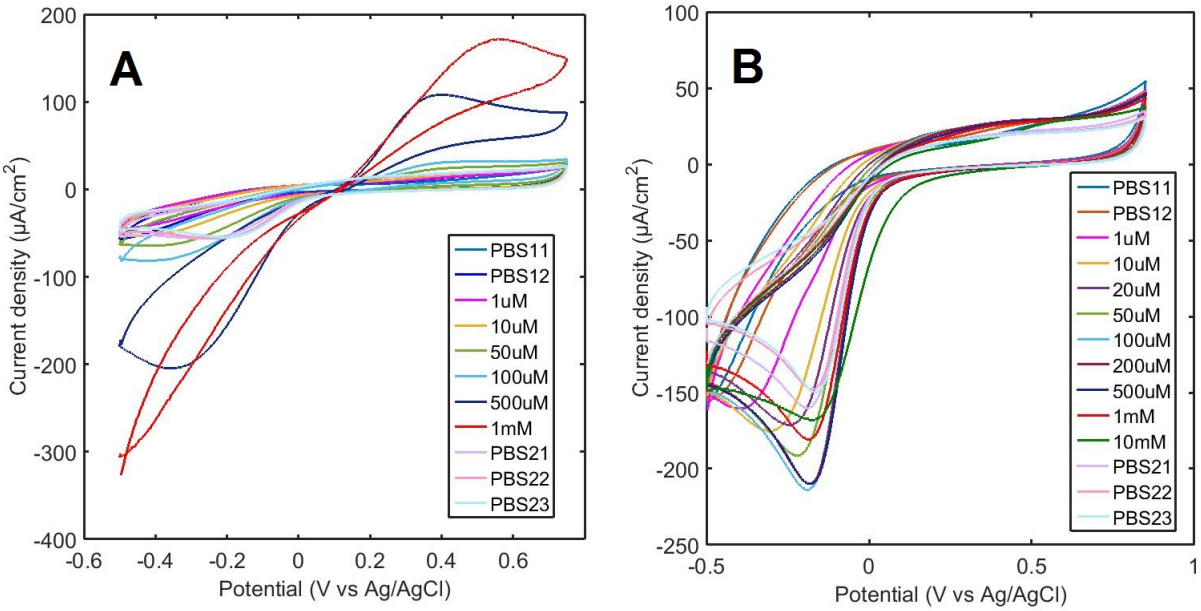

Figure A6 – H_2O_2 measurement with (A) CPt/APTES sample and glutamate measurements with (B) CPt/APTES/GlOx sample. Scan rate was 50 mV/s.

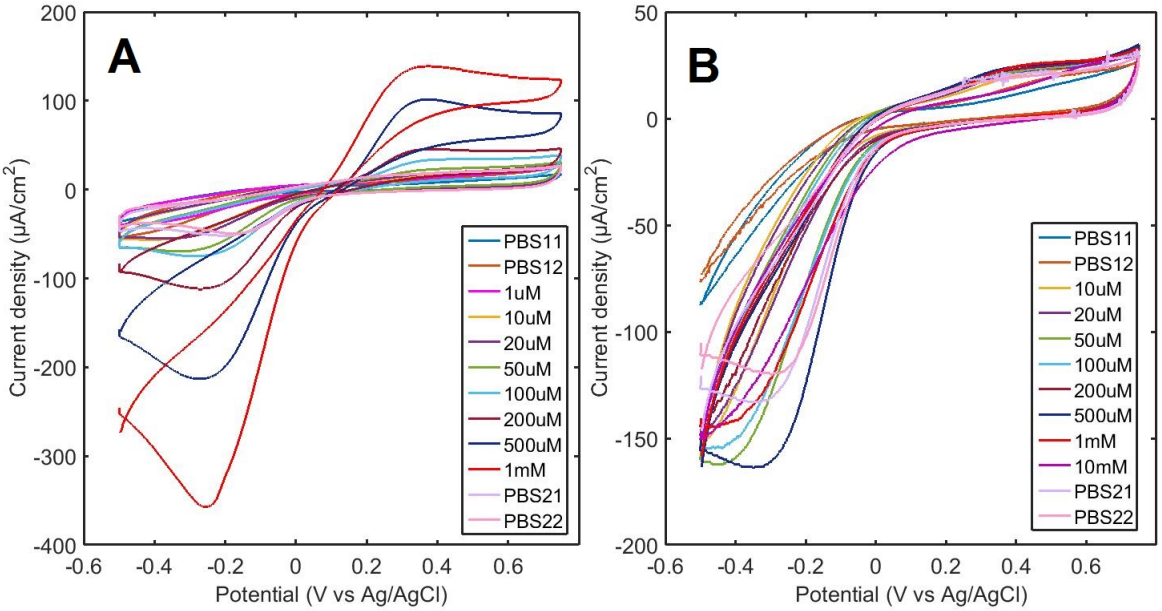

Figure A7 – H_2O_2 measurement with (A) CPt/TESPSA sample and glutamate measurements with (B) CPt/TESPSA/GlOx sample. Scan rate was 50 mV/s.

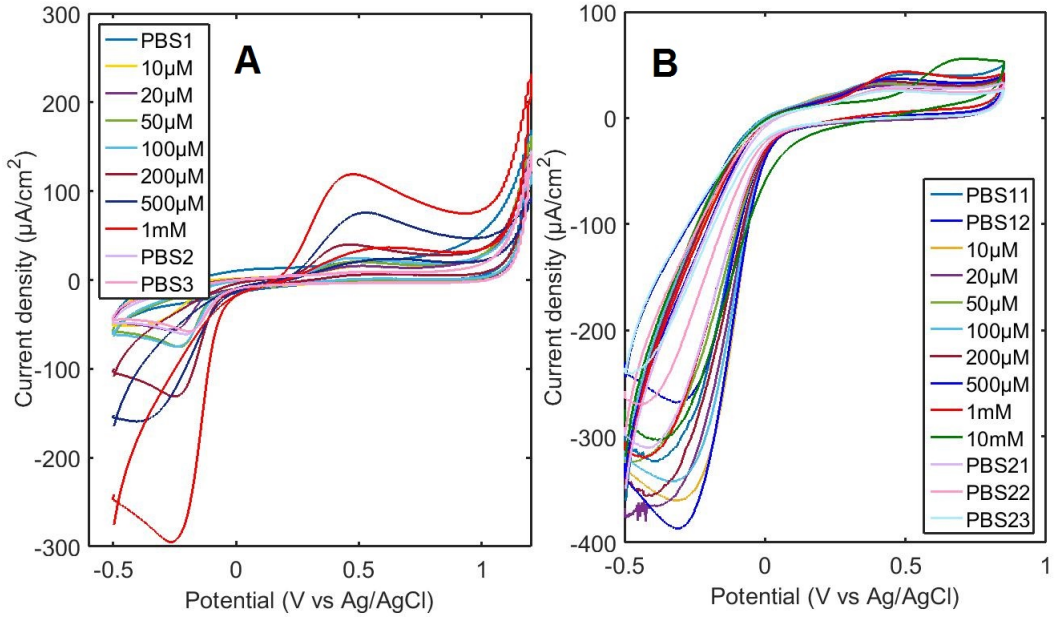

Figure A8 – H_2O_2 measurement with (A) CPt/PANI sample and glutamate measurements with (B) CPt/PANI/GlOx sample. Scan rate was 50 mV/s.

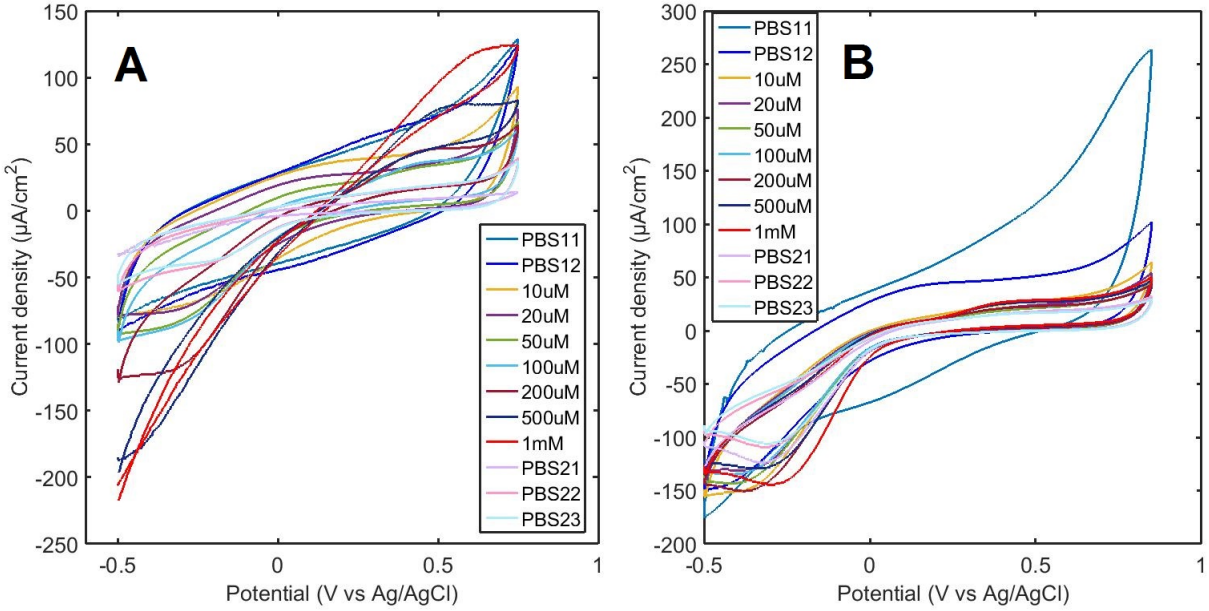

Figure A9 – H_2O_2 measurement with (A) CPt/PPy sample and glutamate measurements with (B) CPt/PPy/GlOx sample. Scan rate was 50 mV/s.

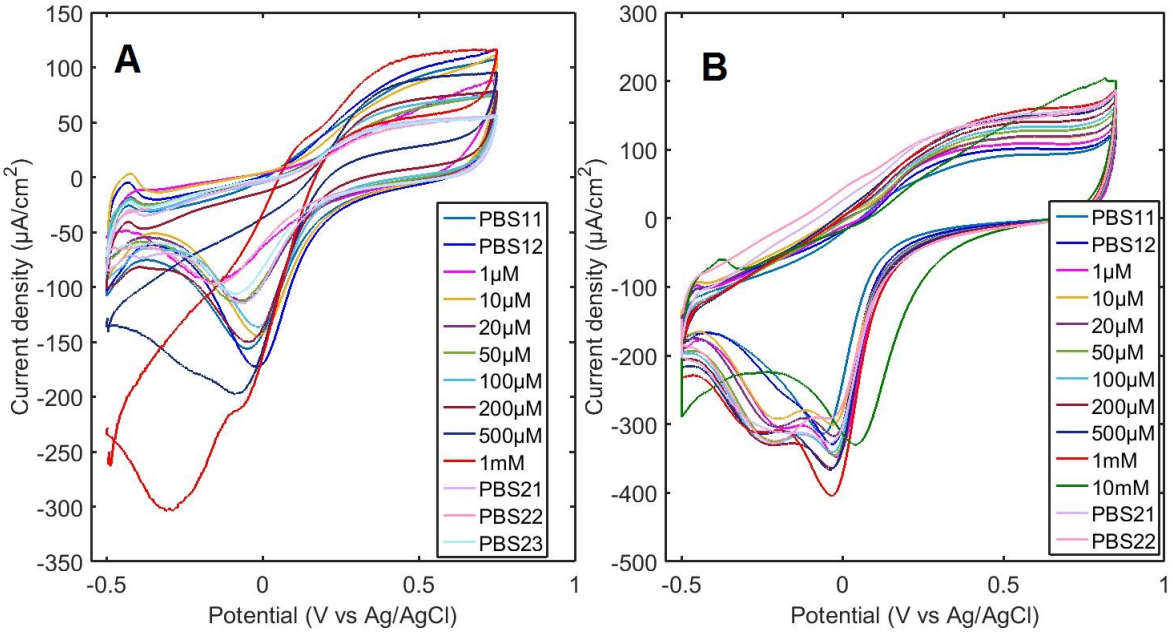

Figure A10 – H_2O_2 measurement with (A) Pt/APTES sample and glutamate measurements with (B) Pt/APTES/GlOx sample. Scan rate was 50 mV/s.

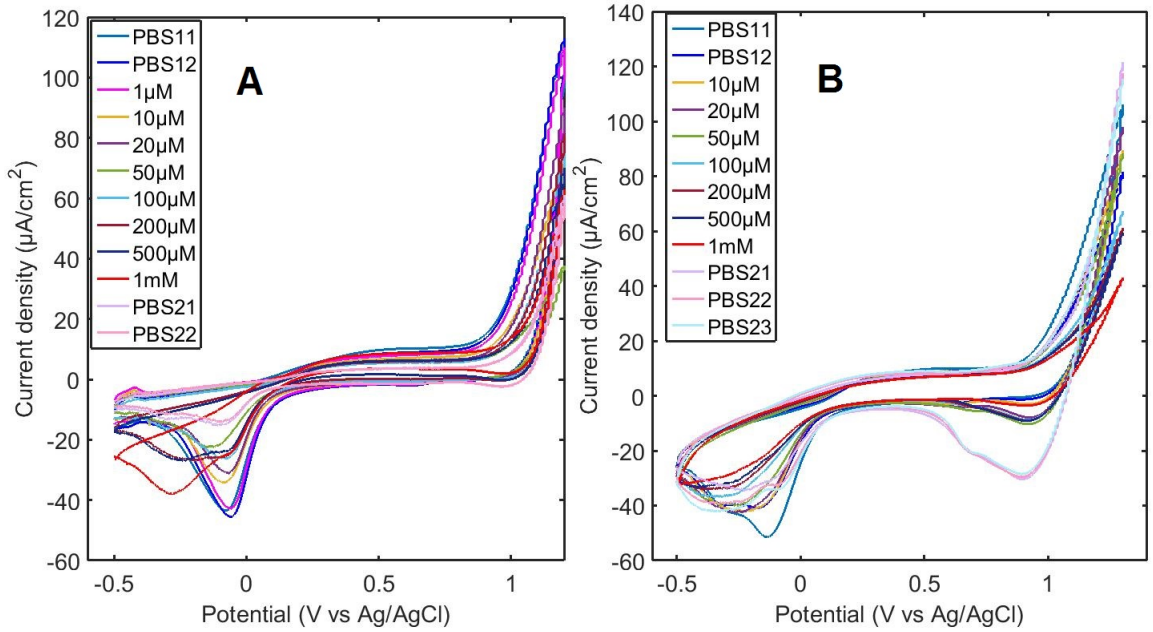

Figure A11 – H_2O_2 measurement with (A) Pt/TESPSA sample and glutamate measurements with (B) Pt/TESPSA/GlOx sample. Scan rate was 50 mV/s.

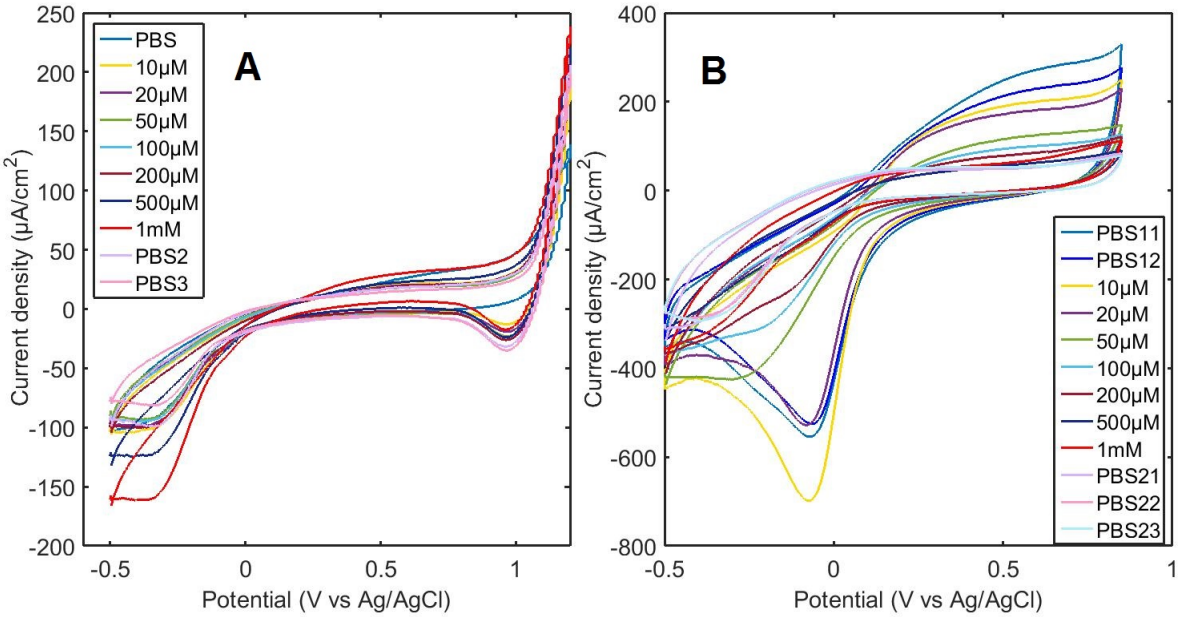

Figure A12 – H_2O_2 measurement with (A) Pt/PANI sample and glutamate measurements with (B) Pt/PANI/GlOx sample. Scan rate was 50 mV/s.

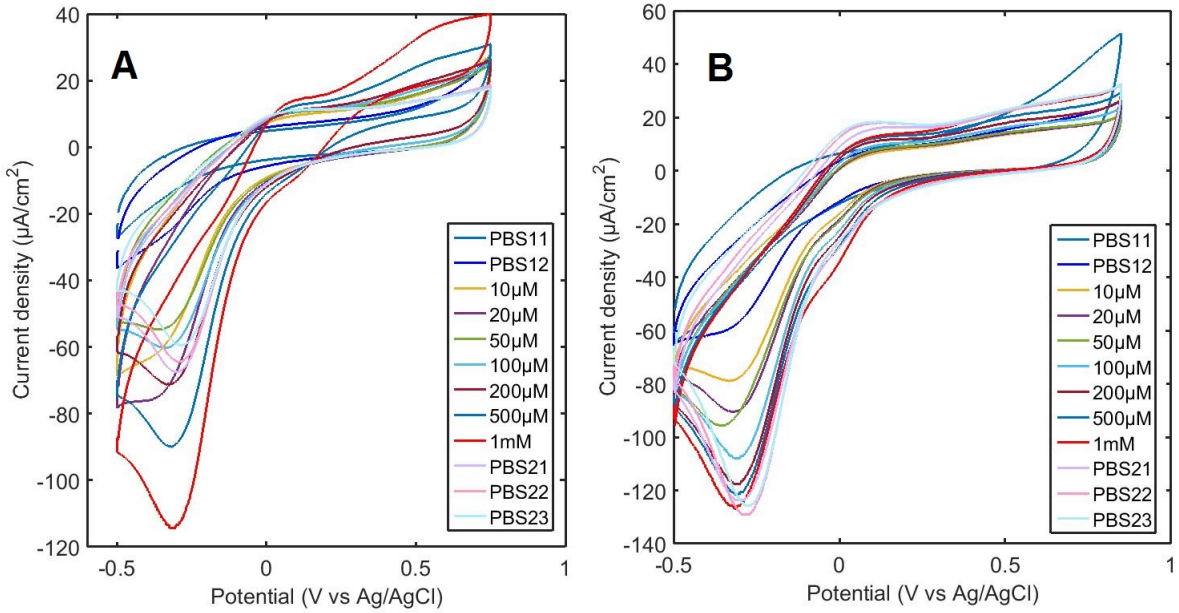

Figure A13 – H_2O_2 measurement with (A) Pt/PPy sample and glutamate measurements with (B) Pt/PPy/GlOx sample. Scan rate was 50 mV/s.

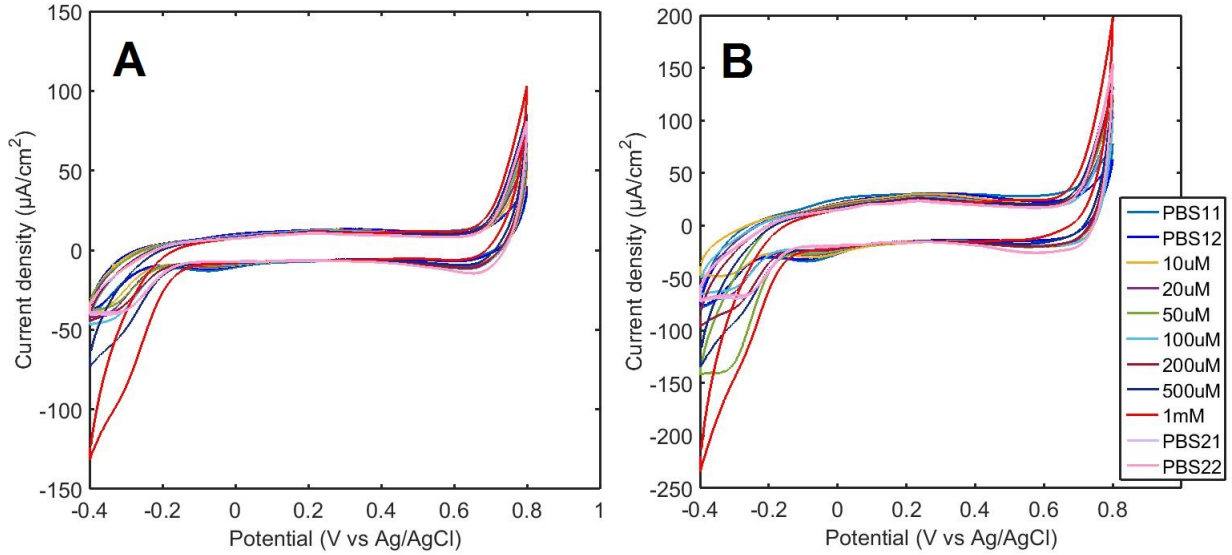

Figure A14 – H_2O_2 measurement with (A) AuNP(a)/PANI sample and with (B) AuNP(b)/PANI sample. Scan rate was 50 mV/s.